SELF–INTERSECTING CURVES ON A PAIR OF PANTS AND PERIODIC ORBITS OF HAMILTONIAN FLOWS

FERNANDO CAMACHO–CADENA

ABSTRACT. The character variety $\mathscr{X}(S,G)$ associated to an oriented compact surface S with boundary and a real reductive Lie group G admits a Poisson structure and is foliated by symplectic leaves. When G is a matrix group, any closed curve $c \in \pi_1(S)$ induces a trace function $\mathsf{tr}_c\colon [\rho] \mapsto \mathsf{tr}(\rho(c))$ on $\mathscr{X}(S,G)$. In this article, we study the Hamiltonian flows of trace functions associated to self–intersecting curves. We prove that when $G = \mathsf{PSL}(3,\mathbb{R})$ and S is the pair of pants, every orbit of the Hamiltonian flow of the trace of a figure eight curve on S is periodic and has a unique fixed point. The proof uses explicit computations in Fock–Goncharov coordinates. As an application, we prove a similar statement for the trace of the Θ–web. Finally, we focus on the symplectic leaf corresponding to the unipotent locus, and derive similar results for two more self–intersecting curves: the commutator, and a curve going k times around a boundary component.

1. INTRODUCTION

Let S be an oriented compact surface of genus g with $n \geq 1$ boundary components, of negative Euler characteristic and with fundamental group $\pi_1(S)$. Let G be a real reductive Lie group, and assume that it is a matrix group. Associated to S and G is the *character variety*

$$\mathscr{X}(S,G) \coloneqq \mathsf{Hom}(\pi_1(S),G) /\!\!/ G,$$

where G acts on representations by conjugation. The character variety has a natural Poisson structure, which is defined on each symplectic leaf [Gol84, GHJW97]. The symplectic leaves correspond to relative character varieties, that is, given a tuple of conjugacy classes $\mathcal{C} = (C_1,\dots,C_n)$ in G, the *relative character variety associated to* $\mathcal{C}$ is

$$\mathscr{X}_{\mathcal{C}}(S,G) \coloneqq \{\rho \in \mathsf{Hom}(\pi_1(S),G) :\ \rho(c_i) \in C_i, i = 1,\dots,n\} /\!\!/ G,$$

where the $c_i \in \pi_1(S)$ are chosen generators for each boundary component of S.

Perhaps the best known example of this is the Teichmüller space of S, i.e. the space of complete hyperbolic structures on S up to isotopy. In this case, $G = \mathsf{PSL}(2,\mathbb{R})$. The relative character varieties are given by prescribing the length of boundary components and the symplectic structure on them is given by the Weil–Petersson symplectic form

This project received funding from the Deutsche Forschungsgemeinschaft (DFG, German Research Foundation) – Project-ID 281071066 – TRR 191, as well as from the European Research Council (ERC) under the European Union's Horizon 2020 research and innovation programme (grant agreement No 101018839). The author acknowledges the support of the Institut Henri Poincaré (UAR 839 CNRS-Sorbonne Université), and LabEx CARMIN (ANR-10-LABX-59-01).

[Wol83].

An important class of functions on character varieties are trace functions associated to closed curves on S. Namely, any curve $c \in \pi_1(S)$ defines a *trace function*

$$\begin{aligned} \mathsf{tr}_c \colon \mathscr{X}(S,G) &\to \mathbb{R} \\ [\rho] &\mapsto \mathsf{tr}(\rho(c)). \end{aligned}$$

By restricting a trace function tr_c to a symplectic leaf $\mathcal{Q} \subset \mathscr{X}(S,G)$, we obtain its associated *Hamiltonian flow*. This is the flow associated to the *Hamiltonian vector field* Htr_c given by $\omega_{\mathcal{Q}}(\cdot, \mathsf{Htr}_c) = d\,\mathsf{tr}_c(\cdot)$, where $\omega_{\mathcal{Q}}$ is the symplectic form of $\mathcal{Q}$. In the case of Teichmüller space, trace functions are directly related to length functions. Moreover, when c is a simple closed curve, Wolpert [Wol82] found that the Hamiltonian flows of tr_c correspond to twist flows.

In more generality, when G is any real reductive Lie group and c is a simple closed curve, Goldman fully described the Hamiltonian flow of the function tr_c [Gol86]. However, both in Teichmüller space and on general character varieties, the study of Hamiltonian flows associated to self–intersecting curves is much more limited. In the case when S is a closed surface, Farre and Wienhard together with the author introduced invariant multi–functions in [CCFW24], generalizing [Gol86]. In that article, the authors found a geometric and qualtitative description of Hamiltonian flows associated to trace functions coming from self–intersecting curves. Namely, if the curve fills a subsurface S_0 of S, then the Hamiltonian flow only deforms the complement of S_0 in S. Even though the result gave insight into the Hamiltonian flow, its behavior on the surface S_0 remained unknown outside some simple cases.

In this article, we continue the study of Hamiltonian flows associated to trace functions of self–intersecting curves. To do this, we turn to the framework of Fock and Goncharov [FG06]. A *framed representation* is a representation $\rho \colon \pi_1(S) \to \mathsf{PSL}(d,\mathbb{R})$ together with the data of n full flags $F_1, \dots, F_n$ in $\mathbb{R}^d$ associated to each boundary component such that $\rho(c_i) \cdot F_i = F_i$ for each $i = 1, \dots, n$. Fock and Goncharov define a set of coordinates on the space of framed representations depending on a triangulation of S (see Section 3). The positivity of the coordinates does not depend on the triangulation and therefore defines the set of *positive framed representations*, which we denote by $\widehat{\mathscr{X}_d}^+(S)$.

The space of positive framed representations comes equipped with a Poisson structure [FR99, FG06]. Its symplectic leaves identify with relative character varieties through the projection $\widehat{\mathscr{X}_d}^+(S) \to \mathscr{X}_d(S)$ which forgets the framing, and where we abbreviate $\mathscr{X}(S, \mathsf{PSL}(d,\mathbb{R}))$ by $\mathscr{X}_d(S)$. The symplectic structure on the symplectic leaves coincides with the symplectic structure on the relative character varieties up to a constant [Sun21, Theorem 1.1]. Fock and Goncharov describe the Poisson structure explicitly in coordinates (see Section 3.3), and the reconstruction of the representation from the coordinates is also explicit. This allows us to work with explicit computations to deduce results on Hamiltonian flows of trace functions associated to self–intersecting curves.

Here we take the case $G = \mathsf{PSL}(3,\mathbb{R})$, where the space of positive framed representations coincides with the space of *framed real convex projective structures* on S [FG07]. These are triples $[\mathsf{dev}, \rho, \nu]$, where $\rho\colon \pi_1(S) \to \mathsf{PSL}(3,\mathbb{R})$ is a representation, known as the *holonomy*, $\mathsf{dev}\colon \widetilde{S} \to \mathbb{RP}^2$ is a ρ–equivariant diffeomorphism onto a properly convex domain in $\mathbb{RP}^2$, known as the *developing map*, and ν is a framing of ρ (see Section 2.3). We denote the space of framed real convex projective structures on S by $\widehat{\mathfrak{C}}(S)$.

In this article, we focus on the pair of pants P. The symplectic leaves in $\widehat{\mathfrak{C}}(P)$ are two dimensional [Gol90], and hence using Fock–Goncharov coordinates, we can plot level sets of trace functions to understand and guess the behavior of their associated Hamiltonian flows. We pick a presentation of the fundamental group $\pi_1(P) = \langle \alpha, \beta, \gamma \,|\, \alpha\beta\gamma = 1\rangle$ with α, β, γ corresponding to the peripheral loops as in Figure 1.

Let $\delta = \alpha\gamma^{-1}$ be a *figure eight curve* in P, as shown in Figure 1. Picking a symplectic leaf (see Section 4.2 for more details), Figure 2 shows the level sets of tr_δ using coordinates σ_1 and τ_1 (see Section 6.2 for a more detailed description of which symplectic leaf the plot corresponds to).

Our main result is the following, which confirms the heuristic picture in Figure 2.

Theorem A (Theorem 5.1)**.** *Let $\delta = \alpha\gamma^{-1}$ be a figure eight curve on a pair of pants P and let $\mathcal{Q}$ be any symplectic leaf in $\widehat{\mathfrak{C}}(P)$. Then the restriction of the trace function $\mathsf{tr}_\delta\big|_{\mathcal{Q}}\colon \mathcal{Q} \to \mathbb{R}$ attains a unique minimum. Moreover, every orbit of the Hamiltonian flow of $\mathsf{tr}_\delta\big|_{\mathcal{Q}}$ is periodic and there is a unique fixed point.*

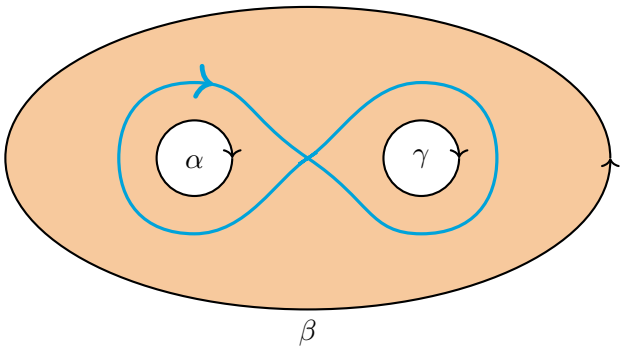

FIGURE 1. A pair of pants, the generators for its fundamental group, and a figure eight curve.

Theorem A has the following application. Sikora in [Sik01] (see also [DKS24]) introduced the notion of 3–webs, which are 3–regular bipartite graphs on a surface. Similar to the case of closed curves, a web m defines a trace function $\mathsf{tr}_m\colon \widehat{\mathfrak{C}}(P) \to \mathbb{R}$. For the case of the Θ–*web*, shown in Figure 3, its trace, when restricted to a symplectic leaf, is given by $C - \mathsf{tr}_\delta$ for a constant C depending on the symplectic leaf (see Section 5.5). Thus by Theorem A, we immediately obtain the following.

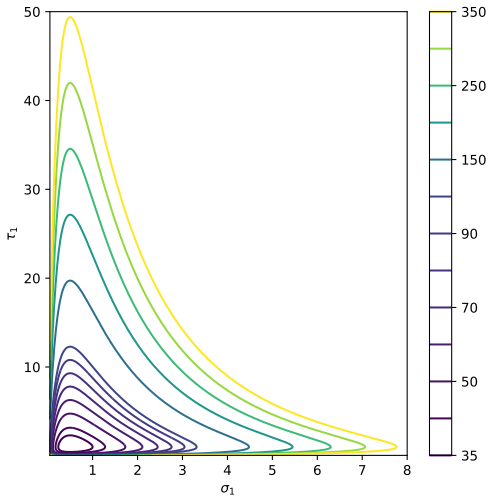

FIGURE 2. Level sets of tr_δ on the unipotent locus.

Corollary B (Corollary 5.7)**.** *Let m_Θ be the Θ–web and $\mathcal{Q}$ be any symplectic leaf in $\widehat{\mathfrak{C}}(P)$. Then the restriction of the trace function $\mathsf{tr}_{m_\Theta}\big|_{\mathcal{Q}}\colon \mathcal{Q} \to \mathbb{R}$ attains a unique maximum. Moreover, every orbit of the Hamiltonian flow of $\mathsf{tr}_{m_\Theta}\big|_{\mathcal{Q}}$ is periodic and there is a unique fixed point.*

One may also consider the function $\mathsf{tr}_\delta + \mathsf{tr}_{\delta^{-1}}$. This function may be more natural in the sense that the map $c \mapsto \mathsf{tr}_c + \mathsf{tr}_{c^{-1}}$ is invariant under taking inverses of the curve. In particular, the function only depends on the curve and *not* on its orientation. We note that in the case of the group $\mathsf{SL}(2,\mathbb{R})$, the function $c \mapsto \mathsf{tr}_c$ is already invariant under taking inverses. For the symmetric function $\mathsf{tr}_\delta + \mathsf{tr}_{\delta^{-1}}$ in the $\mathsf{PSL}(3,\mathbb{R})$ case, we obtain a similar result as Theorem A as well as more information about the fixed point. Recall that a real convex projective structure on P is said to be *hyperbolic* if its holonomy representation factors through an irreducible representation $\mathsf{PSL}(2,\mathbb{R}) \to \mathsf{PSL}(3,\mathbb{R})$ (see Section 4.3).

Theorem C. *Let $\delta = \alpha\gamma^{-1}$ be a figure eight curve on a pair of pants P and let $\mathcal{Q}$ be any symplectic leaf in $\widehat{\mathfrak{C}}(P)$. Then the following statements hold.*

(a) *[Theorem A.1] The restriction of the function $\mathsf{tr}_\delta + \mathsf{tr}_{\delta^{-1}}\big|_{\mathcal{Q}}\colon \mathcal{Q} \to \mathbb{R}$ attains a unique minimum. Moreover, every orbit of the Hamiltonian flow of $\mathsf{tr}_\delta + \mathsf{tr}_{\delta^{-1}}\big|_{\mathcal{Q}}$ is periodic, and there is a unique fixed point.*

(b) *[Theorem 5.8] Let $\mathcal{Q}$ be a symplectic leaf containing a hyperbolic structure. Then the fixed point of $\mathsf{tr}_\delta + \mathsf{tr}_{\delta^{-1}}\big|_{\mathcal{Q}}$ is the unique hyperbolic structure in $\mathcal{Q}$.*

1.1. **Idea of the proof of Theorem A.** The proof of Theorem A relies on the following observation, which is a direct consequence of Kerckhoff's work on the Nielsen realization problem in [Ker83]. To state the observation we first make some definitions. Let $S =$

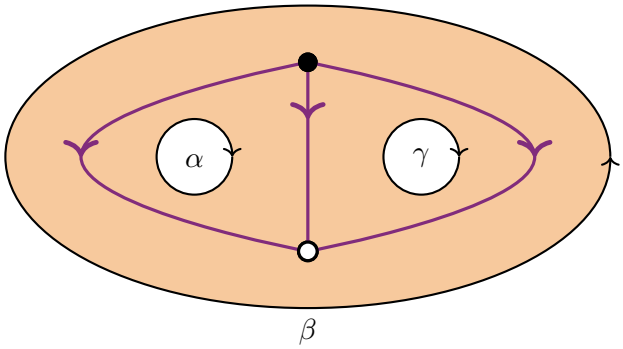

FIGURE 3. The Θ–web on a pair of pants shown in purple.

$S_{g,n,b}$ be a surface of genus g with $n \geq 0$ boundary components and $b \geq 0$ punctures such that $2g-2+n+b > 0$, meaning that S admits complete hyperbolic metrics. For a complete hyperbolic metric m with geodesic boundary, let ℓ_c^m be the hyperbolic length of the geodesic representative of a closed curve c on S. Let $c_1, \ldots, c_n$ denote the boundary curves of S. Fix a *length vector* $L = (\ell_1, \ldots, \ell_n) \in \mathbb{R}^n_{>0}$ and let

$$\mathcal{T}_L(S) \coloneqq \{m \text{ a complete hyperbolic metric on } S : \ \ell^m_{c_i} = \ell_i \text{ for all } i = 1, \ldots, n\}/\mathsf{Diff_0(S)},$$

called the *Teichmüller space* of S. The dimension of $\mathcal{T}_L(S)$ is $6g - 6 + 2n + 2b$.

The Teichmüller space $\mathcal{T}_L(S)$ carries the well–known Weil–Petersson symplectic structure. Moreover, any curve c in S defines a length function

$$\ell_c \colon \mathcal{T}_L(S) \to \mathbb{R}_{>0}.$$

Using the Weil–Petersson symplectic structure, any length function gives rise to a Hamiltonian flow.

A curve c in S is said to be *filling* if its complement in S is a disjoint union of disks, once punctured disks, and annuli which are homotopic to the boundary of S.

Theorem D (Consequence of [Ker83])**.** *Let S be one of the surfaces $S_{1,0,1}, S_{1,1,0}, S_{0,0,4}, S_{0,1,3}, S_{0,2,2}, S_{0,3,1}, S_{0,4,0}$. Let c be a filling curve in S and L a length vector. Then every orbit of the Hamiltonian flow of the function ℓ_c restricted to the Teichmüller space $\mathcal{T}_L(S)$ is periodic and there is a unique fixed point.*

This observation is analogous to Theorem A since the figure eight curve δ is a filling curve in the pair of pants P. The proof uses the notion of an *earthquake*, which is a type of deformation in Teichmüller space. We do not define it here, as we will only need to know some facts about it. For any $t \in \mathbb{R}$, we will write $E_t \colon \mathcal{T}_L(S) \to \mathcal{T}_L(S)$ for an earthquake path in Teichmüller space.

The proof of the theorem hinges on the following four facts:

Fact 1. The Teichmüller space of the surfaces $S_{1,0,1}$, $S_{1,1,0}$, $S_{0,0,4}$, $S_{0,1,3}$, $S_{0,2,2}$, $S_{0,3,1}$, $S_{0,4,0}$ is two–dimensional. Moreover,

these are the only surfaces whose Teichmüller space is two–dimensional. These surfaces are the one–holed torus with either a cusp or a boundary component, and the rest are four–holed spheres with different combinations of boundary components or cusps.

Fact 2 (Properness, Lemma 3.1 in [Ker83])**.** If c is a filling curve in S, then the function $\ell_c \colon \mathcal{T}_L(S) \to \mathbb{R}_{>0}$ is a proper function.

Fact 3 (Earthquake Theorem, [Thu86])**.** Any two points in $\mathcal{T}_L(S)$ can be connected via an earthquake path.

Fact 4 (Strict convexity, Theorem 2 in [Ker83])**.** Let E_t be an earthquake path. Then if c is a filling curve, the function $t \mapsto \ell_c(E_t(m))$ is a strictly convex function for any $m \in \mathcal{T}_L(S)$.

With these three results, we can prove Theorem D.

Proof. [of Theorem D] To start, we make the same observation made in [Ker83, pp. 236], which we restate here. Since the function ℓ_c is proper by Fact 2 and ℓ_c is a positive function, it realizes a minimum. By Fact 4, ℓ_c is strictly convex along any earthquake path. Since any pair of points in $\mathcal{T}_L(S)$ can be connected by an earthquake path by Fact 3, ℓ_c attains a unique minimum. In particular, the function ℓ_c has a unique critical point. Therefore, the Hamiltonian flow of ℓ_c has a unique fixed point, corresponding to the minimum.

Now we show that every orbit is periodic. Let M be a non–empty level set of ℓ_c that does not correspond to the fixed point. In particular, M is a regular level set and therefore a smooth codimension one submanifold of $\mathcal{T}_L(S)$. The Hamiltonian flow of ℓ_c preserves the level sets of ℓ_c (see for example [MS17, pp. 99]). Properness of ℓ_c implies that M is compact. By the fact that $\mathcal{T}_L(S)$ is two–dimensional by Fact 1, M is a compact one–dimensional manifold. Therefore M is a topological circle. Once again, since M does not contain any fixed points, the Hamiltonian vector field restricted to M is bounded away from zero. This implies that the orbit is the whole level set M and is therefore periodic. □

The strategy to prove Theorem A is to prove analogous results to Facts 1, 2, 3 and 4 for the symplectic leaves of $\widehat{\mathfrak{C}}(P)$, where P is the pair of pants. As mentioned above, a symplectic leaf $\mathcal{Q}$ of $\widehat{\mathfrak{C}}(P)$ is a two–dimensional manifold (see Lemma 4.4 for their parameterization). Hence, we already have an analogue of Fact 1. For properness (Fact 2), we prove the following.

Proposition E (Proposition 5.3)**.** *Let $\delta = \alpha\gamma^{-1}$ be the figure eight curve and let $\mathcal{Q} \subset \widehat{\mathfrak{C}}(P)$ be a symplectic leaf. Then the function $\mathsf{tr}_\delta\big|_{\mathcal{Q}} \colon \mathcal{Q} \to \mathbb{R}$ is proper and positive. In particular, it realizes a minimum in $\mathcal{Q}$.*

This is proved by explicit computations of the trace function in Fock–Goncharov coordinates. There is no proper analogue of the earthquake theorem, but we work with two flows, the *eruption* and the *hexagon* flow (in analogy with the flows defined in [WZ18, SWZ20]), which we discuss in Section 4.4. These flows commute, and any two

points in $\mathcal{Q}$ can be connected by a combination of these two flows, as stated in Lemma 4.15. This provides a working analogue of Fact 3.

For an analogue of Fact 4 about the convexity of length functions along earthquake paths, we prove the following result, which seems to be of independent interest.

Theorem F (Theorem 5.4)**.** *Let $\delta = \alpha\gamma^{-1}$ be a figure eight curve and let $\mathcal{Q} \subset \widehat{\mathfrak{C}}(P)$ be a symplectic leaf. Then the trace function $\mathsf{tr}_\delta\big|_{\mathcal{Q}} \colon \mathcal{Q} \to \mathbb{R}$ is strictly convex along the eruption and the hexagon flows.*

The proof relies heavily on the positivity of the Fock–Goncharov coordinates.

Remark 1.1. As shown in [BL23], certain notions of length functions on geodesic laminations are convex along Hamiltonian flows of length functions. Theorem F gives another type of flow along which length functions of certain curves (here interpreted as a trace function) are convex.

The proof of Theorem A is then exactly the same as that of Theorem D using all of the above results. The individual proofs of Proposition E and Theorem F go through explicit computations using Mathematica and the Fock–Goncharov coordinates.

Remark 1.2. In Equation (19) we also provide a formula for the Hamiltonian vector field of a function given in coordinates σ_1, τ_1 of a symplectic leaf. The resulting expressions for the trace of the figure eight curve are explicit, but it is still hard to find a closed–form formula for the solution of the differential equation. However, we can use Mathematica (and Python) to numerically solve the equations. Throughout the paper, we show some of the numerical solutions in simple cases.

1.2. **Beyond the figure eight curve.** Theorem D seems to suggest that if γ is any *filling* curve in P and $\mathcal{Q} \subset \widehat{\mathfrak{C}}(P)$ is a symplectic leaf, then an analogue of Theorem A should hold. Namely, that every orbit of the Hamiltonian flow of $\mathsf{tr}_\gamma\big|_{\mathcal{Q}}$ is periodic and that there is a unique fixed point corresponding to the minimum of the function. As our methods rely on explicit computations, they do not allow to make a very general statement about any curve. However, to provide evidence for the periodicity of Hamiltonian flows associated to filling curves, we provide two more examples.

For this, we focus on the *unipotent locus* $\mathfrak{U} \subset \widehat{\mathfrak{C}}(P)$ (see Definition 4.9). These are the framed convex projective structures whose holonomies for the peripheral curves are *unipotent*, by which we mean that all of the eigenvalues are equal to one. With the same methods as above, we prove

Theorem G (Theorem 6.1 and Theorem 6.6)**.** *Consider the curves $[\alpha, \gamma]$ (see Figure 12) and $\alpha^k\gamma^{-1}$ for $k \in \mathbb{N}_{>0}$ (see Figure 15). The restriction of the trace functions $\mathsf{tr}_{[\alpha,\gamma]}\big|_{\mathfrak{U}} \colon \mathfrak{U} \to \mathbb{R}$ and $\mathsf{tr}_{\alpha^k\gamma^{-1}}\big|_{\mathfrak{U}} \colon \mathfrak{U} \to \mathbb{R}$ attain a unique minimum. Moreover, every orbit of the Hamiltonian flows of $\mathsf{tr}_{[\alpha,\gamma]}\big|_{\mathfrak{U}}$ and $\mathsf{tr}_{\alpha^k\gamma^{-1}}\big|_{\mathfrak{U}}$ is periodic and there is a unique fixed point.*

In Section 6 we also find the fixed points of the Hamiltonian flows appearing in the above theorem.

1.2.1. *Conjugating matrices for eruption and hexagon flows.* In the unipotent locus, the expressions for the holonomies of the matrices simplify significantly, allowing us to make even more computations. The symplectic leaves of $\widehat{\mathfrak{C}}(P)$ correspond to relative character varieties (see Lemma 4.6), which themselves are subsets of $\mathscr{X}_3(P)$ where the holonomies of the peripheral elements are in fixed chosen conjugacy classes. Since $\pi_1(P)$ is generated by the peripheral elements α, β and γ and the flows remain in a symplectic leaf, the flows must be realized by a conjugation of the peripheral elements. In Theorem 6.11 we find matrices $\zeta_t^\alpha, \zeta_t^\beta, \zeta_t^\gamma$ in $\mathsf{PSL}(3,\mathbb{R})$ such that the flow of representations

$$\rho_t = \begin{cases} \alpha \mapsto \zeta_t^\alpha \rho(\alpha)(\zeta_t^\alpha)^{-1} \\ \beta \mapsto \zeta_t^\beta \rho(\beta)(\zeta_t^\beta)^{-1} \\ \gamma \mapsto \zeta_t^\gamma \rho(\gamma)(\zeta_t^\gamma)^{-1} \end{cases}$$

covers the holonomies of the eruption flow on the unipotent locus $\mathfrak{U}$. Since ρ_t are representations of the fundamental group of the pair of pants, the above matrices are a solution to

$$\zeta_t^\alpha \rho(\alpha)(\zeta_t^\alpha)^{-1} \zeta_t^\beta \rho(\beta)(\zeta_t^\beta)^{-1} \zeta_t^\gamma \rho(\gamma)(\zeta_t^\gamma)^{-1} = \mathsf{id}.$$

This is a particular instance of a solution to the *Deligne–Simpson problem* [Kos04] and is also solved in our particular case in [KO24, Section 4.2]. Similarly, we describe in Theorem 6.12 the hexagon flow in terms of conjugations of the peripheral elements.

1.3. **Questions.** In this article we only address very specific self–intersecting curves and as mentioned above, our methods rely on explicit computations. We may therefore ask the following

Question 1.3. Let c be a filling curve (equivalently a self–intersecting curve) in the pair of pants P. Is every orbit of the Hamiltonian flow of tr_c restricted to a symplectic leaf $\mathcal{Q} \subset \widehat{\mathfrak{C}}(P)$ periodic with a unique fixed point?

An important fact used to prove Theorem A and Theorem D is that the symplectic leaves all have dimension two. This is a consequence of the topology of the surfaces we work with. This then motivates the following

Question 1.4. Let c be a filling curve in a surface S with negative Euler characteristic. Do there exist periodic orbits of the Hamiltonian flow of tr_c restricted to a symplectic leaf $\mathcal{Q} \subset \widehat{\mathfrak{C}}(S)$?

We may ask the same question when considering length functions on the Teichmüller space $\mathcal{T}_L(S)$. In this case, the length function of any filling curve is proper and there is a unique minimum. The above question therefore only asks if there exist periodic orbits (outside of the minimum).

1.4. **Brief explanation for the Mathematica code.** Most of the results in this article are aided by computations done with Mathematica, and plots made using Python. The code can be downloaded here https://github.com/CamachoCadena/Periodic-orbits-of-Hamiltonian-flows.git.

In order to run the Mathematica code, all sections must be run in the order they appear. The code is adapted so that it can take in different inputs; therefore not all the equations

in this article will appear as output of the code. Rather, the user must run the appropriate sections of the code, potentially giving inputs themselves, so that the desired output is shown. Throughout the article, we will explain which sections are necessary to run. The sections in the code are numbered, and we briefly explain their contents and where they are used.

(a) *Fock–Goncharov's reconstruction of the holonomy through coordinates:* From the construction recalled in Section 3.2, this section computes the holonomies of the boundary curves as shown in Section 3.4.
(b) *Casimir functions (ratios of eigenvalues):* Computes the ratios of eigenvalues of the boundary curves presented in Lemma 3.3, as well as the Jacobian matrix induced by the Casimir functions used in the proof of Lemma 4.1.
(c) *Parameterization of symplectic leaves:* This is the computation needed in Lemma 4.4.
(d) *Functions on symplectic leaves:* Defines trace functions on the symplectic leaves. The functions are used throughout Sections 5 and 6.
(e) *Hamiltonian vector field:* Computes the Hamiltonian vector field in a symplectic leaf. This is used in Sections 5.4, 6.1 and 6.2.
(f) *Convexity:* Computes second derivatives along different flows and is used in the proof of Theorem 5.4, Proposition 6.4.
(g) *Computations for $\alpha^k\gamma^{-1}$ in the unipotent locus:* Computes second derivatives along different flows used in the proof of Proposition 6.9, as well as the Hamiltonian vector field in Section 6.2.
(h) *Conjugating matrices for the eruption flow:* Verifies Theorem 6.11.
(i) *Conjugating matrices for the hexagon flow:* Verifies Theorem 6.12.

The Python code is used to make plots and find numerical solutions to differential equations, as well as for Remark 5.6. It is not used in any of the proofs.

1.5. **Organization of the article.** In Section 2 we recall some basics in Poisson geometry, cross ratios, and framed convex projective structures. In Section 3 we recall the Fock–Goncharov coordinates and give the matrices of boundary curves of the pair of pants in coordinates. In Section 4 we compute the Poisson structure of $\widehat{\mathfrak{C}}(P)$, find the Casimir functions, parameterize the symplectic leaves, and give a formula for the symplectic form. In Section 5 we prove Theorem A and Corollary B. In Section 6 we focus on the unipotent locus and prove Theorem G, as well as Theorems 6.11 and 6.12.

Acknowledgements. I would like to thank my advisors Anna Wienhard and James Farre for suggesting the problem, suggesting to explore it computationally and for helpful discussions. I would especially like to thank Marit Bobb for explaining and helping me compute the symplectic form on symplectic leaves from the Poisson structure in Section 4.1. Finally, I would like to thank Bill Goldman for suggesting to consider the symmetric trace, Zachary Greenberg for discussions on Fock–Goncharov coordinates, and Tengren Zhang for his remarks on framed representations.

Contents

2. Preliminaries

2.1. **Some Poisson geometry.** Here we follow [CFM21] and [Wei83]. We begin with a definition.

Definition 2.1. A *Poisson manifold* M is a smooth manifold endowed with a *Poisson bracket* $\{\cdot,\cdot\}$ on $C^\infty(M)$.

Given a function $f \in C^\infty(M)$, its *Hamiltonian vector field* is the vector field $\mathsf{H}f \in \Gamma(\mathsf{T}M)$ satisfying

$$dg(\mathsf{H}f) = \{g, f\} \tag{1}$$

for every $g \in C^\infty(M)$. The flow of the Hamiltonian vector field of a function $f \in C^\infty(M)$ at time $t \in \mathbb{R}$ is denoted by $\Phi_f^t \colon M \to M$.

Lemma 2.2. *Let $f, g \in C^\infty(M)$ and assume that there is a constant $c \in \mathbb{R}$ such that $\{f, g\} \equiv c$. Then the Hamiltonian vector fields $\mathsf{H}f$ and $\mathsf{H}g$ commute.*

Proof. Since $\{f, g\} \equiv c$, it follows that $\mathsf{H}\{f, g\} \equiv 0$. Then by the fact that $\mathsf{H}\{f, g\} = [\mathsf{H}_f, \mathsf{H}_g]$ (see for example [CdS01, Section 18.3]), the lemma follows. □

The Poisson bracket defines a *cosymplectic structure*, which is a map $\omega^\vee \colon \Omega^1(M) \times \Omega^1(M) \to C^\infty(M)$ given locally by

$$\omega^\vee(dx, dy) = \{x, y\},$$

for local coordinates x, y on M. The *radical* of the cosymplectic structure is the subspace

$$\mathsf{Rad}(\omega^\vee) \coloneqq \{\alpha \in \Omega^1(M) : \omega^\vee(\alpha, \cdot) \equiv 0\}.$$

The dimension of the fibers of $\Omega^1(M)/\mathsf{Rad}(\omega^\vee)$ is called the *rank* of the Poisson structure.

Definition 2.3. A *Casimir function* is a function $f \in C^\infty(M)$ such that

$$\{f, g\} = 0$$

for every $g \in C^\infty(M)$. The set of Casimir functions forms a ring, denoted by $\mathscr{C}(M)$.

From the cosymplectic form, we obtain a map

$$[\omega^\vee] \colon \Omega^1(M)/\mathsf{Rad}(\omega^\vee) \to \Gamma(\mathsf{T}M)$$

defined by

$$\beta([\omega^\vee]([\alpha])) = \omega^\vee(\alpha, \beta)$$

for any $\alpha, \beta \in \Omega^1(M)$.

The image of the map $[\omega^\vee]$ is given by

$$\{X \in \Gamma(\mathsf{T}M) : \ \beta(X) \equiv 0 \quad \text{for every } \beta \in \mathsf{Rad}(\omega^\vee)\}, \tag{2}$$

and vector fields in the image of $[\omega^\vee]$ are generated by Hamiltonian vector fields.

An *orbit* in a Poisson manifold is an equivalence class $\mathcal{Q} \subseteq M$ given by the following relation. Two points $p, q \in M$ are equivalent if there exist functions $f_1, \dots, f_k \in C^\infty(M)$ such that

$$\Phi^1_{f_1} \circ \cdots \circ \Phi^1_{f_k}(p) = q.$$

It is a classical result that orbits in Poisson manifolds are symplectic submanifolds, whose symplectic structure is inherited by the Poisson structure, see for example [CFM21, Theorem 4.1].

Definition 2.4. A *symplectic leaf* of a Poisson manifold is a pair $(\mathcal{Q}, \omega_\mathcal{Q})$, where $\mathcal{Q}$ is an orbit, and $\omega_\mathcal{Q}$ is the induced symplectic structure. The *symplectic foliation* of M is the collection of symplectic leaves

$$\mathscr{L} = \{(\mathcal{Q}, \omega_\mathcal{Q}) : \ \mathcal{Q} \text{ is a symplectic leaf}\}.$$

Remark 2.5. In the special case when the rank of the Poisson structure is constant, a symplectic leaf is the common level set of the Casimir functions. This result is due to Weinstein in [Wei83, pp. 529].

Since the symplectic leaves are orbits, we give the following standard definition, in which we abuse nomenclature.

Definition 2.6. A collection of functions $\{f_1, \dots, f_k\} \subset C^\infty(M)$ whose Hamiltonian flows generate every symplectic leaf in $\mathscr{L}$ are called the *Hamiltonians* of the Poisson structure.

2.2. **The full flag variety and invariants of flags.** Here we describe the full flag variety of $\mathbb{R}^3$ and, following [FG06, FG07], give definitions of cross ratios and triple ratios. These are later used in Section 3.1 to describe Fock and Goncharov's parameterization of framed positive representations.

The *(full) flag variety of* $\mathbb{R}^3$, denoted by $\mathscr{F}$, is the space of tuples $(p, \ell) \in \mathbb{RP}^2 \times (\mathbb{RP}^2)^*$ such that $\ell(p) = 0$. We say that two of flags (p_1, ℓ_1) and (p_2, ℓ_2) are *transverse* or *in generic position* if $\ell_1(p_2) \neq 0 \neq \ell_2(p_1)$. With this, define $\mathscr{F}_n$ to be the set of ordered n–tuples of flags that are pairwise transverse.

The kernel of a projective class of a linear functional defines a projective line in $\mathbb{RP}^2$. If $(p, \ell) \in \mathscr{F}$, then this means that p is contained in the projective line defined by ℓ. Throughout, we will not make a distinction between projective classes of linear functionals, which we write as row vectors, and projective lines.

Given any four pairwise distinct projective lines $\ell_1, \ell_2, \ell_3, \ell_4$ in $\mathbb{RP}^2$ that go through a point $p \in \mathbb{RP}^2$, we can define their *cross ratio*. Namely, we take another projective line

h which intersects $\ell_1, \dots, \ell_4$ at distinct points $p_1, \dots, p_4$ respectively, and that are not equal to p. Then take any identification of h with $\mathbb{RP}^1 \cong \mathbb{R} \cup \{\infty\}$ sending p_i to x_i. The cross ratio of $(\ell_1, \dots, \ell_4)$ is

$$\mathsf{cr}(\ell_1, \dots, \ell_4) \coloneqq \frac{(x_1 - x_2)(x_3 - x_4)}{(x_1 - x_4)(x_2 - x_3)}.$$

This convention for the cross ratio is the one such that $\mathsf{cr}(\infty, -1, 0, x_4) = x_4$. The cross ratio is a projective invariant, meaning that if $g \in \mathsf{PSL}(3, \mathbb{R})$, then $\mathsf{cr}(g \cdot \ell_1, g \cdot \ell_2, g \cdot \ell_3, g \cdot \ell_4) = \mathsf{cr}(\ell_1, \dots, \ell_4)$.

The cross ratio on projective lines is used to define projective invariants of generic 4–tuples of flags. For two distinct points $p, q \in \mathbb{RP}^2$, let $\overline{pq}$ be the projective line containing p and q.

Definition 2.7. Let $(F_1, F_2, F_3, F_4) = ((p_1, \ell_1), (p_2, \ell_2), (p_3, \ell_3), (p_4, \ell_4)) \in \mathscr{F}_4$. Let

$$\mathsf{cr}_1(F_1, F_2, F_3, F_4) \coloneqq -\frac{\ell_1(p_2)(\overline{p_1p_3})(p_4)}{\ell_1(p_4)(\overline{p_1p_3})(p_2)}, \tag{3}$$

$$\mathsf{cr}_2(F_1, F_2, F_3, F_4) \coloneqq -\frac{\ell_3(p_4)(\overline{p_1p_3})(p_2)}{\ell_3(p_2)(\overline{p_1p_3})(p_4)}. \tag{4}$$

These cross ratios can also be defined geometrically as follows.

Lemma 2.8. *Let* $(F_1, F_2, F_3, F_4) = ((p_1, \ell_1), (p_2, \ell_2), (p_3, \ell_3), (p_4, \ell_4)) \in \mathscr{F}_4$. *Then*

$$\mathsf{cr}(\ell_1, \overline{p_1p_2}, \overline{p_1p_3}, \overline{p_1p_4}) = \mathsf{cr}_1(F_1, F_2, F_3, F_4),$$
$$\mathsf{cr}(\ell_3, \overline{p_3p_4}, \overline{p_3p_1}, \overline{p_3p_2}) = \mathsf{cr}_2(F_1, F_2, F_3, F_4).$$

Note the lines $\ell_1, \overline{p_1p_2}, \overline{p_1p_3}, \overline{p_1p_4}$ all pass through p_1 and hence it makes sense to compute their cross ratio. The expressions on the left hand–side of the lemma are the invariants used by Fock and Goncharov in [FG07], and the lemma is included to give the formula for the cross ratios without having to pick identifications with $\mathbb{RP}^1$ (similarly to the invariants defined in [BD17]). As we will not use this lemma in the article, its proof is delayed to Appendix B. Up to a sign, these are the cross ratios used in [WZ18] to parameterize the space of convex projective structures on a surface.

Another invariant of flags is the triple ratio.

Definition 2.9. Let $(F_1, F_2, F_3) = ((p_1, \ell_1), (p_2, \ell_2), (p_3, \ell_3)) \in \mathscr{F}_3$. The *triple ratio* of these flags is given by

$$\mathsf{T}(F_1, F_2, F_3) = \frac{\ell_1(p_2)\ell_2(p_3)\ell_3(p_1)}{\ell_1(p_3)\ell_2(p_1)\ell_3(p_2)}.$$

The triple ratio is also invariant under the $\mathsf{PSL}(3, \mathbb{R})$ action, that is, for every $g \in \mathsf{PSL}(3, \mathbb{R})$ and $(F_1, F_2, F_3) \in \mathscr{F}_3$,

$$\mathsf{T}(g \cdot F_1, g \cdot F_2, g \cdot F_3) = \mathsf{T}(F_1, F_2, F_3).$$

2.3. **Convex projective structures on surfaces and framings.** In this section, we recall the notion of $\mathbb{RP}^2$ surfaces and their corresponding deformation spaces from [Gol90] and also following [LZ21]. Throughout, S is a closed surface with $n \geq 1$ boundary components. Denote the boundary loops by $c_1, \ldots, c_n \in \pi_1(S)$. Such loops are called *peripheral loops*.

Definition 2.10. An $\mathbb{RP}^2$ *surface* Σ is a smooth surface with boundary with a maximal collection of charts $\{\psi_\alpha \colon U_\alpha \to \mathbb{RP}^2\}_\alpha$ such that

- Each $U_\alpha \subset \Sigma$ is a connected, simply connected open subset of the interior of Σ.
- For any ψ_α, ψ_β with $U_\alpha \cap U_\beta \neq \emptyset$, the map $\psi_\alpha \circ \psi_\beta^{-1} \colon U_\alpha \cap U_\beta \to \psi_\alpha(U_\alpha \cap U_\beta)$ is the restriction of a projective transformation of $\mathbb{RP}^2$.

Let Σ and Σ' be two $\mathbb{RP}^2$ surfaces with atlases $\{\psi_\alpha\}_\alpha$ and $\{\psi'_\beta\}_\beta$ respectively. A diffeomorphism $f \colon \Sigma \to \Sigma'$ is called a *projective isomorphism* if for any U_α and U'_β such that $f(U_\alpha) \cap U_\beta \neq \emptyset$, the following map

$$\psi'_\beta \circ f \circ \psi_\alpha^{-1} \colon \psi_\alpha(U_\alpha \cap f^{-1}(U'_\beta)) \to \psi'_\beta(f(U_\alpha) \cap U_\beta)$$

is the restriction of a projective map on $\mathbb{RP}^2$ on each connected component.

The universal cover $\widetilde{\Sigma}$ of Σ is also an $\mathbb{RP}^2$ surface. And hence, by Theorem 2.2 in [Gol90], there exists a smooth map $\mathsf{dev}_\Sigma \colon \widetilde{\Sigma} \to \mathbb{RP}^2$, and a representation $\rho_\Sigma \colon \pi_1(\Sigma) \to \mathsf{PSL}(3, \mathbb{R})$ such that the following diagram

$$\begin{array}{ccc} \widetilde{\Sigma} & \xrightarrow{\mathsf{dev}_\Sigma} & \mathbb{RP}^2 \\ {\scriptstyle\gamma}\downarrow & & \downarrow{\scriptstyle\rho_\Sigma(\gamma)} \\ \widetilde{\Sigma} & \xrightarrow{\mathsf{dev}_\Sigma} & \mathbb{RP}^2 \end{array}$$

commutes for every $\gamma \in \pi_1(\Sigma)$. The map dev_Σ is called a *developing map*, and ρ_Σ the *holonomy*; together, the pair $(\mathsf{dev}_\Sigma, \rho_\Sigma)$ is called a *developing pair* for Σ. Moreover, if $(\mathsf{dev}'_\Sigma, \rho'_\Sigma)$ is another developing pair for Σ, there exists an element $g \in \mathsf{PSL}(3, \mathbb{R})$ such that

$$(\mathsf{dev}'_\Sigma, \rho'_\Sigma) = (g \cdot \mathsf{dev}_\Sigma, g \cdot \rho_\Sigma \cdot g^{-1}).$$

We now focus on a particular class of $\mathbb{RP}^2$ surfaces.

Definition 2.11.

- A *properly convex domain* $\Omega \subset \mathbb{RP}^2$ is an open subset whose closure does not contain any projective lines, and for any distinct $p, q \in \Omega$, there is a projective line segment connecting p and q and that is completely contained in Ω.
- A connected $\mathbb{RP}^2$ surface is *convex* if some developing map of Σ is a diffeomorphism onto a properly convex domain in $\mathbb{RP}^2$ and it extends to the boundary. Moreover, we require that the development map sends boundary components to either points or line segments. If a boundary component is sent to a point, it is said to *cuspidal*.

Definition 2.12. The *deformation space of convex projective structures on S* is

$$\mathfrak{C}(S) \coloneqq \left\{ \begin{array}{l} (f,\Sigma) : \ \Sigma \text{ is a convex } \mathbb{RP}^2 \text{ surface} \\ \text{and } f\colon S \to \Sigma \text{ is a diffeomorphism} \end{array} \right\} / \sim \tag{5}$$

where $(f_1,\Sigma_1) \sim (f_2,\Sigma_2)$ if $f_1 \circ f_2^{-1}\colon \Sigma_2 \to \Sigma_1$ is homotopic to a projective isomorphism from Σ_2 to Σ_1. An equivalence class $[f,\Sigma] \in \mathfrak{C}(S)$ is then called a *(marked) convex projective structure on S*.

The holonomy of an $\mathbb{RP}^2$ surface provides a map

$$\mathsf{hol}\colon \mathfrak{C}(S) \to \mathscr{X}_3(S) \coloneqq \mathsf{Hom}(\pi_1(S), \mathsf{PSL}(3,\mathbb{R})) /\!\!/ \mathsf{PSL}(3,\mathbb{R})$$

as follows. Given a pair $(f,\Sigma) \in \mathfrak{C}(S)$, we obtain, up to conjugation, a representation $\rho_\Sigma\colon \pi_1(\Sigma) \to \mathsf{PSL}(3,\mathbb{R})$ and hence a representation $f^*\rho_\Sigma\colon \pi_1(S) \to \mathsf{PSL}(3,\mathbb{R})$. Moreover, if two pairs (f,Σ) and (f',Σ') are equivalent, then the corresponding representations also differ by a conjugation. We denote the image of hol by $\mathscr{X}_3^+(S)$.

In order to describe Fock–Goncharov coordinates, we need to have additional data on a convex projective structure, which is a framing. Recall that the boundary curves of S are denoted by $c_i \in \pi_1(S)$ for $i = 1,\dots,n$.

Definition 2.13. A *framed representation* is a tuple $(\rho, F_1,\dots,F_n)$, where $\rho\colon \pi_1(S) \to \mathsf{PSL}(3,\mathbb{R})$ is a representation, and $F_1,\dots,F_n \in \mathscr{F}$ are flags such that $\rho(c_i)\cdot F_i = F_i$ for $i = 1,\dots,n$. The quotient of the space of framed representations by $\mathsf{PSL}(3,\mathbb{R})$ will be written as $\widehat{\mathscr{X}_3}(S)$.

Definition 2.14. A *framed convex projective structure on S* is a triple $[f,\Sigma,\nu]$, where $[f,\Sigma]$ is convex projective structure on S and ν is a framing of the holonomy representation. The space of framed convex $\mathbb{RP}^2$ structures on S is denoted by $\widehat{\mathfrak{C}}(S)$.

Fock and Goncharov provide a map

$$\widehat{\mathsf{hol}}\colon \widehat{\mathfrak{C}}(S) \to \widehat{\mathscr{X}_3}(S).$$

in [FG07, Theorem 2.5] in which they assign a framing to the holonomy representations of a convex projective structure. We do not describe the map here, and simply use its existence.

Definition 2.15. [FG07] The image $\widehat{\mathsf{hol}}\left(\widehat{\mathfrak{C}}(S)\right) \subset \widehat{\mathscr{X}_3}(S)$ will be denoted by $\widehat{\mathscr{X}_3^+}(S)$, and is known as the space of *positive framed representations*.

There is a natural map

$$\begin{aligned} \mu\colon \widehat{\mathscr{X}_3^+}(S) &\to \mathscr{X}_3^+(S) \\ [(\rho, F_1,\dots,F_n)] &\mapsto [\rho] \end{aligned}$$

which forgets the framing. This map is a ramified $2^n\colon 1$ cover [FG07, FG06] (see also [Pal13]). The map ramifies over those representations where at least one of the $\rho(c_i)$ fixes fewer than 6 flags, namely when $\rho(c_i)$ does not have 3 distinct positive eigenvalues.

The space of positive representations is foliated itself by the following subsets. Recall that $c_1,\dots,c_n \in \pi_1(S)$ are the peripheral elements.

Definition 2.16. Let $\mathcal{C} = (C_1, \dots, C_n)$ be a tuple of conjugacy classes in $\mathsf{PSL}(3,\mathbb{R})$. The *relative character variety* associated to $\mathcal{C}$ is the subspace of the space of positive representations given by

$$\mathscr{X}^+_{3,\mathcal{C}}(S) := \{[\rho] \in \mathscr{X}^+_3(S) : \ \rho(c_i) \in C_i \text{ for all } i = 1, \dots, n\}.$$

Remark 2.17. The relative character varieties are naturally equipped with a symplectic structure [Gol84, GHJW97]. We do not describe the symplectic structure here, as, up to a constant, the symplectic structure coincides with the symplectic structure from the symplectic leaves of $\widehat{\mathfrak{C}}(S)$ through the map $\mu \circ \widehat{\mathsf{hol}}$ [FG07, Section 5],[Sun21]. Using the Fock–Goncharov coordinates which we recall in Section 3.1, we describe the symplectic structure on the symplectic leaves explicitly in the case when S is a pair of pants.

3. Fock–Goncharov coordinates

Let S be a surface of genus g with $n \geq 1$ boundary components so that $2g - 2 + n > 0$. Here we recall the Fock–Goncharov coordinates for framed convex projective structures. In the construction of Fock and Goncharov, a surface with punctures is required. Their construction is combinatorial and we therefore interpret the boundary of our surfaces as punctures by shrinking them to points. **We stress that whenever we refer to (framed) convex projective structures, S has boundary components. Whenever we work with Fock–Goncharov coordinates, we interpret the boundaries as punctures. This is the same convention used in [FG07].**

We will describe the coordinates, explain how to reconstruct a representation from the coordinates, the Poisson structure, and give explicit matrices for the generators of the fundamental group of the pair of pants. The content of this section recalls constructions and results from [FG07] (and more generally [FG06]) and includes more explicit computations that allow us to derive the results of this article. To see another overview of the Fock–Goncharov results, see [CTT20, Pal13].

3.1. **The coordinates.** In the first step, we interpret the boundary components of S as punctures. Begin by taking an *ideal triangulation* $\mathscr{T}$ of S, meaning a triangulation of S with vertices at the punctures. The triangulation consists of $2\,|\chi(S)|$ ideal triangles and $6g + 3n - 6$ edges.

Fock and Goncharov define an isomorphism

$$\varphi_{\mathscr{T}} : \widehat{\mathfrak{C}}(S) \to \mathbb{R}^{16g-16+8n}_{>0}$$

in [FG07, Theorem 2.5] giving coordinates on the space of framed convex projective structures. The map is defined as follows. First lift the triangulation $\mathscr{T}$ to a triangulation $\widetilde{\mathscr{T}}$ of the universal cover $\widetilde{S}$. Let $[f, \Sigma, \nu] \in \widehat{\mathfrak{C}}(S)$ and let dev_Σ be a developing map for (f, Σ). We describe the two types of inavariants associated to a framed convex projective structure.

The first is a cross ratio associated to edges of the triangulation. Let E be an edge of the triangulation $\mathscr{T}$ with vertices $p_{\mathsf{E},1}$ and $p_{\mathsf{E},2}$. The edge E has two triangles $\triangle_1$ and $\triangle_2$ on either side with vertices $\{p_{\mathsf{E},1}, p_{\mathsf{E},2}, p_{\triangle,1}\}$ and $\{p_{\mathsf{E},1}, p_{\mathsf{E},2}, p_{\triangle,2}\}$ respectively. Take

lifts $\{\widetilde{p}_{\mathsf{E},1}, \widetilde{p}_{\mathsf{E},2}, \widetilde{p}_{\triangle,1}, \widetilde{p}_{\triangle,2}\}$ of the four points $\{p_{\mathsf{E},1}, p_{\mathsf{E},2}, p_{\triangle,1}, p_{\triangle,2}\}$ to the universal cover so that $\{\widetilde{p}_{\mathsf{E},1}, \widetilde{p}_{\mathsf{E},2}, \widetilde{p}_{\triangle,1}\}$ are endpoints of a single lift $\widetilde{\triangle}_1$ of $\triangle_1$, $\{\widetilde{p}_{\mathsf{E},1}, \widetilde{p}_{\mathsf{E},2}, \widetilde{p}_{\triangle,2}\}$ are endpoints of a single lift $\widetilde{\triangle}_2$ of $\triangle_2$, and so that these lifts of the ideal triangles share the edge $\widetilde{\mathsf{E}}$ with lifts of the endpoints $\{\widetilde{p}_{\mathsf{E},1}, \widetilde{p}_{\mathsf{E},2}\}$. See Figure 4 for this setup. Up to renaming the points, we may choose an ordering of the lifts $\{\widetilde{p}_{\mathsf{E},1}, \widetilde{p}_{\mathsf{E},2}, \widetilde{p}_{\triangle,1}, \widetilde{p}_{\triangle,2}\}$ such that

$$\widetilde{p}_{\mathsf{E},1} \prec \widetilde{p}_{\triangle,1} \prec \widetilde{p}_{\mathsf{E},2} \prec \widetilde{p}_{\triangle,2} \prec \widetilde{p}_{\mathsf{E},1},$$

where $\prec$ denotes the counterclockwise ordering on the circle.

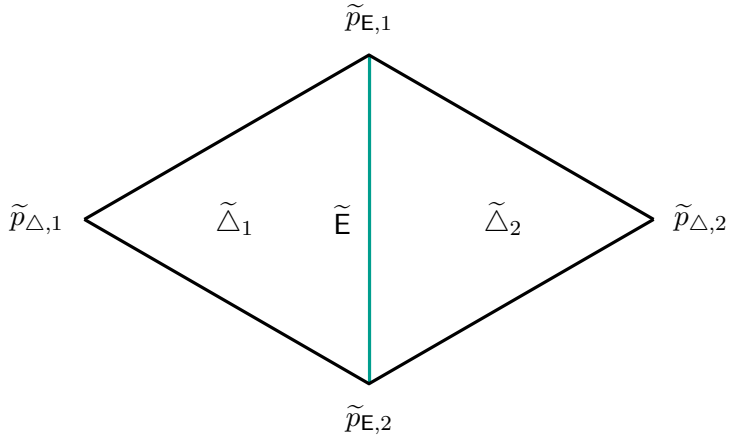

FIGURE 4. Computing edge invariants.

Through the developing map dev_Σ and the assignment of a framed representation, we obtain for each of the vertices, flags $F_{\mathsf{E},1}, F_{\triangle,1}, F_{\mathsf{E},2}, F_{\triangle,2} \in \mathscr{F}$ respectively. Now we can define the coordinates

$$\sigma^1_{\mathsf{E}}([f,\Sigma,\nu]) \coloneqq \mathsf{cr}_1(F_{\mathsf{E},1}, F_{\triangle,1}, F_{\mathsf{E},2}, F_{\triangle,2})$$
$$\sigma^2_{\mathsf{E}}([f,\Sigma,\nu]) \coloneqq \mathsf{cr}_2(F_{\mathsf{E},1}, F_{\triangle,1}, F_{\mathsf{E},2}, F_{\triangle,2})$$

The second type of coordinate is the triple ratio associated to ideal triangles. Let $\triangle$ be an ideal triangle in $\mathscr{T}$ with vertices p_1, p_2, p_3. Take lifts $\{\widetilde{p}_1, \widetilde{p}_2, \widetilde{p}_3\}$ of the three vertices to the universal cover such that $\{\widetilde{p}_1, \widetilde{p}_2, \widetilde{p}_3\}$ are vertices of a lift of $\triangle$. Up to renaming, assume that the vertices are ordered such that $\widetilde{p}_1 \prec \widetilde{p}_2 \prec \widetilde{p}_3 \prec \widetilde{p}_1$. Similarly as above, the developing map dev_Σ together with the associated framing, we obtain three flags $F_1, F_2, F_3 \in \mathscr{F}$. Then let

$$\tau_\triangle([f,\Sigma,\nu]) \coloneqq \mathsf{T}(F_1, F_2, F_3).$$

The map $\varphi_{\mathscr{T}}$ is then defined as

$$[f,\Sigma]_\nu \mapsto \left(\left(\sigma^1_{\mathsf{E}}([f,\Sigma,\nu]), \sigma^2_{\mathsf{E}}([f,\Sigma,\nu])\right)_{\mathsf{E}}, (\tau_\triangle([f,\Sigma,\nu]))_\triangle\right)$$

as the edges E and triangles $\triangle$ vary in the triangulation $\mathscr{T}$. The fact that all of these coordinates are positive is the content of Lemma 2.3 and Lemma 2.4 in [FG07].

Remark 3.1. We stress here that these coordinates, although closely related to the Bonahon–Dreyer coordinates in [BD17] for closed surfaces, are not exactly the same coordinates. The difference lies in that the cross ratios and triple ratios are taken with respect to slightly different tuples of flags. This becomes evident in the computation of the holonomies, where we observe that the Bonahon–Dreyer closed leaf inequalities have a slightly different form.

3.2. **Reconstructing the representation from coordinates.** Recall that there is a natural map

$$\widehat{\mathscr{X}_3^+}(S) := \widehat{\mathsf{hol}}\left(\widehat{\mathfrak{C}}(S)\right) \to \mathscr{X}_3^+(S)$$

which simply forgets the framing. In particular, there is a map

$$\vartheta\colon \widehat{\mathfrak{C}}(S) \to \mathscr{X}_3^+(S)$$

which factors through the holonomy map $\widehat{\mathsf{hol}}$. In this section, we describe how to obtain a representation (up to conjugation) from coordinates, as described in [FG07, Section 5]. Fix an ideal triangulation $\mathscr{T}$ of S (after shrinking the boundaries to punctures).

We begin by constructing an embedded quiver $\mathsf{Q}_{\mathscr{T}}$ on S as follows:

- On the interior of each edge E of the triangulation, place two distinct vertices $v_{\mathsf{E},1}$ and $v_{\mathsf{E},2}$.
- On the interior of each ideal triangle $\triangle$, place an additional vertex $v_{\triangle}$.
- On an ideal triangle $\triangle$, place three 3–cycles as in Figure 5.

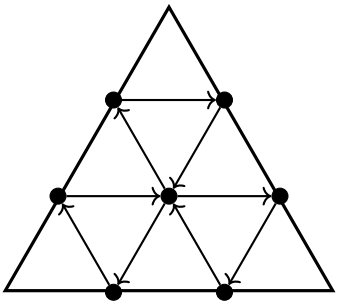

FIGURE 5. Quiver embedded in an ideal triangle.

Each vertex in the quiver $\mathsf{Q}_{\mathscr{T}}$ is itself a coordinate function as follows. For each vertex $v_{\triangle}$, we assign the coordinate function $\tau_{\triangle}$. For an edge E with vertices $p_{\mathsf{E},1}, p_{\mathsf{E},2}$ (the vertices here being the punctures of the surface), let $\{\widetilde{p}_{\mathsf{E},1}, \widetilde{p}_{\mathsf{E},2}, \widetilde{p}_{\triangle,1}, \widetilde{p}_{\triangle,2}\}$ be the vertices of the lifts of the endpoints of the two triangles sharing the edge E as in Section 3.1. Up to renaming, we may assume that the vertex $v_{\mathsf{E},1}$ is the one closest to $p_{\mathsf{E},1}$. Then assign to the vertex $v_{\mathsf{E},i}$ the coordinate function σ^i_{E} whenever $\widetilde{p}_{\mathsf{E},1} \prec \widetilde{p}_{\triangle,1} \prec \widetilde{p}_{\mathsf{E},2} \prec \widetilde{p}_{\triangle,2} \prec \widetilde{p}_{\mathsf{E},1}$.

With the quiver $\mathsf{Q}_{\mathscr{T}}$ and the coordinate functions on the vertices, construct a new oriented graph $\Gamma = (V, E)$ on the surface as follows:

- Place three vertices in the interior of each triangle $\triangle$ of the triangulation $\mathscr{T}$ and create a counterclockwise 3–cycle connecting the vertices.

- For a given edge E of the triangulation, place an edge (with an arbitrary orientation), connecting the vertices of Γ closest to the edge E.

The graph Γ is shown in Figure 6 for two adjacent ideal triangles.

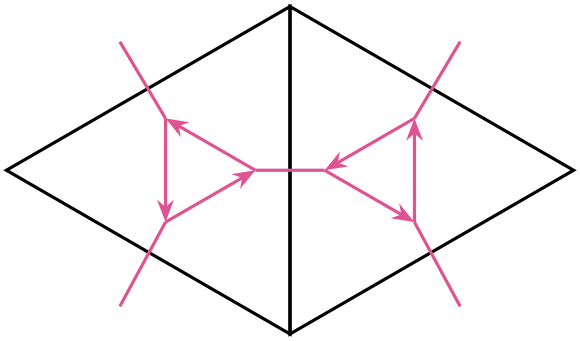

FIGURE 6. A portion of the graph Γ used to reconstruct the holonomy from the Fock–Goncharov coordinates.

For $x, z, w > 0$, define the following matrices in $\mathsf{PSL}(3,\mathbb{R})$:

$$T(x) \coloneqq \frac{1}{x^{1/3}}\begin{bmatrix} 0 & 0 & 1 \\ 0 & -1 & -1 \\ x & 1+x & 1 \end{bmatrix}, \quad E(z,w) \coloneqq \frac{z^{1/3}}{w^{1/3}}\begin{bmatrix} 0 & 0 & \frac{1}{z} \\ 0 & -1 & 0 \\ w & 0 & 0 \end{bmatrix}.$$

Now we are ready to describe the map ϑ. Let $[f,\Sigma,\nu] \in \widehat{\mathfrak{C}}(S)$ with its corresponding coordinates given by $\varphi_{\mathscr{T}}$. Consider the lift $\widetilde{\Gamma}$ of Γ to the universal cover $\widetilde{S}$ and fix a vertex p of $\widetilde{\Gamma}$. For a curve $\alpha \in \pi_1(S)$, we describe the holonomy $\vartheta([f,\Sigma,\nu])(\alpha)$ (we abuse notation here picking a representative in the equivalence class of representations). Lift α to a curve $\widetilde{\alpha} \subset \widetilde{S}$ starting at the point p and homotope it (relative endpoints) so that it lies on the graph $\widetilde{\Gamma}$[1]. The endpoint of this path is $\alpha \cdot p$ (interpreting α as a deck transformation). The holonomy $\vartheta([f,\Sigma,\nu])(\alpha)$ is the following product in the matrices $T(x)$ and $E(z,w)$. Every time the curve $\widetilde{\alpha}$ goes through an edge in $\widetilde{\Gamma}$ internal to a triangle $\triangle$, multiply with the matrix $T(\tau_{\triangle}([f,\Sigma,\nu]))^{\varepsilon}$, where $\varepsilon \in \{\pm 1\}$ depending on whether the edge is crossed according to the orientation of $\widetilde{\Gamma}$ or not. Whenever the path $\widetilde{\alpha}$ goes through an edge crossing an edge E of the triangulation, multiply with the matrix $E(\sigma^1_{\mathsf{E}}([f,\Sigma,\nu]), \sigma^2_{\mathsf{E}}([f,\Sigma,\nu]))$ where we assume that the vertex $v_{\mathsf{E},1}$ of the quiver $\mathsf{Q}_{\mathscr{T}}$ lies to the right of the segment of $\widetilde{\alpha}$ crossing E. The matrices are multiplied from left to right as $\widetilde{\alpha}$ traverses edges of $\widetilde{\Gamma}$.

Remark 3.2. Since the coordinates given by $\varphi_{\mathscr{T}}$ are projective invariants, the matrices $T(x)$ and $E(z,w)$ do not depend on the lifts chosen for the triangles or edges.

[1]Here we have chosen a covering $\widetilde{S} \to S$ whose associated group of deck transformations we identify with the fundamental group $\pi_1(S,p)$.

3.3. **The Poisson structure.** Given a triangulation $\mathscr{T}$ and its associated quiver $\mathsf{Q}_{\mathscr{T}}$ as in Section 3.1, the Poisson structure on $\widehat{\mathfrak{C}}(S) \cong \mathbb{R}_{>0}^{16g-16+8n}$ is given as follows. For coordinate functions $X_i, X_j \colon \widehat{\mathfrak{C}}(S) \to \mathbb{R}_{>0}$, their Poisson bracket is given by the function

$$\{X_i, X_j\} = 2\varepsilon_{ij} X_i X_j, \tag{6}$$

where

$$\varepsilon_{ij} = \#\{\text{arrows from } i \text{ to } j\} - \#\{\text{arrows from } j \text{ to } i\}$$

in the quiver $\mathsf{Q}_{\mathscr{T}}$ where the coordinates are thought of as vertices [FG07, Section 5.1].

3.4. **Describing the holonomies for convex projective structures on a pair of pants.** In Section 3.2, we described how Fock and Goncharov reconstruct a representation given their coordinates for a general surface. In this section, we focus on the case when $S = P$ is a pair of pants. Shrinking the boundaries to punctures, we name the punctures p_α, p_β and p_γ and choose generators α, β, γ for the fundamental group $\pi_1(P)$ satisfying the relation $\alpha\beta\gamma = 1$, and each going around the respective puncture. We then pick the ideal triangulation $\mathscr{T}$ of P given by the two triangles $\triangle_1, \triangle_2$ with vertices $p_\alpha, p_\beta, p_\gamma$ each. The associated quiver $\mathsf{Q}_{\mathscr{T}}$ is shown in Figure 7. For the pair of pants, we have the Fock–Goncharov coordinates

$$\begin{aligned} \varphi_{\mathscr{T}} \colon \widehat{\mathfrak{C}}(P) &\to \mathbb{R}^8_{>0} \\ [f, \Sigma, \nu] &\mapsto (\sigma_1, \dots, \sigma_6, \tau_1, \tau_2) \end{aligned}$$

where we renamed the coordinates as in Figure 7 dropping the dependence on the edge and triangle in the notation. Following the construction of the map $\vartheta \colon \widehat{\mathfrak{C}}(P) \to \mathscr{X}_3^+(S)$ in Section 3.2, and following Figure 8, we obtain that an equivalence class $[\rho]$ in the image of ϑ with coming from the coordinates $(\sigma_1, \dots, \sigma_6, \tau_1, \tau_2)$ is given by

$$\begin{aligned} \rho(\alpha) &= E(\sigma_2, \sigma_1) T(\tau_2) E(\sigma_3, \sigma_4) T(\tau_1) \\ &= \begin{bmatrix} \sqrt[3]{\frac{\tau_1^2 \tau_2^2}{\sigma_1 \sigma_2^2 \sigma_3^2 \sigma_4}} & \frac{\sqrt[3]{\frac{\sigma_2\sigma_3}{\sigma_1\sigma_4\tau_1\tau_2}}(\sigma_3\tau_2 + \sigma_3 + \tau_1\tau_2 + \tau_2)}{\sigma_2\sigma_3} & \frac{\sqrt[3]{\frac{\sigma_2\sigma_3}{\sigma_1\sigma_4\tau_1\tau_2}}(\sigma_3(\sigma_4 + \tau_2 + 1) + \tau_2)}{\sigma_2\sigma_3} \\ 0 & \sqrt[3]{\frac{\sigma_2\sigma_3}{\sigma_1\sigma_4\tau_1\tau_2}} & (\sigma_4 + 1)\sqrt[3]{\frac{\sigma_2\sigma_3}{\sigma_1\sigma_4\tau_1\tau_2}} \\ 0 & 0 & \sqrt[3]{\frac{\sigma_1^2\sigma_2\sigma_3\sigma_4^2}{\tau_1\tau_2}} \end{bmatrix}, \\ \rho(\gamma) &= T(\tau_1) E(\sigma_6, \sigma_5) T(\tau_2) E(\sigma_1, \sigma_2) \\ &= \begin{bmatrix} \sqrt[3]{\frac{\sigma_1\sigma_2^2\sigma_5^2\sigma_6}{\tau_1\tau_2}} & 0 & 0 \\ -\sigma_2(\sigma_5 + 1)\sqrt[3]{\frac{\sigma_1\sigma_6}{\sigma_2\sigma_5\tau_1\tau_2}} & \sqrt[3]{\frac{\sigma_1\sigma_6}{\sigma_2\sigma_5\tau_1\tau_2}} & 0 \\ \frac{\sigma_2(\sigma_6(\sigma_5 + \tau_1 + 1) + \tau_1)\sqrt[3]{\frac{\sigma_1\sigma_6}{\sigma_2\sigma_5\tau_1\tau_2}}}{\sigma_6} & -\frac{\sqrt[3]{\frac{\sigma_1\sigma_6}{\sigma_2\sigma_5\tau_1\tau_2}}(\sigma_6(\tau_1+1) + \tau_1(\tau_2+1))}{\sigma_6} & \sqrt[3]{\frac{\tau_1^2\tau_2^2}{\sigma_1^2\sigma_2\sigma_5\sigma_6^2}} \end{bmatrix} \\ \rho(\beta) &= T(\tau_1)^{-1} E(\sigma_4, \sigma_3) T(\tau_2) E(\sigma_5, \sigma_6) T(\tau_1)^{-1}. \end{aligned}$$

The expression for $\rho(\beta)$ is too complicated to fit in one line, so we give it here in terms of its entries:

$$\rho(\beta)_{11} = \frac{\sqrt[3]{\frac{\sigma_4\sigma_5}{\sigma_3\sigma_6\tau_1\tau_2}}\left(\sigma_4\sigma_5\left(\sigma_6\left(\sigma_3+\tau_1+1\right)+\tau_1+1\right)+\tau_1\left(\sigma_5\left(\sigma_6+\tau_2+1\right)+\tau_2\right)\right)}{\sigma_4\sigma_5},$$

$$\rho(\beta)_{12} = \frac{\sqrt[3]{\frac{\sigma_4\sigma_5}{\sigma_3\sigma_6\tau_1^4\tau_2}}\left(\sigma_4\left(\tau_1+1\right)\left(\sigma_6\left(\sigma_3+\tau_1+1\right)+\tau_1\right)+\tau_1\left(\sigma_6\left(\tau_1+1\right)+\tau_1\left(\tau_2+1\right)\right)\right)}{\sigma_4},$$

$$\rho(\beta)_{13} = \frac{\sigma_6\left(\sigma_4\left(\sigma_3+\tau_1+1\right)+\tau_1\right)\sqrt[3]{\frac{\sigma_4\sigma_5}{\sigma_3\sigma_6\tau_1^4\tau_2}}}{\sigma_4},$$

$$\rho(\beta)_{21} = -\frac{\tau_1^{2/3}\left(\sigma_5\left(\sigma_6+\sigma_4\left(\sigma_6+1\right)+\tau_2+1\right)+\tau_2\right)}{\sqrt[3]{\sigma_3\sigma_4^2\sigma_5^2\sigma_6\tau_2}},$$

$$\rho(\beta)_{22} = -\frac{\sqrt[3]{\frac{\sigma_4\sigma_5}{\sigma_3\sigma_6\tau_1\tau_2}}\left(\left(\sigma_4+1\right)\sigma_6\left(\tau_1+1\right)+\tau_1\left(\sigma_4+\tau_2+1\right)\right)}{\sigma_4},$$

$$\rho(\beta)_{23} = -\frac{\left(\sigma_4+1\right)\sigma_6\sqrt[3]{\frac{\sigma_4\sigma_5}{\sigma_3\sigma_6\tau_1\tau_2}}}{\sigma_4},$$

$$\rho(\beta)_{31} = \frac{\tau_1^{2/3}\left(\sigma_5\left(\sigma_6+\tau_2+1\right)+\tau_2\right)}{\sqrt[3]{\sigma_3\sigma_4^2\sigma_5^2\sigma_6\tau_2}},$$

$$\rho(\beta)_{32} = \frac{\sqrt[3]{\frac{\sigma_4\sigma_5}{\sigma_3\sigma_6\tau_1\tau_2}}\left(\sigma_6\left(\tau_1+1\right)+\tau_1\left(\tau_2+1\right)\right)}{\sigma_4},$$

$$\rho(\beta)_{33} = \sqrt[3]{\frac{\sigma_5\sigma_6^2}{\sigma_3\sigma_4^2\tau_1\tau_2}}.$$

The computations are found in Section 1 of the Mathematica code. From a direct computation found in Section 2 of the Mathematica code, we obtain the following.

Lemma 3.3. *Let* $(\sigma_1,\ldots,\sigma_6,\tau_1,\tau_2)\in\widehat{\mathfrak{C}}(P)$. *Then the ratios of pairs of eigenvalues of* $\vartheta(\sigma_1,\ldots,\sigma_6,\tau_1,\tau_2)(\alpha)$ *are given by*

$$\sigma_1\sigma_4 \text{ and } \frac{\tau_1\tau_2}{\sigma_2\sigma_3}.$$

The ratios of pairs of eigenvalues of $\vartheta(\sigma_1,\ldots,\sigma_6,\tau_1,\tau_2)(\beta)$ *are given by*

$$\sigma_3\sigma_6 \text{ and } \frac{\tau_1\tau_2}{\sigma_4\sigma_5}.$$

The ratios of pairs of eigenvalues of $\vartheta(\sigma_1,\ldots,\sigma_6,\tau_1,\tau_2)(\gamma)$ *are given by*

$$\sigma_2\sigma_5 \text{ and } \frac{\tau_1\tau_2}{\sigma_1\sigma_6}.$$

4. The Poisson structure and symplectic leaves for the pair of pants

Here we describe explicitly the Poisson structure, symplectic leaves, Casimir functions, Hamiltonian functions, and flows for the pair of pants P. We also find an explicit parameterization of the symplectic leaves, allowing us to provide a closed–form formula

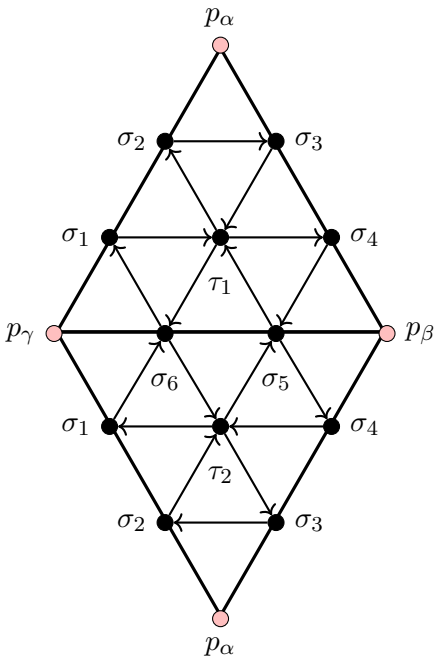

FIGURE 7. Quiver on ideal triangulation of a pair of pants. The top is triangle $\triangle_1$ and the bottom is triangle $\triangle_2$. The gluing pattern can be seen from the identification of the edge invariants. The punctures p_α, p_β and p_γ are drawn in pink.

for the symplectic structure.

4.1. **Poisson structure.** Fix an ideal triangulation $\mathscr{T} = \{\triangle_1, \triangle_2\}$ of P with vertices $p_\alpha, p_\beta, p_\gamma$ as in Section 3.4. Let τ_i denote the triple ratio coordinate for the triangle $\triangle_i$. Then let $\sigma_1, \sigma_2, \ldots, \sigma_6$ be the coordinates on the edges as shown in Figure 7. Using the basis $X_i = \sigma_i$ for $i = 1, \ldots, 6$ and $X_7 = \tau_1, X_8 = \tau_2$, the matrix ε_{ij} from (6) is

$$(\varepsilon_{ij})_{i,j=1,\ldots,8} = \begin{bmatrix} 0 & 0 & 0 & 0 & 0 & 0 & 1 & -1 \\ 0 & 0 & 0 & 0 & 0 & 0 & -1 & 1 \\ 0 & 0 & 0 & 0 & 0 & 0 & 1 & -1 \\ 0 & 0 & 0 & 0 & 0 & 0 & -1 & 1 \\ 0 & 0 & 0 & 0 & 0 & 0 & 1 & -1 \\ 0 & 0 & 0 & 0 & 0 & 0 & -1 & 1 \\ -1 & 1 & -1 & 1 & -1 & 1 & 0 & 0 \\ 1 & -1 & 1 & -1 & 1 & -1 & 0 & 0 \end{bmatrix}. \tag{7}$$

We compute that the radical of the associated cosymplectic structure is given by

$$\begin{aligned} \mathsf{Rad}(\omega^\vee) = \langle &\tau_1 \cdot d\tau_2 + \tau_2 \cdot d\tau_1, \sigma_1 \cdot d\sigma_2 + \sigma_2 \cdot d\sigma_1, \sigma_2 \cdot d\sigma_3 + \sigma_3 \cdot d\sigma_2, \\ &\sigma_3 \cdot d\sigma_4 + \sigma_4 \cdot d\sigma_3, \sigma_5 \cdot d\sigma_6 + \sigma_6 \cdot d\sigma_5 \rangle. \end{aligned}$$

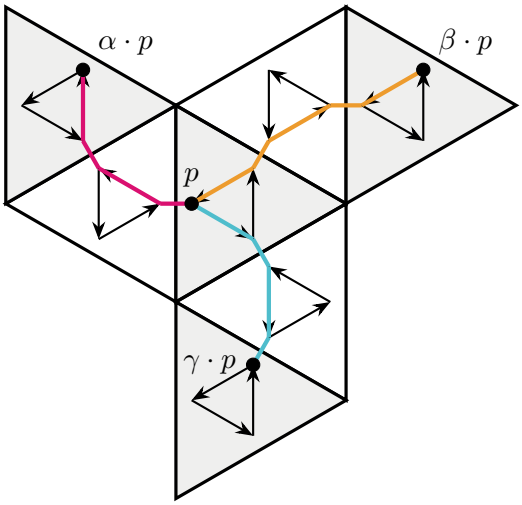

FIGURE 8. Computing the holonomies of the peripheral curves. To avoid a crowded figure, we do not include the labels for the coordinates functions. This figure shows part of the universal cover $\widetilde{P}$. The filled grey triangles correspond to lifts of $\triangle_1$ (whose triangle invariant is τ_1), and the non–filled triangles are lifts of $\triangle_2$. To compute the holonomy, we pick an arbitrary point p in the embedded graph Γ from Figure 6. The pink curve corresponds to a lift of α, the orange curve corresponds to a lift of β, and the teal curve corresponds to a lift of γ. The respective endpoints of the lifts are labeled in the figure.

Since the coordinates are positive, $\mathsf{Rad}(\omega^\vee)$ has constant dimension along $\widehat{\mathfrak{C}}(P)$. In particular by Remark 2.5, the symplectic leaves of $\widehat{\mathfrak{C}}(P)$ are determined by the common level sets of the Casimir functions.

4.2. **Casimir functions and symplectic leaves.** Here we give expressions for the Casimir functions and parameterize the symplectic leaves in terms of their common level sets.

Lemma 4.1. *The ring $\mathscr{C} \subset C^\infty(\widehat{\mathfrak{C}}(P))$ of Casimir functions of $(\widehat{\mathfrak{C}}(P), \{\cdot,\cdot\})$ is generated by the functions*

$$\ell_{\alpha,1} \coloneqq \sigma_1\sigma_4, \qquad \ell_{\alpha,2} \coloneqq \frac{\tau_1\tau_2}{\sigma_2\sigma_3}, \tag{8}$$

$$\ell_{\beta,1} \coloneqq \sigma_3\sigma_6, \qquad \ell_{\beta,2} \coloneqq \frac{\tau_1\tau_2}{\sigma_4\sigma_5}, \tag{9}$$

$$\ell_{\gamma,1} \coloneqq \sigma_2\sigma_5, \qquad \ell_{\gamma,2} \coloneqq \frac{\tau_1\tau_2}{\sigma_1\sigma_6}. \tag{10}$$

Remark 4.2. Note that from Lemma 3.3, the Casimir functions are exactly the eigenvalue ratios of the holonomies of the curves α, β and γ respectively.

Proof. Since the Poisson bracket is bilinear, it is enough to prove that the above functions are Casimir on a basis. By the definition of the Hamiltonian vector field in

(1), we have that for any coordinate function X_i

$$\{\ell_{\alpha,1}, X_i\} = \{\sigma_1\sigma_4, X_i\} = \sigma_1\{\sigma_4, X_i\} + \sigma_4\{\sigma_1, X_i\},$$
$$\{\ell_{\alpha,2}, X_i\} = \left\{\frac{\tau_1\tau_2}{\sigma_2\sigma_3}, X_i\right\} = \frac{\tau_2}{\sigma_2\sigma_3}\{\tau_1, X_i\} + \frac{\tau_1}{\sigma_2\sigma_3}\{\tau_2, X_i\} - \frac{\tau_1\tau_2}{\sigma_2^2\sigma_3}\{\sigma_2, X_i\} - \frac{\tau_1\tau_2}{\sigma_2\sigma_3^2}\{\sigma_3, X_i\},$$
$$\{\ell_{\beta,1}, X_i\} = \{\sigma_3\sigma_6, X_i\} = \sigma_3\{\sigma_6, X_i\} + \sigma_6\{\sigma_3, X_i\},$$
$$\{\ell_{\beta,2}, X_i\} = \left\{\frac{\tau_1\tau_2}{\sigma_4\sigma_5}, X_i\right\} = \frac{\tau_2}{\sigma_4\sigma_5}\{\tau_1, X_i\} + \frac{\tau_1}{\sigma_4\sigma_5}\{\tau_2, X_i\} - \frac{\tau_1\tau_2}{\sigma_4^2\sigma_5}\{\sigma_4, X_i\} - \frac{\tau_1\tau_2}{\sigma_4\sigma_5^2}\{\sigma_5, X_i\},$$
$$\{\ell_{\gamma,1}, X_i\} = \{\sigma_2\sigma_5, X_i\} = \sigma_2\{\sigma_5, X_i\} + \sigma_5\{\sigma_2, X_i\},$$
$$\{\ell_{\gamma,2}, X_i\} = \left\{\frac{\tau_1\tau_2}{\sigma_1\sigma_6}, X_i\right\} = \frac{\tau_2}{\sigma_1\sigma_6}\{\tau_1, X_i\} + \frac{\tau_1}{\sigma_1\sigma_6}\{\tau_2, X_i\} - \frac{\tau_1\tau_2}{\sigma_1^2\sigma_6}\{\sigma_1, X_i\} - \frac{\tau_1\tau_2}{\sigma_1\sigma_6^2}\{\sigma_6, X_i\}.$$

The fact that the functions in the proposition are Casimir then immediately follows from the form of the matrix in (7) defining the Poisson structure.

To see that the functions generate the ring of Casimirs, we observe that the (fibers) of the dimension of the radical $\mathsf{Rad}(\omega^\vee)$ is 6. Hence, we need to show that the Jacobian matrix of the family of functions $\{\ell_{\alpha,1}, \ell_{\alpha,2}, \ell_{\beta,1}, \ell_{\beta,2}, \ell_{\gamma,1}, \ell_{\gamma,2}\}$ always has rank 6. Indeed, we compute in Section 2 of the Mathematica code that the kernel of the Jacobian matrix

$$\left(\frac{\partial f}{\partial X_i}\right)_{\substack{f\in\{\ell_{\alpha,1},\ell_{\alpha,2},\ell_{\beta,1},\ell_{\beta,2},\ell_{\gamma,1},\ell_{\gamma,2}\},\\ X_i\in\{\sigma_1,\ldots,\sigma_6,\tau_1,\tau_2\}}}$$

is given by

$$\left\langle \tau_1\frac{\partial}{\partial\tau_1} - \tau_2\frac{\partial}{\partial\tau_2}, \sum_{i=1}^{6}(-1)^{i+1}\sigma_i\frac{\partial}{\partial\sigma_i}\right\rangle. \tag{11}$$

Since the coordinates are always positive, the rank of the Jacobian matrix is always 6, as desired. □

Remark 4.3. These equations correspond to the *(weak) closed leaf inequalities* of Bonahon–Dreyer in [BD14] (for the pair of pants case, see [LZ21, pp. 27]). One can observe however that the equations themselves look slightly different. This is due to the fact that flags used in the Bonahon–Dreyer coordinates differ from the flags used by Fock–Goncharov (see Remark 3.1).

Lemma 4.4. *Let* $L = (\ell_{\alpha,1}, \ell_{\alpha,2}, \ell_{\beta,1}, \ell_{\beta,2}.\ell_{\gamma,1}, \ell_{\gamma,2}) \in \mathbb{R}^6_{>0}$. *Let*

$$\sigma_{2,L}(\sigma_1, \tau_1) \coloneqq \frac{(\ell_{\alpha,1}\ell_{\beta,2}\ell_{\gamma,1})^{2/3}}{\sigma_1(\ell_{\alpha,2}\ell_{\beta,1}\ell_{\gamma,2})^{1/3}},$$
$$\sigma_{3,L}(\sigma_1, \tau_1) \coloneqq \frac{(\ell_{\beta,1}\ell_{\gamma,2})^{2/3}\sigma_1}{(\ell_{\alpha,1}\ell_{\alpha,2}\ell_{\beta,2}\ell_{\gamma,1})^{1/3}},$$
$$\sigma_{4,L}(\sigma_1, \tau_1) \coloneqq \frac{\ell_{\alpha,1}}{\sigma_1},$$

$$\sigma_{5,L}(\sigma_1,\tau_1) \coloneqq \frac{(\ell_{\alpha,2}\ell_{\beta,1}\ell_{\gamma,1}\ell_{\gamma,2})^{1/3}\sigma_1}{(\ell_{\alpha,1}\ell_{\beta,2})^{2/3}},$$
$$\sigma_{6,L}(\sigma_1,\tau_1) \coloneqq \frac{(\ell_{\alpha,1}\ell_{\alpha,2}\ell_{\beta,1}\ell_{\beta,2}\ell_{\gamma,1})^{1/3}}{\ell_{\gamma,2}^{2/3}\sigma_1},$$
$$\tau_{2,L}(\sigma_1,\tau_1) \coloneqq \frac{(\ell_{\alpha,1}\ell_{\alpha,2}\ell_{\beta,1}\ell_{\beta,2}\ell_{\gamma,1}\ell_{\gamma,2})^{1/3}}{\tau_1}.$$

The symplectic leaf corresponding to L, denoted by $\mathcal{Q}_L$ is given by

$$\mathcal{Q}_L = \{(\sigma_1,\sigma_{2,L},\sigma_{3,L},\sigma_{4,L},\sigma_{5,L},\sigma_{6,L},\tau_1,\tau_{2,L}) \in \widehat{\mathfrak{C}}(P) : \sigma_1,\tau_1 > 0\}.$$

In particular, any symplectic leaf is two–dimensional. In the description of the set, we dropped the dependence of the functions $\sigma_{i,L}$ and $\tau_{2,L}$ for readability.

Proof. The proof is a computation solving for $\sigma_2,\dots,\sigma_6$ and τ_2 in terms of σ_1,τ_1 and the vector L, found in Section 3 of the Mathematica code. □

Definition 4.5. We call a vector $L \in \mathbb{R}^6_{>0}$ that defines a symplectic leaf a *length vector*.

The symplectic leaves in $\widehat{\mathfrak{C}}(P)$ correspond precisely to the relative character varieties in $\mathscr{X}_3^+(P)$ via the map ϑ.

Lemma 4.6. *For any $L \in \mathbb{R}^6_{>0}$, the map*

$$\vartheta\big|_{\mathcal{Q}_L} : \mathcal{Q}_L \to \mathscr{X}^+_{3,\mathcal{C}}(P)$$

is an isomorphism.

To prove this lemma, we need the following result due to Marquis.

Theorem 4.7. [Mar10] *Let $[\rho] \in \mathscr{X}_3^+(S)$. If γ is a peripheral element, then the conjugacy class of $\rho(\gamma)$ has to contain*

$$\begin{pmatrix}1&1&0\\0&1&1\\0&0&1\end{pmatrix}, \begin{pmatrix}\lambda_1&0&0\\0&\lambda_2&1\\0&0&\lambda_2\end{pmatrix} \text{ or } \begin{pmatrix}\lambda_1&0&0\\0&\lambda_2&0\\0&0&\lambda_3\end{pmatrix}$$

for some pairwise distinct and positive $\lambda_1,\lambda_2,\lambda_3$.

Proof. [of Lemma 4.6] By definition, the map $\vartheta\colon \widehat{\mathscr{X}_3^+}(P) \to \mathscr{X}_3^+(P)$ is surjective. Then since $\widehat{\mathscr{X}_3^+}(P)$ is foliated by the symplectic leaves $\mathcal{Q}_L$ as L ranges in $\mathbb{R}^6_{>0}$, we only have to show that for each $L \in \mathbb{R}^6_{>0}$ there is a tuple of conjugacy classes $\mathcal{C}(L)$ such that $\vartheta(\mathcal{Q}_L) \subset \mathscr{X}^+_{3,\mathcal{C}(L)}(P)$ and that restricted to a symplectic leaf, ϑ is injective.

The eigenvalue ratios of the peripheral holonomies are exactly the Casimir functions (see Remark 4.2). By Theorem 4.7, we see that the conjugacy class of the holonomy of a peripheral lement is completely determined by the eigenvalue ratios, and hence there is a map $L \mapsto \mathcal{C}(L)$. In particular, $\vartheta(\mathcal{Q}_L) \subset \mathscr{X}^+_{3,\mathcal{C}(L)}(P)$. To see that the restriction to a symplectic leaf is injective, note that changing the framing changes the invariants. Therefore the framed convex projective structures with different framings lie in different

symplectic leaves. Since the only ambiguity in the map ϑ comes from the framing, this implies that ϑ is injective when restricted to the symplectic leaves. □

Remark 4.8. The map $L \mapsto \mathcal{C}(L)$ is in general not injective, meaning that two symplectic leaves may be mapped to the same relative character variety. Indeed, if L contains a pair $\ell_{x,1} \neq \ell_{x,2} \neq 1$ for $x \in \{\alpha, \beta, \gamma\}$, then interchanging $\ell_{x,1}$ with $\ell_{x,2}$ will define the same conjugacy class. This is because the Weyl group action on $\mathsf{PSL}(3,\mathbb{R})$ can interchange the order of the eigenvalues. However, in the case when $\mathcal{C}$ consists of only unipotent conjugacy classes, there is only one vector $L \in \mathbb{R}^6_{>0}$ mapping to $\mathcal{C}$, namely the vector $(1,1,1,1,1,1)$.

In Section 6 we will focus on a special symplectic leaf, corresponding to the case when the peripheral holonomies are *unipotent*. An element in $\mathsf{PSL}(3,\mathbb{R})$ is unipotent if all of its eigenvalues are equal to one.

Definition 4.9. The *unipotent locus* of $\widehat{\mathfrak{C}}(P)$, denoted by $\mathfrak{U}$, is the symplectic leaf where the Casimir functions are all equal to 1. That is

$$\mathfrak{U} := \mathcal{Q}_{(1,1,1,1,1,1)}$$

in the notation of Lemma 4.4. Through the map ϑ, $\mathfrak{U}$ is identified with the relative character variety where all the peripheral elements are unipotent.

Putting the spaces of framed convex projective structures, symplectic leaves, and framed representations, together with their counterparts without the framing, we provide the diagram below describing the relationships between all of these spaces:

$$\begin{array}{ccc}
\widehat{\mathfrak{C}}(P) & \longrightarrow & \mathfrak{C}(P) \\
\Big\downarrow{\scriptstyle \widehat{\mathsf{hol}}} & \searrow^{\vartheta} & \Big\downarrow{\scriptstyle \mathsf{hol}} \\
\mathbb{R}^8_{>0} \cong \widehat{\mathscr{X}_3^+}(P) & \xrightarrow[\mu]{} & \mathscr{X}_3^+(P) \\
\cup\mathrm{I} & & \cup\mathrm{I} \\
\mathbb{R}^2_{>0} \cong \mathcal{Q}_L & \xrightarrow{\cong} & \mathscr{X}^+_{3,\mathcal{C}}(P)
\end{array}$$

On the left are spaces which include framed structures, and on the right are the non–framed structures. The map ϑ is from Section 3.2, which forgets the framing of the holonomy representation, the map μ from Section 2.3 forgets the framing. The isomorphism at the bottom of the diagram is the content of Lemma 4.6.

4.3. **The Fuchsian locus.** A (framed) convex projective structure on P is said to be *hyperbolic* (or *Fuchsian*) if it corresponds to a hyperbolic structure on P (either with cusps or with geodesic boundary). In terms of its holonomy representation, this means that it factors through an irreducible representation $\mathsf{PSL}(2,\mathbb{R}) \to \mathsf{PSL}(3,\mathbb{R})$. As we are dealing with a pair of pants, there is a unique hyperbolic structure once the lengths of the boundary data are fixed. In particular, a symplectic leaf contains at most one hyperbolic structure. Since all ideal triangles in $\mathbb{H}^2 \subset \mathbb{RP}^2$ are equivalent, one can compute that

the triple ratio of an ideal triangle is always equal to one. Moreover, there is a single cross ratio that can be associated to a quadruple of flags, and hence in the coordinates, we have that

$$\sigma_1 = \sigma_2, \quad \sigma_3 = \sigma_4 \quad \text{and} \quad \sigma_5 = \sigma_6. \tag{12}$$

Let $F = (\ell_\alpha, \ell_\beta, \ell_\gamma) \in \mathbb{R}^3_{>0}$. By Lemma 4.4, we observe that the only symplectic leaves that contain a hyperbolic structure are the ones corresponding to the length vectors

$$L(F) = \left(\ell_\alpha, \frac{1}{\ell_\alpha}, \ell_\beta, \frac{1}{\ell_\beta}, \ell_\gamma, \frac{1}{\ell_\gamma}\right). \tag{13}$$

Moreover, by solving the Casimir equations from Lemma 4.1, we have that for $F = (\ell_\alpha, \ell_\beta, \ell_\gamma) \in \mathbb{R}^3_{>0}$, the Fuchsian structure in $\mathcal{Q}_{L(F)}$ is given by the coordinates

$$(\sigma_1, \dots, \sigma_6, \tau_1, \tau_2) = \left(\sqrt{\frac{\ell_\alpha \ell_\gamma}{\ell_\beta}}, \sqrt{\frac{\ell_\beta}{\ell_\alpha \ell_\gamma}}, \sqrt{\frac{\ell_\alpha \ell_\beta}{\ell_\gamma}}, \sqrt{\frac{\ell_\gamma}{\ell_\alpha \ell_\beta}}, \sqrt{\frac{\ell_\beta \ell_\gamma}{\ell_\alpha}}, \sqrt{\frac{\ell_\alpha}{\ell_\beta \ell_\gamma}}, 1, 1\right). \tag{14}$$

4.4. **Hamiltonian vector fields and flows.** Following the discussion surrounding Equation (2) regarding the symplectic leaves, we compute that for a point $p = (\sigma_1, \dots, \sigma_6, \tau_1, \tau_2) \in \widehat{\mathfrak{C}}(P)$ and the symplectic leaf $\mathcal{Q}$ going through p:

$$\mathsf{T}_p\mathcal{Q} = \left\langle \tau_1 \frac{\partial}{\partial \tau_1} - \tau_2 \frac{\partial}{\partial \tau_2}, \sum_{i=1}^{6} (-1)^{i+1} \sigma_i \frac{\partial}{\partial \sigma_i} \right\rangle. \tag{15}$$

Equivalently, by the fact the rank of the Poisson structure is constant (Remark 2.5), we see that $\mathsf{T}_p\mathcal{Q}$ is exactly the kernel of the Jacobian matrix associated to the Casimir functions in Proposition 4.1 (see Equation (11)).

Recall from Definition 2.6, that the Hamiltonian functions are a family of functions generating the symplectic leaves.

Proposition 4.10. *The Hamiltonian functions generating the symplectic leaves of $\widehat{\mathfrak{C}}(P)$ are given by*

$$\mathcal{I} = \frac{\log \tau_1 - \log \tau_2}{4},$$
$$\mathcal{E} = -\frac{1}{12} \sum_{i=1}^{6} (-1)^{i+1} \log \sigma_i.$$

Their Hamiltonian vector fields are given by

$$\mathsf{H}_{\mathcal{I}} = \sum_{i=1}^{6} (-1)^{i+1} \sigma_i \frac{\partial}{\partial \sigma_i}, \quad \text{and}$$
$$\mathsf{H}_{\mathcal{E}} = \tau_1 \frac{\partial}{\partial \tau_1} - \tau_2 \frac{\partial}{\partial \tau_2}.$$

Moreover, their Poisson bracket is

$$\{\mathcal{I}, \mathcal{E}\} = \frac{1}{2} \tag{16}$$

In particular, the Hamiltonian flows of $\mathcal{I}$ and $\mathcal{E}$ commute.

Proof. To see that the functions $\mathcal{I}$ and $\mathcal{E}$ generate the symplectic leaves, observe that according to Equation (15), the vector fields $\mathsf{H}_{\mathcal{I}}$ and $\mathsf{H}_{\mathcal{E}}$ generate the tangent space to the symplectic leaves. We begin by showing that the Hamiltonian vector fields $\mathsf{H}_{\mathcal{I}}$ and $\mathsf{H}_{\mathcal{E}}$ are indeed the Hamiltonian vector fields of the functions $\mathcal{I}$ and $\mathcal{E}$. To see that the Hamiltonian vector fields are those in the proposition, it is enough to check Equation (1) on the coordinate functions. We compute that for any coordinate function X_j

$$\begin{aligned}\{X_j, \mathcal{I}\} &= \frac{1}{4}\left(-\{\log \tau_1, X_j\} + \{\log \tau_2, X_j\}\right) \\ &= \frac{1}{4}\left(\frac{1}{\tau_2} d\tau_2(\mathsf{H}_{X_j}) - \frac{1}{\tau_1} d\tau_1(\mathsf{H}_{X_j})\right) \\ &= \frac{1}{4}\left(\frac{1}{\tau_2}\{\tau_2, X_j\} - \frac{1}{\tau_1}\{\tau_1, X_j\}\right).\end{aligned}$$

In particular, from the matrix (7) and the Poisson structure (6), we obtain that

$$\{\sigma_i, \mathcal{I}\} = (-1)^{i+1}\sigma_i, \qquad \{\tau_i, \mathcal{I}\} = 0.$$

On the other hand,

$$dX_j(\mathsf{H}_{\mathcal{I}}) = \sum_{i=1}^{6} (-1)^{i+1}\sigma_i \, dX_j\left(\frac{\partial}{\partial \sigma_i}\right)$$

and we see from the above equations that indeed $\{X_j, \mathcal{I}\} = dX_j(\mathsf{H}_{\mathcal{I}})$ as desired.

Following a similar computation for the function $\mathcal{E}$, we see that for any coordinate function X_j:

$$\{X_j, \mathcal{E}\} = \frac{1}{12}\sum_{i=1}^{6} \frac{(-1)^i}{\sigma_i}\{X_j, \sigma_i\}.$$

It follows that

$$\{\sigma_i, \mathcal{E}\} = 0, \qquad \{\tau_i, \mathcal{E}\} = \tau_i.$$

On the other hand,

$$dX_j(\mathsf{H}_{\mathcal{E}}) = \tau_1 \, dX_j\left(\frac{\partial}{\partial \tau_1}\right) - \tau_2 \, dX_j\left(\frac{\partial}{\partial \tau_2}\right)$$

and we see from the above equations that indeed $\{X_j, \mathcal{E}\} = dX_j(\mathsf{H}_{\mathcal{E}})$ for every coordinate function. These computations prove the first part of the proposition.

To see that the flows commute, we compute that their Poisson bracket is given by

$$\{\mathcal{I}, \mathcal{E}\} = \frac{1}{48}\left(\sum_{i=1}^{6} \frac{(-1)^i}{\tau_1\sigma_i}\{\tau_1, \sigma_i\} + \sum_{i=1}^{6} \frac{(-1)^{i+1}}{\tau_2\sigma_i}\{\tau_2, \sigma_i\}\right) = \frac{1}{2}.$$

Since the Poisson bracket is constant, the corresponding Hamiltonian vector fields commute by Lemma 2.2. □

The expression for the vector fields allows us to solve for the Hamiltonian flow itself.

Corollary 4.11. *The Hamiltonian flows of the Hamiltonian functions are given by*

$$\widehat{\Phi}^t_{\mathcal{E}}\colon (\sigma_1,\dots,\sigma_6,\tau_1,\tau_2)\mapsto(\sigma_1,\dots,\sigma_6,e^t\tau_1,e^{-t}\tau_2)$$
$$\widehat{\Phi}^t_{\mathcal{I}}\colon (\sigma_1,\dots,\sigma_6,\tau_1,\tau_2)\mapsto(e^t\sigma_1,e^{-t}\sigma_2,e^t\sigma_3,e^{-t}\sigma_4,e^t\sigma_5,e^{-t}\sigma_6,\tau_1,\tau_2).$$

Proof. This corollary is an immediate consequence of the form of the Hamiltonian vector fields in Proposition 4.10. That is, the above flows solve the ordinary differential equations defined by the corresponding vector fields. □

Similar flows already appear in [WZ18, SWZ20]. Given their similarity, we adopt the same names for the flows.

Definition 4.12. [WZ18, SWZ20] The Hamiltonian flow of the function $\mathcal{E}$ is called the *eruption flow*, and the Hamiltonian flow of the function $\mathcal{I}$ is called the *hexagon flow*.

Remark 4.13. The difference between the flows in [WZ18, SWZ20] and the flows in this article, is that the invariants used by Fock and Goncharov in [FG07] are different from the ones used in the above papers.

These two flows give a symplectic trivialization of the two–dimensional symplectic leaves. In particular, it means that for any pairs $q_1,q_2\in\widehat{\mathfrak{C}}(P)$, there are unique numbers $s,t\in\mathbb{R}$ such that

$$q_2=\widehat{\Phi}^t_{\mathcal{I}}\circ\widehat{\Phi}^s_{\mathcal{E}}(q_1)=\widehat{\Phi}^s_{\mathcal{E}}\circ\widehat{\Phi}^t_{\mathcal{I}}(q_1). \tag{17}$$

This fact motivates the following.

Definition 4.14. Let $a\in\mathbb{R}$. Any of the two flows

$$\widehat{\Phi}^t_{\mathcal{I}}\circ\widehat{\Phi}^{at}_{\mathcal{E}}\quad\text{or}\quad\widehat{\Phi}^{at}_{\mathcal{I}}\circ\widehat{\Phi}^t_{\mathcal{E}}$$

is called a *mixed flow*. A mixed flow defined by $a\in\mathbb{R}$ will be written as Ψ^t_a.

The following is a direct consequence of Equation (17), and is the required analogue of Fact 3 in the introduction, allowing to connect any pair of points in a simplectic leaf via a mixed flow.

Lemma 4.15. *Let $L\in\mathbb{R}^6_{>0}$ define a symplectic leaf $\mathcal{Q}_L\subset\widehat{\mathfrak{C}}(P)$. For any pair $q_1,q_2\in\mathcal{Q}_L$, there is a constant $a\in\mathbb{R}$ defining a mixed flow and a time $t\in\mathbb{R}$ such that $q_2=\Psi^t_a(q_1)$.*

4.5. **The symplectic form on a symplectic leaf.** Here we compute the symplectic form on the leaves explicitly first by using the functions $\mathcal{I}$ and $\mathcal{E}$. We then use the parametrization of the symplectic leaves in Lemma 4.4 to give a more useful expression for the symplectic form.

Lemma 4.16. *Let $\mathcal{Q}$ be a symplectic leaf of $\widehat{\mathfrak{C}}(P)$. The symplectic form $\omega_{\mathcal{Q}}$ is given by*

$$\omega_{\mathcal{Q}}=2\,d\mathcal{I}\wedge d\mathcal{E}.$$

In terms of the Fock–Goncharov coordinates, the symplectic form reads

$$\omega_{\mathcal{Q}}=\frac{1}{24}\sum_{i=1}^{6}(-1)^i\left(\frac{1}{\tau_1\sigma_i}d\tau_1\wedge d\sigma_i-\frac{1}{\tau_2\sigma_i}d\tau_2\wedge d\sigma_i\right). \tag{18}$$

Remark 4.17. The form of the symplectic structure here is analogous to the Darboux system given by Sun and Zhang in [SZ17, Corollary 7.11]. Recall from Remark 4.13 that the difference lies in the description of the invariants associated to flags.

Proof. By Proposition 4.10, we only need to compute $\omega_{\mathcal{Q}}(\mathsf{H}_{\mathcal{I}}, \mathsf{H}_{\mathcal{E}})$. By Equation (16) we have that

$$\omega_{\mathcal{Q}}(\mathsf{H}_{\mathcal{I}}, \mathsf{H}_{\mathcal{E}}) = \{\mathcal{I}, \mathcal{E}\} = \frac{1}{2}.$$

On the other hand,

$$2d\mathcal{I} \wedge d\mathcal{E}(\mathsf{H}_{\mathcal{I}}, \mathsf{H}_{\mathcal{E}}) = 2\{\mathcal{I}, \mathcal{E}\}^2 = \frac{1}{2}$$

as desired. Writing the symplectic form in terms of Fock–Goncharov coordinates is a computation using the expression of the functions in Proposition 4.10. □

This expression allows us to compute the Hamiltonian vector fields and Hamiltonian flows of all the coordinate functions.

Corollary 4.18. *The Hamiltonian vector field of the coordinate functions* $\sigma_1, \dots, \sigma_6, \tau_1, \tau_2$ *is given by*

$$\mathsf{H}_{\sigma_i} = (-1)^{i+1}\sigma_i \mathsf{H}_{\mathcal{E}}, \quad \mathsf{H}_{\tau_1} = \tau_1 \mathsf{H}_{\mathcal{I}}, \quad \text{and } \mathsf{H}_{\tau_2} = -\tau_2 \mathsf{H}_{\mathcal{I}}.$$

In particular, their corresponding Hamiltonian flows are given by

$$\begin{aligned}
\widehat{\Phi}^t_{\sigma_i}(\sigma_1, \dots, \sigma_6, \tau_1, \tau_2) &\mapsto \left(\sigma_1, \dots, \sigma_6, e^{(-1)^i t\sigma_i}\tau_1, e^{(-1)^{i+1}t\sigma_i}\tau_2\right), \\
\widehat{\Phi}^t_{\tau_1}(\sigma_1, \dots, \sigma_6, \tau_1, \tau_2) &\mapsto \left(e^{t\tau_1}\sigma_1, e^{-t\tau_1}\sigma_2, e^{t\tau_1}\sigma_3, e^{-t\tau_1}\sigma_4, e^{t\tau_1}\sigma_5, e^{-t\tau_1}\sigma_6, \tau_1, \tau_2\right), \\
\widehat{\Phi}^t_{\tau_2}(\sigma_1, \dots, \sigma_6, \tau_1, \tau_2) &\mapsto \left(e^{-t\tau_2}\sigma_1, e^{t\tau_2}\sigma_2, e^{-t\tau_2}\sigma_3, e^{t\tau_2}\sigma_4, e^{-t\tau_2}\sigma_5, e^{t\tau_2}\sigma_6, \tau_1, \tau_2\right).
\end{aligned}$$

Proof. The computation of the Hamiltonian vector fields is a direct application of the expression of $\omega_{\mathcal{Q}}$ in Fock–Goncharov coordinates in Equation (18). Similarly, the solutions to the ordinary differential equations arising from the vector fields are seen to be given by the flows in the corollary. □

Restricted to symplectic leaves determined by a length vector $L \in \mathbb{R}^6_{>0}$, we can use the coordinates σ_1 and τ_1 as in Lemma 4.4. In the following corollary, we describe the symplectic form in terms of the coordinates σ_1 and τ_1.

Lemma 4.19. *Let* $L = (\ell_{\alpha,1}, \ell_{\alpha,2}, \ell_{\beta,1}, \ell_{\beta,2}, \ell_{\gamma,1}, \ell_{\gamma,2}) \in \mathbb{R}^6_{>0}$. *The symplectic form of the symplectic leaf* $\mathcal{Q}_L$ *parameterized as in Lemma 4.4 is given by*

$$\omega_{\mathcal{Q}_L} = \frac{1}{2\sigma_1\tau_1} d\sigma_1 \wedge d\tau_1.$$

Proof. To prove the formula, we compute that

$$\begin{aligned}
d\sigma_{2,L} &= -\frac{1}{\sigma_1^2}\frac{(\ell_{\alpha,1}\ell_{\beta,2}\ell_{\gamma,1})^{2/3}}{(\ell_{\alpha,2}\ell_{\beta,1}\ell_{\gamma,2})^{1/3}} d\sigma_1, \\
d\sigma_{3,L} &= \frac{(\ell_{\beta,1}\ell_{\gamma,2})^{2/3}}{(\ell_{\alpha,1}\ell_{\alpha,2}\ell_{\beta,2}\ell_{\gamma,1})^{1/3}} d\sigma_1,
\end{aligned}$$

$$d\sigma_{4,L} = -\frac{\ell_{\alpha,1}}{\sigma_1^2} d\sigma_1,$$
$$d\sigma_{5,L} = \frac{(\ell_{\alpha,2}\ell_{\beta,1}\ell_{\gamma,1}\ell_{\gamma,2})^{1/3}}{(\ell_{\alpha,1}\ell_{\beta,2})^{2/3}} d\sigma_1,$$
$$d\sigma_{6,L} = -\frac{1}{\sigma_1^2}\frac{(\ell_{\alpha,1}\ell_{\alpha,2}\ell_{\beta,1}\ell_{\beta,2}\ell_{\gamma,1})^{1/3}}{\ell_{\gamma,2}^{2/3}} d\sigma_1,$$
$$d\tau_{2,L} = -\frac{(\ell_{\alpha,1}\ell_{\alpha,2}\ell_{\beta,1}\ell_{\beta,2}\ell_{\gamma,1}\ell_{\gamma,2})^{1/3}}{\tau_1^2} d\tau_1.$$

Replacing $\sigma_{i,L}, \tau_{2,L}$ and their derivatives in Equation (18), we observe that

$$\omega_{\mathcal{Q}_L} = \frac{1}{24}\sum_{i=1}^{6} \frac{-2}{\tau_1\sigma_1} d\tau_1 \wedge d\sigma_1 = \frac{1}{2\sigma_1\tau_1} d\sigma_1 \wedge d\tau_1$$

as claimed. □

This form of the symplectic structure gives us a straight forward computation of the Hamiltonian vector field of a given function. Namely, let $L \in \mathbb{R}^6_{>0}$ define a symplectic leaf $\mathcal{Q}_L$. Consider a function $\phi\colon \mathcal{Q}_L \cong \mathbb{R}^2_{>0} \to \mathbb{R}$ given in coordinates (σ_1, τ_1) using the parameterization of Lemma 4.4. Then a linear algebra computation shows that the Hamiltonian vector field of ϕ is given by

$$\mathsf{H}_\phi = 2\sigma_1\tau_1\left(-\frac{\partial\phi}{\partial\tau_1}\cdot\frac{\partial}{\partial\sigma_1} + \frac{\partial\phi}{\partial\sigma_1}\cdot\frac{\partial}{\partial\tau_1}\right). \tag{19}$$

Writing down the associated differential equation, we have that a path $(\sigma_1, \tau_1)\colon \mathbb{R} \to \mathcal{Q}_L$ is a flow line of the Hamiltonian vector field of ϕ if

$$\begin{cases} \dot\sigma_1(t) &= -2\sigma_1(t)\tau_1(t)\dfrac{\partial\phi}{\partial\tau_1}(\sigma_1(t),\tau_1(t)), \\ \dot\tau_1(t) &= 2\sigma_1(t)\tau_1(t)\dfrac{\partial\phi}{\partial\sigma_1}(\sigma_1(t),\tau_1(t)). \end{cases} \tag{20}$$

5. Trace of the figure eight curve

We are now ready to address Theorem A. Recall that any closed curve $c \in \pi_1(S)$ defines the function

$$\begin{aligned} \mathsf{tr}_c\colon \widehat{\mathfrak{C}}(P) &\to \mathbb{R} \\ [f,\Sigma,\nu] &\mapsto \mathsf{tr}(\vartheta([f,\Sigma,\nu])(c)). \end{aligned}$$

In this section, we focus on the figure eight curve, i.e. a curve with a single self–intersection. The identification $\widehat{\mathfrak{C}}(P) \cong \mathbb{R}^8_{>0}$ together with the reconstruction of representations from coordinates (recall Section 3.2) allows us to write traces of curves as rational functions in the coordinates.

The main goal of this section is to provide a proof of Theorem A, which we restate here.

Theorem 5.1. *Let $\delta = \alpha\gamma^{-1}$ be the figure eight curve on P and let $L \in \mathbb{R}^6_{>0}$ define a symplectic leaf $\mathcal{Q}_L \subset \widehat{\mathfrak{C}}(P)$. Then the function $\mathsf{tr}_\delta\big|_{\mathcal{Q}_L} \colon \mathcal{Q}_L \to \mathbb{R}$ attains a unique minimum. Moreover, every orbit of the Hamiltonian flow of $\mathsf{tr}_\delta\big|_{\mathcal{Q}_L}$ is periodic and there is a unique fixed point.*

As explained in the introduction, we need to prove Proposition E (analogous to Fact 2) on properness of the trace function, and Theorem F (analogous to Fact 4) on convexity. We begin by presenting the expression for the trace of the figure eight curve in a given symplectic leaf.

Lemma 5.2. *Let $\delta = \alpha\gamma^{-1}$ and $L = (\ell_{\alpha,1}, \ell_{\alpha,2}, \ell_{\beta,1}, \ell_{\beta,2}, \ell_{\gamma,1}, \ell_{\gamma,2}) \in \mathbb{R}^6_{>0}$ be a length vector defining a symplectic leaf $\mathcal{Q}_L$. Then*

$$\begin{gathered}
\mathsf{tr}_\delta\big|_{\mathcal{Q}_L} \colon \mathcal{Q}_L \to \mathbb{R} \\
(\sigma_1, \tau_1) \mapsto \frac{1}{\sigma_1\tau_1\ell_{\alpha,1}^{4/3}\sqrt[3]{\ell_{\beta,1}}\ell_{\beta,2}\left(\ell_{\alpha,2}\ell_{\gamma,1}\ell_{\gamma,2}\right)^{2/3}} \cdot \\
\Big(\sigma_1^3\tau_1^2\ell_{\gamma,2}\sqrt[3]{\ell_{\alpha,2}\ell_{\beta,1}} + \ell_{\alpha,1}^{5/3}\left(\ell_{\beta,2}\ell_{\gamma,1}\ell_{\gamma,2}\right)^{2/3}\left(\left(\sigma_1+\tau_1+1\right)\ell_{\alpha,2}\ell_{\beta,2} + \sigma_1\tau_1^2\right) + \\
+\sigma_1^2\tau_1\left(\ell_{\alpha,2}\ell_{\beta,1}\right)^{2/3}\sqrt[3]{\ell_{\alpha,1}\ell_{\beta,2}\ell_{\gamma,1}\ell_{\gamma,2}}\left(2\sigma_1\ell_{\gamma,2} + \ell_{\gamma,2} + \tau_1\right) + \\
+\sigma_1\ell_{\alpha,1}^{4/3}\left(\ell_{\alpha,2}\ell_{\beta,1}\right)^{2/3}\sqrt[3]{\ell_{\beta,2}\ell_{\gamma,1}\ell_{\gamma,2}}\left(\left(\sigma_1+1\right)\ell_{\beta,2}\ell_{\gamma,2} + \tau_1\left(\sigma_1\ell_{\gamma,2} + \tau_1\right)\right) + \\
+\tau_1\ell_{\alpha,1}^2\ell_{\beta,2}\sqrt[3]{\ell_{\alpha,2}\ell_{\beta,1}}\left(\ell_{\gamma,1}\left(\sigma_1\ell_{\gamma,2} + \sigma_1 + \tau_1 + 1\right) + \sigma_1\ell_{\gamma,2}\right) \\
+\sigma_1^2\left(\ell_{\alpha,1}\ell_{\beta,2}\ell_{\gamma,1}\ell_{\gamma,2}\right)^{2/3}\left(\ell_{\alpha,2}\left(\ell_{\beta,1}\left(\sigma_1\ell_{\gamma,2} + \ell_{\gamma,2} + \tau_1\right) + \tau_1\right) + \tau_1^2\right) \\
+\sigma_1\tau_1\ell_{\alpha,1}\sqrt[3]{\ell_{\alpha,2}\ell_{\beta,1}}(\ell_{\beta,2}\ell_{\gamma,1}(\sigma_1\ell_{\gamma,2} + \ell_{\gamma,2} + \tau_1 + 1) + (\sigma_1+1)\ell_{\beta,2}\ell_{\gamma,2} + \sigma_1\tau_1\ell_{\gamma,2} + \\
+\ell_{\alpha,2}\ell_{\beta,2}\left(\ell_{\gamma,1}\left(\left(\sigma_1+\tau_1+1\right)\ell_{\gamma,2} + \tau_1\right) + \tau_1\ell_{\gamma,2}\right)\Big).
\end{gathered}$$

In the unipotent locus, i.e. when $L = (1,1,1,1,1,1)$, we have that

$$\begin{aligned}
&\mathsf{tr}_\delta \colon \mathfrak{U} \to \mathbb{R} \\
&(\sigma_1, \tau_1) \mapsto \frac{\sigma_1^3\left(\tau_1+1\right)^2 + 3\sigma_1^2\left(\tau_1+1\right)^2 + 3\sigma_1\left(\tau_1^2+3\tau_1+1\right) + \left(\tau_1+1\right)^2}{\sigma_1\tau_1}
\end{aligned}$$

Proof. The proof of this fact is a computation, found in Section 4 of the Mathematica code. The function `traceFigure8` will give the above output with the length vectors as input. For the unipotent locus, replace the length vector with ones. □

5.1. **Properness of the trace function.** We can now prove Proposition E, which we restate here for convenience.

Proposition 5.3. *Let $\delta = \alpha\gamma^{-1}$ and $L = (\ell_{\alpha,1}, \ell_{\alpha,2}, \ell_{\beta,1}, \ell_{\beta,2}, \ell_{\gamma,1}, \ell_{\gamma,2}) \in \mathbb{R}^6_{>0}$ be a length vector defining a symplectic leaf $\mathcal{Q}_L$. Then the function $\mathsf{tr}_\delta \colon \mathcal{Q}_L \to \mathbb{R}$ is proper. In particular, it realizes a minimum in $\mathcal{Q}_L$.*

Proof. By the parameterization in Lemma 4.4, the trace of δ defines the rational function in Lemma 5.2 as a map from $\mathbb{R}^2_{>0}$ to $\mathbb{R}$. Let $(\sigma_{1,n}, \tau_{1,n})_{n\in\mathbb{N}}$ be a sequence such that as n goes to ∞, $(\sigma_{1,n}, \tau_{1,n})$ goes to a tuple in $\{(\infty,\infty), (0,\infty), (\infty,0), (x,0), (0,y) : x, y \geq$

$0\}$, i.e. a sequence escaping every compact set in $\mathbb{R}^2_{>0}$. We need to show that in any of these cases, $\mathsf{tr}_\delta(\sigma_{1,n}, \tau_{1,n}) \to \infty$ as $n \to \infty$. Notice that all the variables are positive and that all the signs on the monomials are positive as well. Hence, it is enough to find terms in the expression in Lemma 5.2 that diverges along any of the above sequences.

(a) Assume $(\sigma_{1,n}, \tau_{1,n}) \to (\infty, \infty)$, then the term

$$\frac{\sigma_{1,n}^3 \tau_{1,n}^2 \ell_{\gamma,2} \sqrt[3]{\ell_{\alpha,2}\ell_{\beta,1}}}{\sigma_{1,n}\tau_{1,n}\ell_{\alpha,1}^{4/3}\sqrt[3]{\ell_{\beta,1}}\ell_{\beta,2}\left(\ell_{\alpha,2}\ell_{\gamma,1}\ell_{\gamma,2}\right)^{2/3}} \xrightarrow{n\to\infty} \infty.$$

(b) Assume $(\sigma_{1,n}, \tau_{1,n}) \to (\infty, 0)$, then the term

$$\frac{2\sigma_{1,n}^3 \tau_{1,n}(\ell_{\alpha,2}\ell_{\beta,1})^{2/3}\sqrt[3]{\ell_{\alpha,1}\ell_{\beta,2}\ell_{\gamma,1}\ell_{\gamma,2}}\ell_{\gamma,2}}{\sigma_{1,n}\tau_{1,n}\ell_{\alpha,1}^{4/3}\sqrt[3]{\ell_{\beta,1}}\ell_{\beta,2}\left(\ell_{\alpha,2}\ell_{\gamma,1}\ell_{\gamma,2}\right)^{2/3}} \xrightarrow{n\to\infty} \infty.$$

(c) Assume $(\sigma_{1,n}, \tau_{1,n}) \to (0, \infty)$, then the term

$$\frac{\ell_{\alpha,1}^{5/3}\left(\ell_{\beta,2}\ell_{\gamma,1}\ell_{\gamma,2}\right)^{2/3}\sigma_{1,n}\tau_{1,n}^2}{\sigma_{1,n}\tau_{1,n}\ell_{\alpha,1}^{4/3}\sqrt[3]{\ell_{\beta,1}}\ell_{\beta,2}\left(\ell_{\alpha,2}\ell_{\gamma,1}\ell_{\gamma,2}\right)^{2/3}} \xrightarrow{n\to\infty} \infty.$$

(d) Assume $(\sigma_{1,n}, \tau_{1,n}) \to (x, 0)$ or $(0, y)$ for $x, y \geq 0$, then the term

$$\frac{\ell_{\alpha,1}^{5/3}(\ell_{\beta,2}\ell_{\gamma,1}\ell_{\gamma,2})^{2/3}\ell_{\alpha,2}\ell_{\beta,2}}{\sigma_{1,n}\tau_{1,n}\ell_{\alpha,1}^{4/3}\sqrt[3]{\ell_{\beta,1}}\ell_{\beta,2}\left(\ell_{\alpha,2}\ell_{\gamma,1}\ell_{\gamma,2}\right)^{2/3}} \xrightarrow{n\to\infty} \infty.$$

This finishes the proof of properness of the function tr_δ on the symplectic leaves. To see that the function realizes a minimum, note that the function is positive. □

5.2. **Convexity of tr_δ.** The next step is to prove Theorem F. Here we once again use more Mathematica for the computations. Since we have explicit expressions for the Hamiltonian flows associated to coordinate functions, as well as the mixed flows, we can use them to compute second derivatives. That is, given a function $\phi\colon \mathcal{Q}_L \to \mathbb{R}$ and a flow $\widehat{\Phi}^t\colon \mathcal{Q}_L \to \mathcal{Q}_L$, we compute

$$t \mapsto \frac{\partial^2}{\partial t^2}\phi\left(\widehat{\Phi}^t(q)\right)$$

for any $q \in \mathcal{Q}_L$ and check whether it is a strictly positive function.

Theorem 5.4. *Let $L \in \mathbb{R}^6_{>0}$ and $\delta = \alpha\gamma^{-1}$ be a figure eight curve. Then the trace function $\mathsf{tr}_\delta\big|_{\mathcal{Q}_L}\colon \mathcal{Q}_L \to \mathbb{R}$ is strictly convex along any mixed flow.*

Proof. Let $L = (\ell_{\alpha,1}, \ell_{\alpha,2}, \ell_{\beta,1}, \ell_{\beta,2}, \ell_{\gamma,1}, \ell_{\gamma,2}) \in \mathbb{R}^6_{>0}$ be a length vector and let $q = (\sigma_1, \tau_1) \in \mathcal{Q}_L$. Let $a \in \mathbb{R}$. We need to check the two different types of mixed flows from Definition 4.14. We begin with the case when the mixed flow defined by a is given by $\Psi_a^t = \widehat{\Phi}_{\mathcal{I}}^{at} \circ \widehat{\Phi}_{\mathcal{E}}^t$. In Section 6 of the Mathematica code, set `testf` equal to `traceFig8`. Then inputting the function `testfMix1` to `SecondDerFlow`, we obtain that

$$\frac{\partial^2}{\partial t^2}\mathsf{tr}_\delta\left(\Psi_a^t(q)\right)=\frac{e^{-t(a+1)}}{\sigma_1\tau_1\ell_{\beta,2}\sqrt[3]{\ell_{\alpha,1}^4\ell_{\alpha,2}^2\ell_{\beta,1}\ell_{\gamma,1}^2\ell_{\gamma,2}^2}}\cdot$$

$$\Bigg(e^t\tau_1\ell_{\alpha,1}^2\ell_{\beta,2}\ell_{\gamma,1}\left(e^t\tau_1(a-1)^2+a^2\right)\sqrt[3]{\ell_{\alpha,2}\ell_{\beta,1}}+\sigma_1\tau_1^2e^{(a+2)t}\ell_{\alpha,1}^{5/3}\left(\ell_{\beta,2}\ell_{\gamma,1}\ell_{\gamma,2}\right)^{2/3}+$$

$$\sigma_1\cdot\Bigg((2a+1)^2\sigma_1^2\tau_1^2e^{(3a+2)t}\ell_{\gamma,2}\sqrt[3]{\ell_{\alpha,2}\ell_{\beta,1}}+(a-1)^2\sigma_1e^{2at}\ell_{\alpha,2}\ell_{\beta,1}\ell_{\gamma,2}^{5/3}\left(\ell_{\alpha,1}\ell_{\beta,2}\ell_{\gamma,1}\right)^{2/3}+$$

$$(1-2a)^2\sigma_1^2e^{3at}\ell_{\alpha,2}\ell_{\beta,1}\ell_{\gamma,2}^{5/3}\left(\ell_{\alpha,1}\ell_{\beta,2}\ell_{\gamma,1}\right)^{2/3}+\tau_1^2e^{(a+2)t}\sqrt[3]{\ell_{\alpha,1}^4\ell_{\alpha,2}^2\ell_{\beta,1}^2\ell_{\beta,2}\ell_{\gamma,1}\ell_{\gamma,2}}+$$

$$8a^2\sigma_1^2\tau_1e^{3at+t}\sqrt[3]{\ell_{\alpha,1}\ell_{\alpha,2}^2\ell_{\beta,1}^2\ell_{\beta,2}\ell_{\gamma,1}\ell_{\gamma,2}^4}+$$

$$(a+1)^2\sigma_1\tau_1^2e^{2(a+1)t}\sqrt[3]{\ell_{\alpha,1}\ell_{\beta,2}\ell_{\gamma,1}\ell_{\gamma,2}}\left(\sqrt[3]{\ell_{\alpha,1}\ell_{\beta,2}\ell_{\gamma,1}\ell_{\gamma,2}}+\left(\ell_{\alpha,2}\ell_{\beta,1}\right)^{2/3}\right)+$$

$$a^2\sigma_1\tau_1e^{2at+t}\Bigg(\left(\ell_{\alpha,2}\left(\ell_{\beta,1}+1\right)\left(\ell_{\alpha,1}\ell_{\beta,2}\ell_{\gamma,1}\ell_{\gamma,2}\right)^{2/3}+\right.$$

$$\left.\sqrt[3]{\ell_{\alpha,1}\ell_{\alpha,2}^2\ell_{\beta,1}^2\ell_{\beta,2}\ell_{\gamma,1}\ell_{\gamma,2}^4}+\sqrt[3]{\ell_{\alpha,1}^4\ell_{\alpha,2}^2\ell_{\beta,1}^2\ell_{\beta,2}\ell_{\gamma,1}\ell_{\gamma,2}^4}\right)\Bigg)+$$

$$\ell_{\alpha,1}\Bigg(\ell_{\alpha,2}\ell_{\beta,2}\left(a^2e^t\tau_1+\sigma_1e^{at}+(a+1)^2\right)\left(\ell_{\alpha,1}\ell_{\beta,2}\ell_{\gamma,1}\ell_{\gamma,2}\right)^{2/3}+$$

$$\sigma_1\Bigg((a+1)^2\sigma_1\tau_1^2e^{2(a+1)t}\ell_{\gamma,2}\sqrt[3]{\ell_{\alpha,2}\ell_{\beta,1}}+\tau_1^2e^{(a+2)t}\ell_{\beta,2}\ell_{\gamma,1}\sqrt[3]{\ell_{\alpha,2}\ell_{\beta,1}}+$$

$$a^2\sigma_1\tau_1e^{2at+t}\ell_{\beta,2}\left(\ell_{\gamma,1}+1\right)\ell_{\gamma,2}\sqrt[3]{\ell_{\alpha,2}\ell_{\beta,1}}+$$

$$e^{at}\ell_{\beta,2}\ell_{\gamma,2}\left(\ell_{\gamma,1}\sqrt[3]{\ell_{\alpha,2}^4\ell_{\beta,1}}+\sqrt[3]{\ell_{\alpha,1}\ell_{\alpha,2}^2\ell_{\beta,1}^2\ell_{\beta,2}\ell_{\gamma,1}\ell_{\gamma,2}}\right)+$$

$$(a-1)^2\sigma_1e^{2at}\ell_{\beta,2}\ell_{\gamma,2}\left(\ell_{\gamma,1}\sqrt[3]{\ell_{\alpha,2}^4\ell_{\beta,1}}+\sqrt[3]{\ell_{\alpha,1}\ell_{\alpha,2}^2\ell_{\beta,1}^2\ell_{\beta,2}\ell_{\gamma,1}\ell_{\gamma,2}}\right)\Bigg)\Bigg)\Bigg)\Bigg).$$

Examining the terms, we see that a always appears either within a square, or in an exponential. Moreover, t also always appears only in an exponential. All the lengths are positive, and so are the coordinates σ_1 and τ_1. Thus, the second derivative is always strictly larger than zero, and hence the function $t\mapsto \mathsf{tr}_\delta\big|_{\mathcal{Q}_L}(\Psi_a^t(q))$ is strictly convex for any $q\in\mathcal{Q}_L$.

The case for the other mixed flow is similar. Consider now the mixed flow $\Psi_a^t=\widehat{\Phi}_{\mathcal{I}}^t\circ\widehat{\Phi}_{\mathcal{E}}^{at}$ and $q=(\sigma_1,\tau_1)\in\mathcal{Q}_L$. In Section 6 of the Mathematica code, set `testf` equal to `traceFig8`. Then inputting the function `testfMix2` to `SecondDerFlow`, we obtain that

$$\frac{\partial^2}{\partial t^2}\mathsf{tr}_\delta\left(\Psi_a^t(q)\right)=\frac{e^{-t(a+1)}}{\sigma_1\tau_1\ell_{\beta,2}\sqrt[3]{\ell_{\alpha,1}^4\ell_{\alpha,2}^2\ell_{\beta,1}\ell_{\gamma,1}^2\ell_{\gamma,2}^2}}\cdot$$

$$\Bigg(a^2\sigma_1\tau_1^2e^{2at+t}\ell_{\alpha,1}^{5/3}\left(\ell_{\beta,2}\ell_{\gamma,1}\ell_{\gamma,2}\right)^{2/3}+\tau_1e^{at}\ell_{\alpha,1}^2\ell_{\beta,2}\ell_{\gamma,1}\left((a-1)^2\tau_1e^{at}+1\right)\sqrt[3]{\ell_{\alpha,2}\ell_{\beta,1}}+$$

$$\sigma_1\Bigg((a+2)^2\sigma_1^2\tau_1^2e^{(2a+3)t}\ell_{\gamma,2}\sqrt[3]{\ell_{\alpha,2}\ell_{\beta,1}}+(a-1)^2\sigma_1e^{2t}\ell_{\alpha,2}\ell_{\beta,1}\ell_{\gamma,2}^{5/3}\left(\ell_{\alpha,1}\ell_{\beta,2}\ell_{\gamma,1}\right)^{2/3}+$$
$$a^2\tau_1^2e^{2at+t}\sqrt[3]{\ell_{\alpha,1}^4\ell_{\alpha,2}^2\ell_{\beta,1}^2\ell_{\beta,2}\ell_{\gamma,1}\ell_{\gamma,2}}+(a-2)^2\sigma_1^2e^{3t}\ell_{\alpha,2}\ell_{\beta,1}\ell_{\gamma,2}^{5/3}\left(\ell_{\alpha,1}\ell_{\beta,2}\ell_{\gamma,1}\right)^{2/3}+$$
$$8\sigma_1^2\tau_1e^{(3+a)t}\sqrt[3]{\ell_{\alpha,1}\ell_{\alpha,2}^2\ell_{\beta,1}^2\ell_{\beta,2}\ell_{\gamma,1}\ell_{\gamma,2}^4}+$$
$$(a+1)^2\sigma_1\tau_1^2e^{2(a+1)t}\sqrt[3]{\ell_{\alpha,1}\ell_{\beta,2}\ell_{\gamma,1}\ell_{\gamma,2}}\left(\sqrt[3]{\ell_{\alpha,1}\ell_{\beta,2}\ell_{\gamma,1}\ell_{\gamma,2}}+\left(\ell_{\alpha,2}\ell_{\beta,1}\right)^{2/3}\right)+$$
$$\sigma_1\tau_1e^{(a+2)t}\Bigg(\ell_{\alpha,2}\left(\ell_{\beta,1}+1\right)\Bigg(\left(\ell_{\alpha,1}\ell_{\beta,2}\ell_{\gamma,1}\ell_{\gamma,2}\right)^{2/3}$$
$$+\sqrt[3]{\ell_{\alpha,1}\ell_{\alpha,2}^2\ell_{\beta,1}^2\ell_{\beta,2}\ell_{\gamma,1}\ell_{\gamma,2}^4}+\sqrt[3]{\ell_{\alpha,1}^4\ell_{\alpha,2}^2\ell_{\beta,1}^2\ell_{\beta,2}\ell_{\gamma,1}\ell_{\gamma,2}^4}\Bigg)\Bigg)+$$
$$\ell_{\alpha,1}\Bigg(\ell_{\alpha,2}\ell_{\beta,2}\left(a^2\sigma_1e^t+\tau_1e^{at}+(a+1)^2\right)\left(\ell_{\alpha,1}\ell_{\beta,2}\ell_{\gamma,1}\ell_{\gamma,2}\right)^{2/3}+$$
$$\sigma_1\Bigg(a^2\tau_1^2e^{2at+t}\ell_{\beta,2}\ell_{\gamma,1}\sqrt[3]{\ell_{\alpha,2}\ell_{\beta,1}}+(a+1)^2\sigma_1\tau_1^2e^{2(a+1)t}\ell_{\gamma,2}\sqrt[3]{\ell_{\alpha,2}\ell_{\beta,1}}+$$
$$\sigma_1\tau_1e^{(a+2)t}\ell_{\beta,2}\left(\ell_{\gamma,1}+1\right)\ell_{\gamma,2}\sqrt[3]{\ell_{\alpha,2}\ell_{\beta,1}}+$$
$$a^2e^t\ell_{\beta,2}\ell_{\gamma,2}\left(\ell_{\gamma,1}\sqrt[3]{\ell_{\alpha,2}^4\ell_{\beta,1}}+\sqrt[3]{\ell_{\alpha,1}\ell_{\alpha,2}^2\ell_{\beta,1}^2\ell_{\beta,2}\ell_{\gamma,1}\ell_{\gamma,2}}\right)+$$
$$(a-1)^2\sigma_1e^{2t}\ell_{\beta,2}\ell_{\gamma,2}\left(\ell_{\gamma,1}\sqrt[3]{\ell_{\alpha,2}^4\ell_{\beta,1}}+\sqrt[3]{\ell_{\alpha,1}\ell_{\alpha,2}^2\ell_{\beta,1}^2\ell_{\beta,2}\ell_{\gamma,1}\ell_{\gamma,2}}\right)\Bigg)\Bigg)\Bigg).$$

Once again, t appears only as an exponential, a appears either as an exponential or within a square, and all of the other variables are positive. Hence, $t\mapsto \mathsf{tr}_\delta\big|_{\mathcal{Q}_L}(\Psi_a^t(q))$ is strictly convex for any $q\in\mathcal{Q}_L$. □

With this strict convexity, we immediately obtain the following.

Corollary 5.5. *Let $L\in\mathbb{R}^6_{>0}$ and $\delta=\alpha\gamma^{-1}$ be a figure eight curve. Then the trace function $\mathsf{tr}_\delta\big|_{\mathcal{Q}_L}:\mathcal{Q}_L\to\mathbb{R}$ has a unique critical point, corresponding to the unique minimum.*

5.3. **Proof of Theorem 5.1.** With the above sections, we can now prove Theorem 5.1, which is exactly the same proof as that of Theorem D.

Proof. [of Theorem 5.1] As stated above in Corollary 5.5, strict convexity of the trace function $\mathsf{tr}_\delta\big|_{\mathcal{Q}_L}$ along any mixed give that there is a unique critical point and corresponds to the unique minimum. Therefore, the Hamiltonian flow of $\mathsf{tr}_\delta\big|_{\mathcal{Q}_L}$ has a unique fixed point.

Now we show that every orbit is periodic. Let M be a non–empty level set of $\mathsf{tr}_\delta\big|_{\mathcal{Q}_L}$ that does not correspond to the fixed point. In particular, M is a a regular level set and therefore a smooth co–dimension one submanifold of $\mathcal{Q}_L$. The Hamiltonian flow of $\mathsf{tr}_\delta\big|_{\mathcal{Q}_L}$ preserves the level sets of $\mathsf{tr}_\delta\big|_{\mathcal{Q}_L}$. Since $\mathsf{tr}_\delta\big|_{\mathcal{Q}_L}$ is a proper function by Proposition 5.3, M is compact. By the fact that $\mathcal{Q}_L$ is two–dimensional ([Gol90], also see Lemma 4.4), M is a compact one–dimensional manifold without boundary. Therefore M

is a topological circle. Once again, since M does not contain any fixed points, the Hamiltonian vector field restricted to M is bounded away from zero. This implies that the orbit is the whole level set M and is therefore periodic. □

5.4. **Numerical solutions to the Hamiltonian flow.** From Equation (19), we can explicitly write down the vector field associated to the trace function tr_δ in coordinates. Let $L \in \mathbb{R}^6_{>0}$ define a symplectic leaf $\mathcal{Q}_L$. By Equation (20), a path $(\sigma_1, \tau_1)\colon \mathbb{R} \to \mathcal{Q}_L$ is a flow line of the Hamiltonian flow of $\mathsf{tr}_\delta\big|_{\mathcal{Q}_L}$ if

$$\dot{\sigma}_1 = \frac{2}{\tau_1(\ell_{\alpha,1}^4\ell_{\alpha,2}^2\ell_{\beta,1}\ell_{\beta,2}^3\ell_{\gamma,1}^2\ell_{\gamma,2}^2)^{1/3}}\cdot$$
$$\Big(\sigma_1^3\left(\ell_{\alpha,2}\ell_{\beta,1}\ell_{\gamma,2}^{5/3}\left(\ell_{\alpha,1}\ell_{\beta,2}\ell_{\gamma,1}\right)^{2/3} - \tau_1^2\ell_{\gamma,2}\sqrt[3]{\ell_{\alpha,2}\ell_{\beta,1}}\right) +$$
$$\ell_{\alpha,1}\ell_{\beta,2}\left(\ell_{\alpha,2}\left(\ell_{\alpha,1}\ell_{\beta,2}\ell_{\gamma,1}\ell_{\gamma,2}\right)^{2/3} - \tau_1^2\ell_{\alpha,1}\ell_{\gamma,1}\sqrt[3]{\ell_{\alpha,2}\ell_{\beta,1}}\right) +$$
$$\sigma_1^2\Big(\ell_{\alpha,2}\ell_{\beta,1}\ell_{\gamma,2}^{5/3}\left(\ell_{\alpha,1}\ell_{\beta,2}\ell_{\gamma,1}\right)^{2/3} + \ell_{\alpha,1}\ell_{\beta,2}\ell_{\gamma,1}\ell_{\gamma,2}\sqrt[3]{\ell_{\alpha,2}^4\ell_{\beta,1}} + \sqrt[3]{\ell_{\alpha,1}^4\ell_{\alpha,2}^2\ell_{\beta,1}^2\ell_{\beta,2}^4\ell_{\gamma,1}\ell_{\gamma,2}^4} -$$
$$\tau_1^2\left(\ell_{\alpha,1}\ell_{\gamma,2}\sqrt[3]{\ell_{\alpha,2}\ell_{\beta,1}} + \left(\ell_{\alpha,1}\ell_{\beta,2}\ell_{\gamma,1}\ell_{\gamma,2}\right)^{2/3} + \sqrt[3]{\ell_{\alpha,1}\ell_{\alpha,2}^2\ell_{\beta,1}^2\ell_{\beta,2}\ell_{\gamma,1}\ell_{\gamma,2}}\right)\Big) +$$
$$\sigma_1\Big(\ell_{\alpha,2}\sqrt[3]{\ell_{\alpha,1}^5\ell_{\beta,2}^5\ell_{\gamma,1}^2\ell_{\gamma,2}^2} + \ell_{\alpha,1}\ell_{\beta,2}\ell_{\gamma,1}\ell_{\gamma,2}\sqrt[3]{\ell_{\alpha,2}^4\ell_{\beta,1}} + \sqrt[3]{\ell_{\alpha,1}^4\ell_{\alpha,2}^2\ell_{\beta,1}^2\ell_{\beta,2}^4\ell_{\gamma,1}\ell_{\gamma,2}^4} -$$
$$\tau_1^2\left(\ell_{\alpha,1}^{5/3}\left(\ell_{\beta,2}\ell_{\gamma,1}\ell_{\gamma,2}\right)^{2/3} + \ell_{\alpha,1}\ell_{\beta,2}\ell_{\gamma,1}\sqrt[3]{\ell_{\alpha,2}\ell_{\beta,1}} + \sqrt[3]{\ell_{\alpha,1}^4\ell_{\alpha,2}^2\ell_{\beta,1}^2\ell_{\beta,2}\ell_{\gamma,1}\ell_{\gamma,2}}\right)\Big)\Big)$$

and

$$\dot{\tau}_1 = \frac{2}{\sigma_1\ell_{\beta,2}\sqrt[3]{\ell_{\alpha,1}^4\ell_{\alpha,2}^2\ell_{\beta,1}\ell_{\gamma,1}^2\ell_{\gamma,2}^2}}\cdot$$
$$\Big(2\sigma_1^3\ell_{\alpha,2}\ell_{\beta,1}\ell_{\gamma,2}^{5/3}\left(\ell_{\alpha,1}\ell_{\beta,2}\ell_{\gamma,1}\right)^{2/3} - \ell_{\alpha,2}\sqrt[3]{\ell_{\alpha,1}^5\ell_{\beta,2}^5\ell_{\gamma,1}^2\ell_{\gamma,2}^2} +$$
$$\sigma_1^2\left(\ell_{\alpha,2}\ell_{\beta,1}\ell_{\gamma,2}^{5/3}\left(\ell_{\alpha,1}\ell_{\beta,2}\ell_{\gamma,1}\right)^{2/3} + \ell_{\alpha,1}\ell_{\beta,2}\ell_{\gamma,1}\ell_{\gamma,2}\sqrt[3]{\ell_{\alpha,2}^4\ell_{\beta,1}} + \sqrt[3]{\ell_{\alpha,1}^4\ell_{\alpha,2}^2\ell_{\beta,1}^2\ell_{\beta,2}^4\ell_{\gamma,1}\ell_{\gamma,2}^4}\right) +$$
$$\tau_1^2\Big(\sigma_1^2\ell_{\alpha,1}\ell_{\gamma,2}\sqrt[3]{\ell_{\alpha,2}\ell_{\beta,1}} - \ell_{\alpha,1}^2\ell_{\beta,2}\ell_{\gamma,1}\sqrt[3]{\ell_{\alpha,2}\ell_{\beta,1}} + \sigma_1^2\ell_{\alpha,1}\ell_{\gamma,2}\sqrt[3]{\ell_{\alpha,2}\ell_{\beta,1}} +$$
$$\sigma_1^2\left(2\sigma_1\ell_{\gamma,2}\sqrt[3]{\ell_{\alpha,2}\ell_{\beta,1}} + \left(\ell_{\alpha,1}\ell_{\beta,2}\ell_{\gamma,1}\ell_{\gamma,2}\right)^{2/3} + \sqrt[3]{\ell_{\alpha,1}\ell_{\alpha,2}^2\ell_{\beta,1}^2\ell_{\beta,2}\ell_{\gamma,1}\ell_{\gamma,2}}\right)\Big) +$$
$$\tau_1\Big(\sigma_1^2\ell_{\alpha,1}\ell_{\beta,2}\left(\ell_{\gamma,1}+1\right)\ell_{\gamma,2}\sqrt[3]{\ell_{\alpha,2}\ell_{\beta,1}} - \ell_{\alpha,1}^2\ell_{\beta,2}\ell_{\gamma,1}\sqrt[3]{\ell_{\alpha,2}\ell_{\beta,1}} - \ell_{\alpha,2}\sqrt[3]{\ell_{\alpha,1}^5\ell_{\beta,2}^5\ell_{\gamma,1}^2\ell_{\gamma,2}^2} +$$
$$4\sigma_1^3\sqrt[3]{\ell_{\alpha,1}\ell_{\alpha,2}^2\ell_{\beta,1}^2\ell_{\beta,2}\ell_{\gamma,1}\ell_{\gamma,2}^4} + \sigma_1^2\Big(\ell_{\alpha,2}\left(\ell_{\beta,1}+1\right)\left(\ell_{\alpha,1}\ell_{\beta,2}\ell_{\gamma,1}\ell_{\gamma,2}\right)^{2/3} +$$
$$\sqrt[3]{\ell_{\alpha,1}\ell_{\alpha,2}^2\ell_{\beta,1}^2\ell_{\beta,2}\ell_{\gamma,1}\ell_{\gamma,2}^4} + \sqrt[3]{\ell_{\alpha,1}^4\ell_{\alpha,2}^2\ell_{\beta,1}^2\ell_{\beta,2}\ell_{\gamma,1}\ell_{\gamma,2}^4}\Big)\Big)\Big).$$

We supressed the dependence of σ_1 and τ_1 on t to make the expressions (mildly) more readable. This equation is computed in Section 5 of the Mathematica code by giving the function `HamiltonianVF` the input function `traceFigure8`.

These are coupled ordinary differential equations, and after some attempts with Mathematica, we were not able to find a closed form solution. In Section 6 we focus on the unipotent locus to have much more simple differential equations, but we were still unable to solve the system of equations symbolically.

However, it is possible to solve the system of differential equations numerically on given symplectic leaves and given initial conditions. We will pick symplectic leaves containing a Fuchsian structure. As in Section 4.3, we let $F = (\ell_\alpha = 3, \ell_\beta = 6, \ell_\gamma = 8)$, which defines a symplectic leaf $\mathcal{Q}_{L(F)}$, and whose Fuchsian representation, in coordinates σ_1, τ_1 as in Lemma 4.4 and from Equation (14), is given by $(\sigma_1^F = 2, \tau_1^F = 1)$. The system of ordinary differential equations describing the Hamiltonian vector field of $\mathsf{tr}_\delta\big|_{\mathcal{Q}_{L(F)}}$ reads (once again suppressing the dependence of the coordinates on t):

$$\begin{cases} \dot{\sigma}_1 &= \dfrac{-6\sigma_1^3\left(\tau_1^2-1\right)+\sigma_1^2\left(17-90\tau_1^2\right)+\sigma_1\left(15-408\tau_1^2\right)-576\tau_1^2+4}{12\tau_1} \\ \dot{\tau}_1 &= \dfrac{(\tau_1+1)\left(12\sigma_1^3(\tau_1+1)+\sigma_1^2(90\tau_1+17)-576\tau_1-4\right)}{12\sigma_1} \end{cases} \tag{21}$$

This equation is computed in Section 5 of the Mathematica code by giving the function `HamiltonianVF` the input function `traceFigure8` with the length vector `3,1/3,6,1/6,8,1/8,1,1`. The numerical solution with initial condition at the Fuchsian locus $(2,1)$ is shown in Figure 9, where we see the periodicity of the flow. We can also see that the Fuchsian structure is not fixed. The level sets of the function $\mathsf{tr}_\delta\big|_{\mathcal{Q}_{L(F)}}$ are shown in Figure 10, where we see that the orbits are closed.

Remark 5.6. Since every orbit is periodic, one may wonder whether the orbits all have the same length and there is a circle action associated to the trace function. However, this is *not* the case with the trace function, as we see in Figure 11.

5.5. **Trace of the Θ–web.** We now prove Corollary B. This is an application of Theorem 5.1 where we show that an analogous version of the theorem holds when tr_δ is replaced by the trace of the Θ–web m_Θ.

A *web* is an embedded 3–regular bipartite graph on the surface P^2. Given a representation $\rho\colon \pi_1(P) \to \mathsf{PSL}(3,\mathbb{R})$ and a web m, [Sik01, Section 4] and [DKS24] define the *trace of the web* m, written as $\mathsf{tr}_m(\rho)$, which is invariant under conjugation. The definition of the trace of a web is in terms of tensor networks, and we do not recall the general definition here. Instead, we give the formula for a specific web.

[2]When considering representations from $\pi_1(P) \to \mathsf{PSL}(d,\mathbb{R})$, [DKS24] define d–webs. Since we are working in the $\mathsf{PSL}(3,\mathbb{R})$ case, we refer to a 3–web simply as a web.

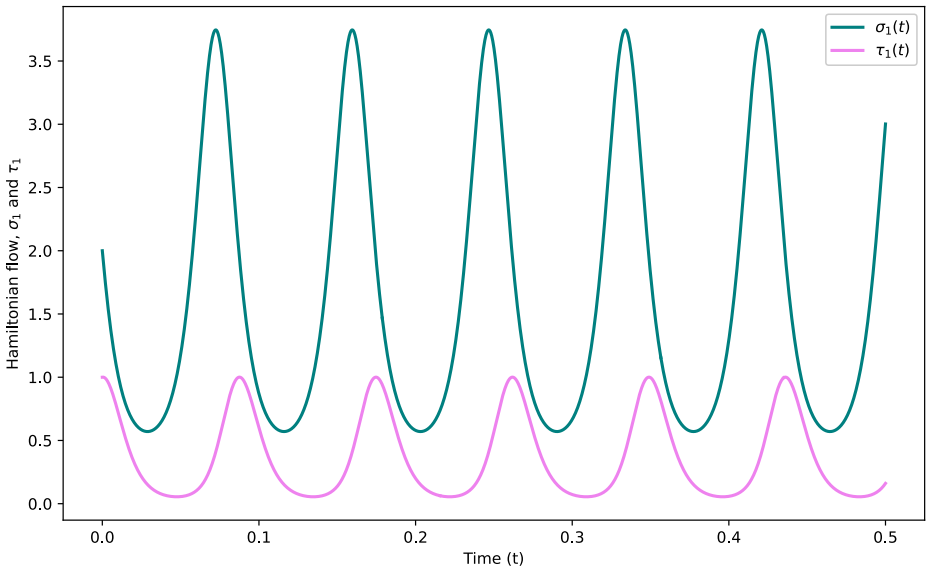

FIGURE 9. Numerical solution to the system of equations (21) with initial condition $(2, 1)$ at the Fuchsian structure.

Let m_Θ be the web with one black and one white vertex, with three edges between them each of multiplicity 1, as in Figure 3. The trace of m_Θ is computed in Section 6.2 of [DKS24] to be

$$\begin{aligned} \mathsf{tr}_{m_\Theta} \colon \mathscr{X}_3(S) &\to \mathbb{R} \\ [\rho] &\mapsto \mathsf{tr}(\rho(\alpha))\mathsf{tr}(\rho(\gamma)) - \mathsf{tr}(\rho(\alpha\gamma^{-1})). \end{aligned}$$

For any $L \in \mathbb{R}^6_{>0}$ there is an induced map

$$\begin{aligned} \widehat{\mathsf{tr}}_{m_\Theta} \colon \mathcal{Q}_L &\to \mathbb{R} \\ [f, \Sigma, \nu] &\mapsto \mathsf{tr}_{m_\Theta}(\vartheta([f, \Sigma, \nu])). \end{aligned}$$

By Lemma 4.6, the quantity $\mathsf{tr}(\rho(\alpha))\mathsf{tr}(\rho(\gamma))$ is constant on the symplectic leaf $\mathcal{Q}_L$; denote this constant by C_L. The trace of the Θ–web is thus given by $[\rho] \mapsto C_L - \mathsf{tr}(\rho(\delta))$, where $\delta = \alpha\gamma^{-1}$ is the figure eight curve from this section. The following is then a direct corollary of Theorem 5.1.

Corollary 5.7. *Let m_Θ be the Θ–web on a pair of pants P. Then for any $L \in \mathbb{R}^6_{>0}$, the trace function $\mathsf{tr}_{m_\Theta}\big|_{\mathcal{Q}_L} \colon \mathcal{Q}_L \to \mathbb{R}$ attains a unique maximum. Moreover, every orbit of the Hamiltonian flow of $\mathsf{tr}_{m_\Theta}\big|_{\mathcal{Q}_L}$ is periodic and there is a unique fixed point.*

5.6. **The symmetrized trace.** In this section, we adress Theorem C. The strategy for the proof is identical to that of Theorem 5.1. Since the computations are very similar to the ones done above, we delay the proof of Theorem C, Part a to Appendix A. Here we prove Part b of Theorem C, which we restate now in more detail.

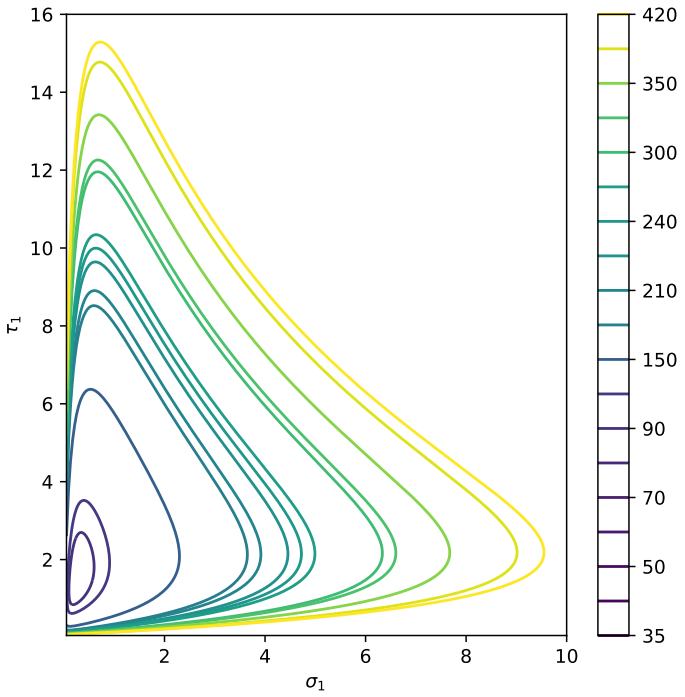

FIGURE 10. Level sets of the function $\mathsf{tr}_\delta\big|_{\mathcal{Q}_{L(F)}}$ for $F = (3, 6, 8)$.

Theorem 5.8. *Let $\delta = \alpha\gamma^{-1}$ be the figure eight curve. Let $F = (\ell_\alpha, \ell_\beta, \ell_\gamma) \in \mathbb{R}^3_{>0}$ define the length vector $L(F) \in \mathbb{R}^6_{>0}$ as in Equation (13). Let $\mathcal{Q}_{L(F)}$ be the symplectic leaf associated to $L(F)$. Then the unique fixed point of the Hamiltonian flow of the function $\mathsf{tr}_\delta + \mathsf{tr}_{\delta^{-1}}\big|_{\mathcal{Q}_F}$ is the unique hyperbolic structure in $\mathcal{Q}_{L(F)}$; which in coordinates is given by*

$$\left(\sqrt{\frac{\ell_\alpha\ell_\gamma}{\ell_\beta}}, \sqrt{\frac{\ell_\beta}{\ell_\alpha\ell_\gamma}}, \sqrt{\frac{\ell_\alpha\ell_\beta}{\ell_\gamma}}, \sqrt{\frac{\ell_\gamma}{\ell_\alpha\ell_\beta}}, \sqrt{\frac{\ell_\beta\ell_\gamma}{\ell_\alpha}}, \sqrt{\frac{\ell_\alpha}{\ell_\beta\ell_\gamma}}, 1, 1\right).$$

Proof. By Part a of Theorem C, we know that the Hamiltonian flow of $\mathsf{tr}_\delta + \mathsf{tr}_{\delta^{-1}}\big|_{\mathcal{Q}_{L(F)}}$ has a unique fixed point. Hence, we only need to show that at the hyperbolic structure, the Hamiltonian vector field is zero. Indeed, using Section 5 of the Mathematica code, we compute that the Hamiltonian vector field is given by

$$\dot{\sigma}_1 = -\frac{1}{\sigma_1\tau_1\ell_\alpha\ell_\beta\ell_\gamma}\cdot$$
$$2\big(\sigma_1^2\ell_\beta\left(\ell_\gamma\left(\sigma_1\left(\tau_1^2\ell_\beta - 1\right) + \tau_1^2 - 1\right) + \sigma_1\left(\left(\sigma_1\left(\tau_1^2 - 1\right) - 1\right)\ell_\beta + \tau_1^2\right)\right) +$$
$$\ell_\alpha^2\ell_\gamma\left(\ell_\gamma\left(\sigma_1\left(\tau_1^2\ell_\beta - 1\right) + \tau_1^2 - 1\right) + \sigma_1\left(\left(\sigma_1\left(\tau_1^2 - 1\right) - 1\right)\ell_\beta + \tau_1^2\right)\right) +$$
$$\sigma_1\ell_\alpha\big(\ell_\gamma\left(\sigma_1^2\ell_\beta\left(\tau_1^2 - \ell_\beta\right) + \sigma_1\left(\tau_1^2 - 1\right)\left(\ell_\beta^2 + 1\right) + \tau_1^2\ell_\beta - 1\right) +$$

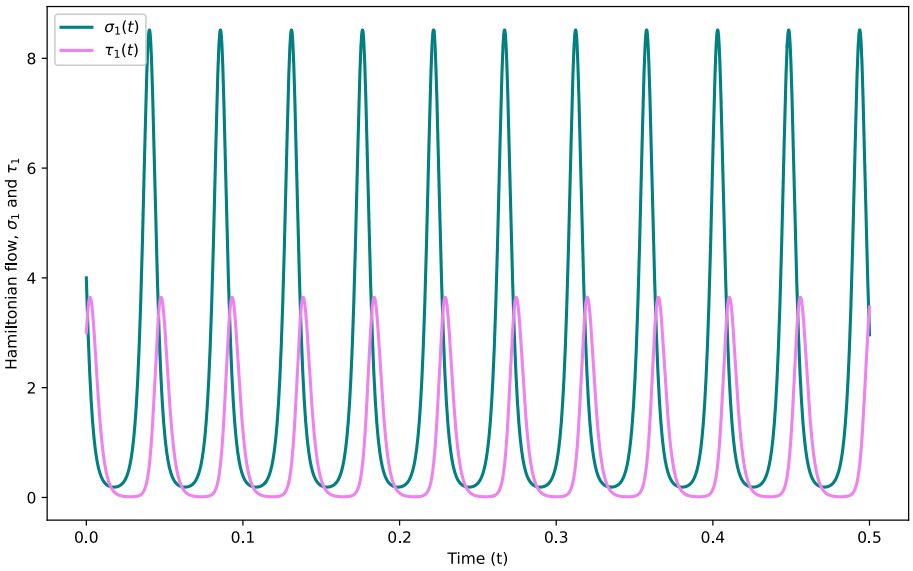

FIGURE 11. Numerical solution to the system of equations (21) with initial conditions $(4, 3)$.

$$\ell_\gamma^2\left(\tau_1^2+\left(\sigma_1\left(\tau_1^2-1\right)-1\right)\ell_\beta\right)+\sigma_1\ell_\beta\left(\tau_1^2+\sigma_1\left(\tau_1^2\ell_\beta-1\right)-1\right)\big)\big),$$

and

$$\begin{aligned}\dot{\tau}=-\frac{2\left(\tau_1+1\right)}{\sigma_1^2\ell_\alpha\ell_\beta\ell_\gamma}\big(&\sigma_1^3\left(-\ell_\beta\right)\left(\tau_1+\tau_1\ell_\beta\ell_\gamma+2\sigma_1\left(\tau_1+1\right)\ell_\beta+\ell_\beta+\ell_\gamma\right)+\\&\sigma_1\ell_\alpha\left(\ell_\gamma-\sigma_1^2\ell_\beta\right)\left(\ell_\beta\left(\tau_1+\ell_\gamma\right)+\tau_1\ell_\gamma+1\right)+\\&\ell_\alpha^2\ell_\gamma\left(\ell_\gamma\left(\sigma_1+2\tau_1+\sigma_1\tau_1\ell_\beta+2\right)+\sigma_1\left(\tau_1+\ell_\beta\right)\right)\big).\end{aligned}$$

A computation in Mathematica then shows that at the values

$$(\sigma_1,\tau_1)=\left(\sqrt{\frac{\ell_\alpha\ell_\gamma}{\ell_\beta}},1\right)$$

make the two above expressions zero. □

6. THE UNIPOTENT LOCUS

In this section, we focus on the symplectic leaf of $\widehat{\mathfrak{C}}(P)$ corresponding to the convex projective structures where all boundaries are cuspidal.

By Lemma 4.4, we see that the unipotent locus is parameterized as

$$\mathfrak{U} = \left\{ \left(\sigma_1, \frac{1}{\sigma_1}, \sigma_1, \frac{1}{\sigma_1}, \sigma_1, \frac{1}{\sigma_1}, \tau_1, \frac{1}{\tau_1} \right) \in \mathbb{R}^8_{>0} : \ \sigma_1, \tau_1 > 0 \right\}.$$

The expressions for traces of curves simplify significantly in this case, and allow us to prove similar results to Theorem 5.1 for a larger class of self–intersecting curves. Namely, we prove Theorem G, which is a version of Theorem 5.1 for the commutator $[\alpha, \gamma]$ and the curve $\alpha^k \gamma^{-1}$ for $k \geq 2$, when restricted to the unipotent locus. Moreover, we find the fixed points of the respective Hamiltonian flows.

As another application of the simplicity of the expressions, we find another way of writing the Hamiltonian flows $\widehat{\Phi}_{\mathcal{E}}$ and $\widehat{\Phi}_{\mathcal{I}}$, which we do in Section 6.3.

6.1. **The commutator.** The first self–intersecting curve we consider apart from the figure eight curve, is the commutator shown in Figure 12.

Following the same proof of Theorem A in Section 5, we show the following.

Theorem 6.1. *The trace function* $\mathsf{tr}_{[\alpha,\gamma]}\big|_{\mathfrak{U}} \colon \mathfrak{U} \to \mathbb{R}$ *attains a unique minimum. Moreover, every orbit of the Hamiltonian flow of* $\mathsf{tr}_{[\alpha,\gamma]}\big|_{\mathfrak{U}}$ *is periodic and there is a unique fixed point.*

Following the same structure as that of Section 5, we begin by using Mathematica to compute the expression for the trace of the commutator on the unipotent locus.

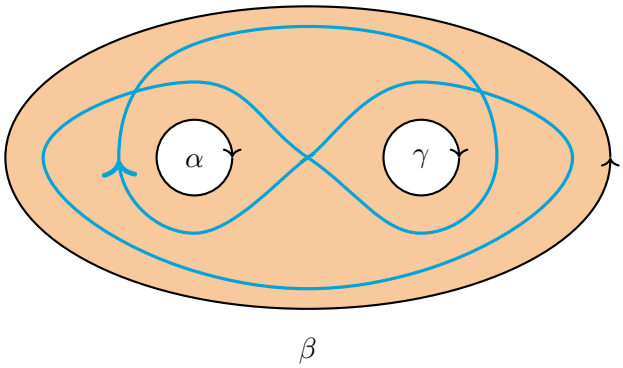

FIGURE 12. The commutator $[\alpha, \gamma]$.

Lemma 6.2. *In coordinates, we have that*

$$\mathsf{tr}_{[\alpha,\gamma]}\big|_{\mathfrak{U}} \colon \mathfrak{U} \to \mathbb{R}$$

$$\begin{aligned}(\sigma_1, \tau_1) \mapsto \frac{1}{\sigma_1^3 \tau_1} \big(& \sigma_1^6 (\tau_1 + 1)^3 + 3\sigma_1^5 (\tau_1 + 1)^2 (2\tau_1 + 1) + 3\sigma_1^4 (\tau_1 + 1)^2 (5\tau_1 + 1) \\ & + \sigma_1^3 \left(20\tau_1^3 + 42\tau_1^2 + 27\tau_1 + 2 \right) + 3\sigma_1^2 (\tau_1 + 1)^2 (5\tau_1 + 1) \\ & + 3\sigma_1 (\tau_1 + 1)^2 (2\tau_1 + 1) + (\tau_1 + 1)^3 \big)\end{aligned}$$

This is computed in Section 4 of the Mathematica code by displaying the function `traceCommutator` with length vector `1,1,1,1,1,1`. With this expression, we move on to show properness.

Proposition 6.3. *The function* $\mathsf{tr}_{[\alpha,\gamma]}\big|_{\mathfrak{U}}\colon \mathfrak{U} \to \mathbb{R}$ *is proper. In particular, it realizes a minimum in* $\mathfrak{U}$.

Proof. Similarly to the proof of Proposition 5.3, let $(\sigma_{1,n}, \tau_{1,n})_{n\in\mathbb{N}}$ be a sequence such that as n goes to ∞, $(\sigma_{1,n}, \tau_{1,n})$ goes to a tuple in $\{(\infty,\infty),(0,\infty),(\infty,0),(x,0),(0,y) : x,y \geq 0\}$. We need to show that for any of these options, $\mathsf{tr}_{[\alpha,\gamma]}(\sigma_{1,n}, \tau_{1.n}) \to \infty$ as $n \to \infty$. Once again, since the function is positive and all signs in front of the monomials are positive, we only need to find single terms in the expression for the trace going to ∞:

(a) Assume $(\sigma_{1,n}, \tau_{1,n}) \to (\infty,\infty)$, then the term
$$\frac{\sigma_{1,n}^6 \tau_{1,n}^3}{\sigma_{1,n}^3 \tau_{1,n}} \xrightarrow{n\to\infty} \infty.$$

(b) Assume $(\sigma_{1,n}, \tau_{1,n}) \to (0,\infty)$, then the term
$$\frac{20\sigma_{1,n}^3 \tau_{1,n}^3}{\sigma_{1,n}^3 \tau_{1,n}} \xrightarrow{n\to\infty} \infty.$$

(c) Assume $(\sigma_{1,n}, \tau_{1,n}) \to (\infty,0)$, then the term
$$\frac{\sigma_{1,n}^6}{\sigma_{1,n}^3 \tau_{1,n}} \xrightarrow{n\to\infty} \infty.$$

(d) Assume $(\sigma_{1,n}, \tau_{1,n}) \to (x,0)$ or $(0,y)$ for $x,y \geq 0$, then the term
$$\frac{1}{\sigma_{1,n}^3 \tau_{1,n}} \xrightarrow{n\to\infty} \infty.$$

This shows that the function $\mathsf{tr}_{[\alpha,\gamma]}\big|_{\mathfrak{U}}\colon \mathfrak{U} \to \mathbb{R}$ is proper. Since the function is also strictly positive, it attains a minimum. □

The next step in the proof of Theorem 6.1 is to show convexity along any mixed flow.

Proposition 6.4. *The function* $\mathsf{tr}_{[\alpha,\gamma]}\big|_{\mathfrak{U}}\colon \mathfrak{U} \to \mathbb{R}$ *is strictly convex along any mixed flow.*

Proof. Consider first the mixed flow $\Psi_a^t = \widehat{\Phi}_{\mathcal{E}}^{at} \circ \widehat{\Phi}_{\mathcal{I}}^{t}$. In Section 6 of the Mathematica code, set `testf` equal to `traceCommutator` using the length vector `1,1,1,1,1,1`. Then inputting the function `testfMix1` to `SecondDerFlow`, we obtain that
$$\frac{\partial^2}{\partial t^2}(\mathsf{tr}_{[\alpha,\gamma]}(\Psi_a^t(\sigma_1,\tau_1))) = \frac{e^{-at}(1+\sigma_1)^4 a^2}{\sigma_1^3\tau_1}\cdot$$
$$\left(3e^{2at}\tau_1^2 + 4e^{3at}\tau_1^3 + 3\sigma_1^2\tau_1^2 e^{2at} + 4\sigma_1^2\tau_1^3 e^{3at} + 3\sigma_1\tau_1^2 e^{2at} + 8\sigma_1\tau_1^3 e^{3at} + \sigma_1 + (\sigma_1-1)^2\right).$$

We observe that for any $a \in \mathbb{R}$ and $t \in \mathbb{R}$, and any σ_1, τ_1, the above expression is positive. Hence $t \mapsto \mathsf{tr}_{[\alpha,\gamma]}\big|_{\mathfrak{U}}(\Psi_a^t(\sigma_1,\tau_1))$ is a strictly convex function.

Now consider the other mixed flow $\Psi_a^t = \widehat{\Phi}_{\mathcal{I}}^{at} \circ \widehat{\Phi}_{\mathcal{E}}^t$. In Section 6 of the Mathematica code, set `testf` equal to `traceCommutator` using the length vector `1,1,1,1,1,1`. Then inputting the function `testfMix2` to `SecondDerFlow`, we obtain that

$$\begin{aligned}\frac{\partial^2}{\partial t^2}(\mathsf{tr}_{[\alpha,\gamma]}(\Psi_a^t(\sigma_1,\tau_1))) &= 21a^2\sigma_1 e^{at} + \frac{21a^2e^{-at}}{\sigma_1} + \frac{48a^2e^{-2at}}{\sigma_1^2} + \frac{27a^2e^{-3at}}{\sigma_1^3} \\ &+\frac{3a^2e^{-at}}{\sigma_1\tau_1} + \frac{12a^2e^{-2at}}{\sigma_1^2\tau_1} + \frac{9a^2e^{-3at}}{\sigma_1^3\tau_1} + 27a^2\sigma_1^3e^{3at} + 48a^2\sigma_1^2e^{2at} \\ &+\frac{9a^2\sigma_1^3e^{3at}}{\tau_1} + \frac{12a^2\sigma_1^2e^{2at}}{\tau_1} + \frac{3a^2\sigma_1 e^{at}}{\tau_1} + \frac{27a^2\tau_1e^{-3at}}{\sigma_1^3} \\ &+60a^2\sigma_1^2\tau_1e^{2at} + 33a^2\sigma_1\tau_1e^{at} + \frac{33a^2\tau_1e^{-at}}{\sigma_1} + \frac{60a^2\tau_1e^{-2at}}{\sigma_1^2} \\ &+27a^2\sigma_1^3\tau_1e^{3at} + \frac{15a^2\tau_1^2e^{-at}}{\sigma_1} + \frac{24a^2\tau_1^2e^{-2at}}{\sigma_1^2} + \frac{9a^2\tau_1^2e^{-3at}}{\sigma_1^3} \\ &+9a^2\sigma_1^3\tau_1^2e^{3at} + 24a^2\sigma_1^2\tau_1^2e^{2at} + 15a^2\sigma_1\tau_1^2e^{at}\end{aligned}$$

We observe again that for any $a \in \mathbb{R}$ and $t \in \mathbb{R}$, and any σ_1, τ_1, the above expression is positive. Hence $t \mapsto \mathsf{tr}_{[\alpha,\gamma]}\big|_{\mathfrak{U}}(\Psi_a^t(\sigma_1,\tau_1))$ is a strictly convex function. □

The proof of Theorem 6.1 then is identical to the proof of Theorem 5.1 in Section 5.3.

The system of differential equations associated to the function $\mathsf{tr}_{[\alpha,\gamma]}\big|_{\mathfrak{U}}$ is given by

$$\begin{cases}\dot{\sigma}_1 = \dfrac{2\left(\sigma_1+1\right)^4\left(\tau_1+1\right)\left(\sigma_1^2\left(2\tau_1^2+\tau_1-1\right)+\sigma_1\left(4\tau_1^2-\tau_1+1\right)+2\tau_1^2+\tau_1-1\right)}{\sigma_1^2\tau_1} \\ \dot{\tau}_1 = \dfrac{6\left(\sigma_1-1\right)\left(\sigma_1+1\right)^3\left(\tau_1+1\right)^2\left(\sigma_1^2\left(\tau_1+1\right)+2\sigma_1\tau_1+\tau_1+1\right)}{\sigma_1^3}\end{cases} \tag{22}$$

This is computed by taking as input to the function `HamiltonianVF` in Section 5 of the Mathematica code, the function `traceCommutator` with length vector `1,1,1,1,1,1`. Once again, a symbolic solution to the differential equation was not possible for us, and we show in Figure 13 a numerical solution. In Figure 14 we show some level sets for the trace function of the commutator on the unipotent locus.

By Theorem 6.1, the function $\mathsf{tr}_{[\alpha,\gamma]}|_{\mathfrak{U}}$ has a unique fixed point, and from the differential equation (22) coming from the Hamiltonian vector field, we immediately obtain the following.

Corollary 6.5. *The fixed point of the Hamiltonian flow of the function* $\mathsf{tr}_{[\alpha,\gamma]}\big|_{\mathfrak{U}}$ *is*

$$(\sigma_1,\tau_1) = \left(1, \frac{\sqrt{33}-1}{16}\right).$$

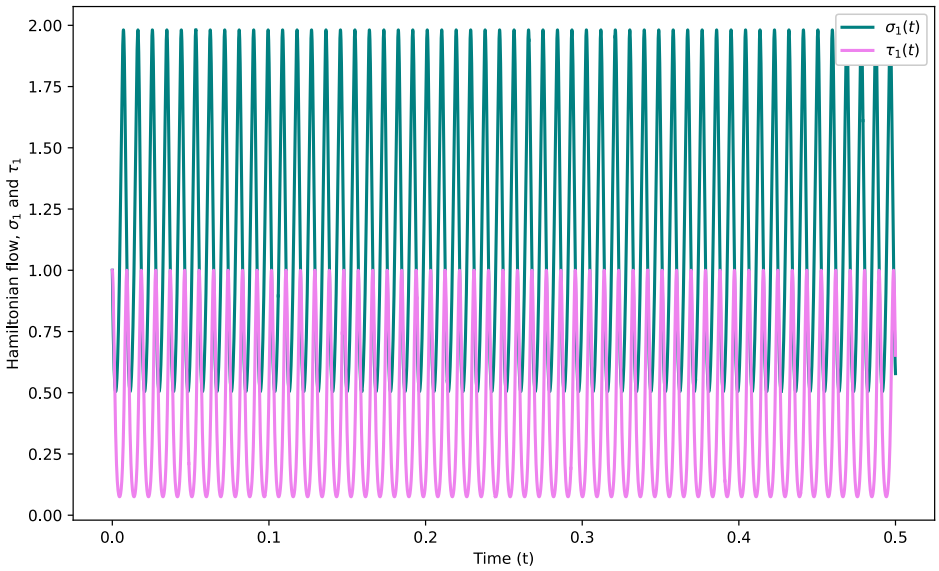

FIGURE 13. Numerical solution to the Hamiltonian flow of $\mathsf{tr}_{[\alpha,\gamma]}\big|_{\mathfrak{U}}$ with initial conditions at the Fuchsian structure $(1,1)$.

This value is also the minimum of the function.

6.2. **Curve with k–self intersections.** Similarly as above, we have the following result for a curve with k–self intersections as in Figure 15.

Theorem 6.6. *Let $k \in \mathbb{N}_{>0}$. The function $\mathsf{tr}_{\alpha^k\gamma^{-1}}\big|_{\mathfrak{U}} \colon \mathfrak{U} \to \mathbb{R}$ attains a unique minimum. Moreover, every orbit of the Hamiltonian flow of $\mathsf{tr}_{\alpha^k\gamma^{-1}}\big|_{\mathfrak{U}}$ is periodic and there is a unique fixed point.*

We begin with a lemma expressing the trace of $\alpha^k\gamma^{-1}$ in the unipotent locus in coordinates.

Lemma 6.7. *In coordinates, we have that*

$$\begin{aligned} \mathsf{tr}_{\alpha^k\gamma^{-1}}\big|_{\mathfrak{U}} \colon \mathfrak{U} &\to \mathbb{R} \\ (\sigma_1,\tau_1) &\mapsto \frac{k^2\,(\sigma_1+1)^{\,3}\,(\tau_1+1)^{\,2} + k\,(\sigma_1+1)^{\,3}\,(\tau_1+1)^{\,2} + 6\sigma_1\tau_1}{2\sigma_1\tau_1} \end{aligned}$$

This is computed in Section 7 of the Mathematica code. We can now show properness.

Proposition 6.8. *The function $\mathsf{tr}_{\alpha^k\gamma^{-1}}\big|_{\mathfrak{U}} \colon \mathfrak{U} \to \mathbb{R}$ is proper for any $k \in \mathbb{N}_{>0}$. In particular, it realizes a minimum in $\mathfrak{U}$.*

Proof. Similarly to the proof of Proposition 5.3, let $(\sigma_{1,n},\tau_{1,n})_{n\in\mathbb{N}}$ be a sequence such that as n goes to ∞, $(\sigma_{1,n},\tau_{1,n})$ goes to a tuple in $\{(\infty,\infty),(0,\infty),(\infty,0),(x,0),(0,y) : x,y \geq 0\}$. As above we show the following.

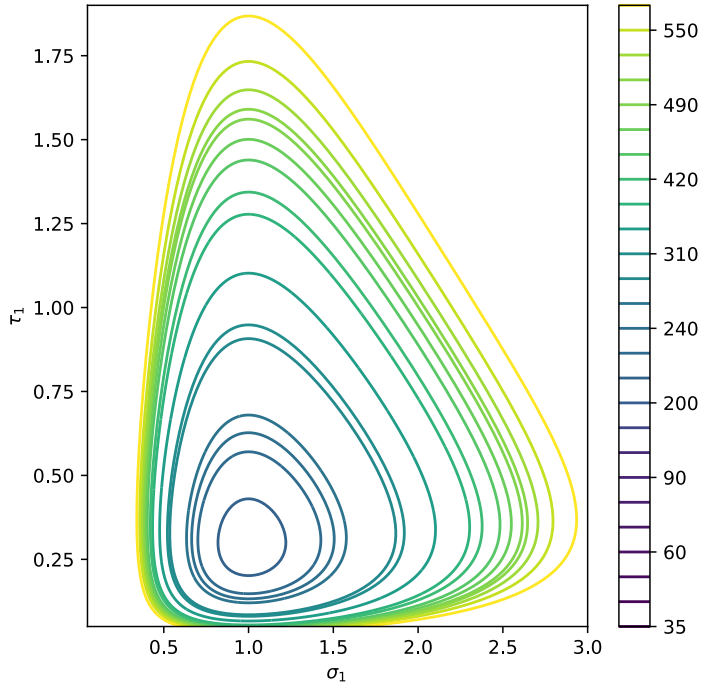

FIGURE 14. Level sets of the function $\mathsf{tr}_{[\alpha,\gamma]}\big|_{\mathfrak{U}}$.

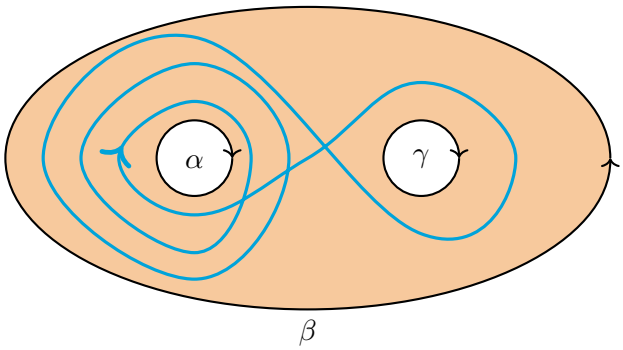

FIGURE 15. An example of the curve $\alpha^k\gamma^{-1}$ with $k=3$.

(a) Assume $(\sigma_{1,n},\tau_{1,n})\to(\infty,\infty)$, then the term

$$\frac{k^2\sigma_{1,n}^3\tau_{1,n}^2}{2\sigma_{1,n}\tau_{1,n}} \xrightarrow{n\to\infty} \infty.$$

(b) Assume $(\sigma_{1,n}, \tau_{1,n}) \to (\infty, 0)$, then the term

$$\frac{k^2\sigma_{1,n}^3}{2\sigma_{1,n}\tau_{1,n}} \xrightarrow{n\to\infty} \infty.$$

(c) Assume $(\sigma_{1,n}, \tau_{1,n}) \to (0, \infty)$, then the term

$$\frac{k^2\tau_{1,n}^2}{2\sigma_{1,n}\tau_{1,n}} \xrightarrow{n\to\infty} \infty.$$

(d) Assume $(\sigma_{1,n}, \tau_{1,n}) \to (x, 0)$ or $(0, y)$ for $x, y \geq 0$, then the term

$$\frac{k^2}{2\sigma_{1,n}\tau_{1,n}} \xrightarrow{n\to\infty} \infty.$$

This shows that the function $\mathsf{tr}_{\alpha^k\gamma^{-1}}\big|_{\mathfrak{U}} \colon \mathfrak{U} \to \mathbb{R}$ is proper. Since the function is strictly positive, it attains a minimum. □

The next step in the proof of Theorem 6.6 is to show convexity along any mixed flow.

Proposition 6.9. *For any $k \in \mathbb{N}_{>0}$, the function $\mathsf{tr}_{\alpha^k\gamma^{-1}}\big|_{\mathfrak{U}}$ is strictly convex along any mixed flow.*

Proof. Consider first the mixed flow $\Psi_a^t = \widehat{\Phi}_{\mathcal{E}}^{at} \circ \widehat{\Phi}_{\mathcal{I}}^{t}$. In Section 7 of the Mathematica code, take as input to the function `SecondDerFlowK` the function `testfMix1K` to get that

$$\frac{\partial^2}{\partial t^2}(\mathsf{tr}_{\alpha^k\gamma^{-1}}(\Psi_a^t(\sigma_1, \tau_1))) = \frac{a^2k(k+1)\,(\sigma_1+1)^{\,3}e^{-at}\left(\tau_1^2e^{2at}+1\right)}{2\sigma_1\tau_1}.$$

For any $a \in \mathbb{R}$, and $t \in \mathbb{R}$ the second derivative is strictly positive, and hence the function $t \mapsto \mathsf{tr}_{\alpha^k\gamma^{-1}}\big|_{\mathfrak{U}}(\Psi_a^t(\sigma_1, \tau_1))$ is strictly convex.

Now consider the other mixed flow $\Psi_a^t = \widehat{\Phi}_{\mathcal{E}}^{t} \circ \widehat{\Phi}_{\mathcal{I}}^{at}$. In Section 7 of the Mathematica code, take as input to the function `SecondDerFlowK` the function `testfMix2K` to get that

$$\frac{\partial^2}{\partial t^2}(\mathsf{tr}_{\alpha^k\gamma^{-1}}(\Psi_a^t(\sigma_1, \tau_1))) = \frac{a^2k(k+1)\,(\tau_1+1)^{\,2}e^{-at}\left(4\sigma_1^3e^{3at}+3\sigma_1^2e^{2at}+1\right)}{2\sigma_1\tau_1}.$$

This quantity is positive and hence the function $t \mapsto \mathsf{tr}_{\alpha^k\gamma^{-1}}\big|_{\mathfrak{U}}(\Psi_a^t(\sigma_1, \tau_1))$ is strictly convex. □

The proof of Theorem 6.6 then is identical to the proof of Theorem 5.1 in Section 5.3. The system of differential equations associated to the function $\mathsf{tr}_{\alpha^k\gamma^{-1}}\big|_{\mathfrak{U}}$ is given by

$$\begin{cases} \dot{\sigma}_1 &= -\dfrac{k(k+1)\,(\sigma_1+1)^{\,3}\left(\tau_1^2-1\right)}{\tau_1} \\ \dot{\tau}_1 &= \dfrac{k(k+1)\,(\sigma_1+1)^{\,2}\,(2\sigma_1-1)\,(\tau_1+1)^{\,2}}{\sigma_1} \end{cases} \tag{23}$$

This is computed at the end of Section 7 of the Mathematica code. Once again, a symbolic solution (even for the case $k = 1$) was not possible for us, and we show in Figure

16 a numerical solution for the case $k = 3$. In Figure 17 we show the level sets for the case $k = 3$, and Figure 2 shows level sets for the case $k = 1$, i.e. for the figure eight curve.

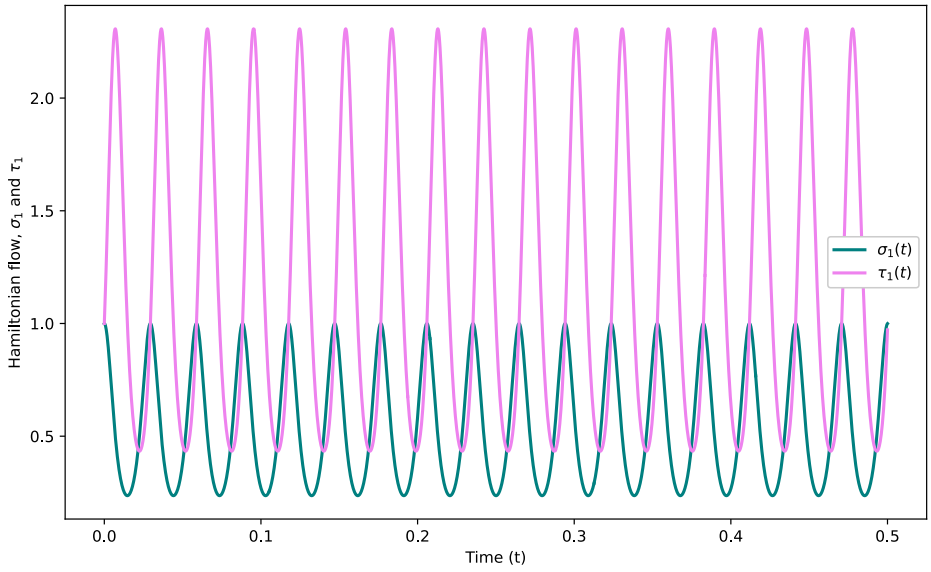

FIGURE 16. Numerical solution to $\mathsf{tr}_{\alpha^3\gamma^{-1}}\big|_{\mathfrak{U}}$ with initial condition at the Fuchsian structure $(1, 1)$.

By Theorem 6.6, the function $\mathsf{tr}_{\alpha^k\gamma^{-1}}|_{\mathfrak{U}}$ has a unique fixed point, and from the differential equation (23) coming from the Hamiltonian vector field, we immediately obtain the following.

Corollary 6.10. *Let $k \in \mathbb{N}_{>0}$. The fixed point of the Hamiltonian flow of the function $\mathsf{tr}_{\alpha^k\gamma^{-1}}\big|_{\mathfrak{U}}$ is*

$$(\sigma_1, \tau_1) = \left(\frac{1}{2}, 1\right).$$

This value is also the minimum of the function. In particular, it does not depend on k.

6.3. **Eruption and hexagon flows with conjugating matrices.** Denote by $\Phi_{\mathcal{I}}$ and respectively by $\Phi_{\mathcal{E}}$ the flows $\vartheta \circ \widehat{\Phi}_{\mathcal{I}}$ and respectively $\vartheta \circ \widehat{\Phi}_{\mathcal{E}}$ on $\mathscr{X}_3^+(P)$. Let $\mathcal{C}$ be tuple of conjugacy classes. Recall that a symplectic leaf $\mathcal{Q}_L$ is mapped through ϑ to the relative character variety $\mathscr{X}_{3,\mathcal{C}}^+(P)$ by Lemma 4.6. Since the fundamental group of P is generated by the three boundary curves, any flow Φ in $\mathscr{X}_{3,\mathcal{C}}^+(P)$ can be written as follows. Let $[\rho] \in \mathscr{X}_{3,\mathcal{C}}^+(P)$. Then the flow $\Phi^t([\rho])$ is covered by a path of representations described by conjugations along the boundary. That is, there exist paths $g_t^\alpha, g_t^\beta, g_t^\gamma \in \mathsf{PSL}(3, \mathbb{R})$

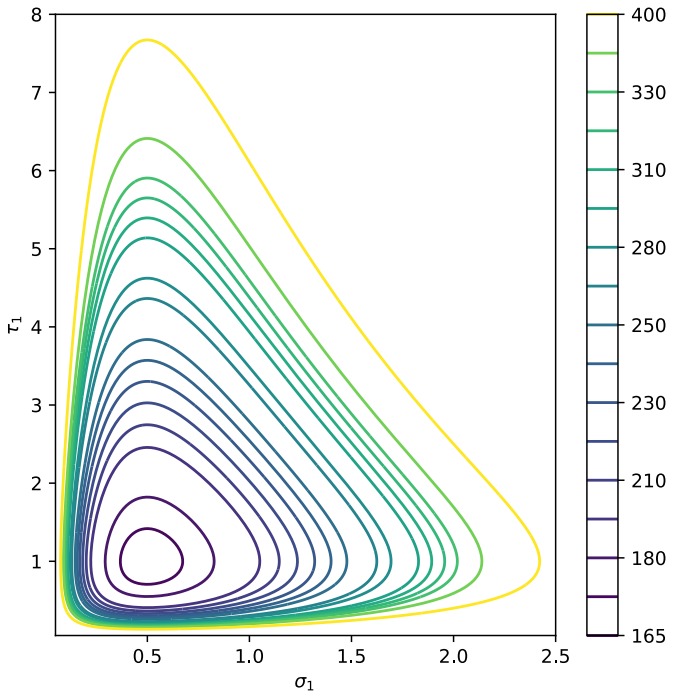

FIGURE 17. Level sets of the function $\mathsf{tr}_{\alpha^3\gamma^{-1}}\big|_{\mathfrak{U}}$.

depending on ρ such that the flow

$$\rho_t = \begin{cases} \alpha \mapsto g_t^{\alpha} \rho(\alpha)(g_t^{\alpha})^{-1} \\ \beta \mapsto g_t^{\beta} \rho(\beta)(g_t^{\beta})^{-1} \\ \gamma \mapsto g_t^{\gamma} \rho(\gamma)(g_t^{\gamma})^{-1} \end{cases} \tag{24}$$

covers the flow Φ on $\mathscr{X}^+_{3,\mathcal{C}}(P)$.

In this section, we find such conjugating matrices for the eruption and hexagon flows when we restrict to the unipotent locus.

The two following results are once again, computations using Mathematica. The conjugating matrices were found by solving matrix equations, and they can be easily checked, since the flows are explicit. The first result finds conjugating matrices for the eruption flow. The matrices were found by finding solutions to the expression in (24). Instead of showing the solution, we simply verify in Sections 8 and 9 of the Mathematica code the following two theorems.

Theorem 6.11. *The flow $\Phi^t_{\mathcal{E}} = \vartheta \circ \widehat{\Phi}^t_{\mathcal{E}}$ on $\mathfrak{U} \subset \mathscr{X}_3^+(P)$ is given by the following conjugations. For $(\sigma_1, \tau_1) \in \mathfrak{U}$, let*

$$\zeta_t^{\alpha} = \begin{pmatrix} \frac{e^{-2t/3}(1+e^t\tau_1)^{2/3}}{(1+\tau_1)^{1/3}} & 0 & 0 \\ 0 & \frac{e^{t/3}(1+\tau_1)^{1/3}}{(1+e^t\tau_1)^{1/3}} & 0 \\ 0 & 0 & \frac{e^{t/3}(1+\tau_1)^{1/3}}{(1+e^t\tau_1)^{1/3}} \end{pmatrix},$$

$$\zeta_t^{\beta} = \frac{(1+\tau_1)^{1/3}}{e^{t/3}\tau_1(1+e^t\tau_1)^{1/3}} \cdot \begin{pmatrix} 0 & -\left((\sigma_1-1)\left(e^t\tau_1+1\right)\right) & -\frac{(\sigma_1\tau_1+\sigma_1-1)\left(e^t\tau_1+1\right)}{\tau_1+1} \\ 0 & \sigma_1+\sigma_1e^t\tau_1-e^t\tau_1 & \frac{\sigma_1(\tau_1+1)\left(e^t\tau_1+1\right)-e^t\tau_1+\tau_1}{\tau_1+1} \\ -e^t\tau_1^2 & -\sigma_1\left(e^t\tau_1+1\right)-e^t\tau_1\left(\tau_1+1\right) & -\sigma_1\left(e^t\tau_1+1\right)-\frac{\tau_1\left(e^t(2\tau_1+1)+1\right)}{\tau_1+1} \end{pmatrix}$$

and

$$\zeta_t^{\gamma} = \begin{pmatrix} \frac{(1+\tau_1)^{1/3}}{(1+e^t\tau_1)^{1/3}} & 0 & 0 \\ 0 & \frac{(1+\tau_1)^{1/3}}{(1+e^t\tau_1)^{1/3}} & 0 \\ 0 & 0 & \frac{(1+\tau_1)^{2/3}}{(1+e^t\tau_1)^{2/3}}. \end{pmatrix}.$$

Then the flow

$$\rho_t = \begin{cases} \alpha \mapsto \zeta_t^{\alpha}\rho(\alpha)(\zeta_t^{\alpha})^{-1} \\ \beta \mapsto \zeta_t^{\beta}\rho(\beta)(\zeta_t^{\beta})^{-1} \\ \gamma \mapsto \zeta_t^{\gamma}\rho(\gamma)(\zeta_t^{\gamma})^{-1} \end{cases}$$

covers the flow $\Phi^t_{\mathcal{E}}$.

The next result is analogous to the above theorem, and concerns the hexagon flow.

Theorem 6.12. *The flow $\Phi^t_{\mathcal{I}} = \vartheta \circ \widehat{\Phi}^t_{\mathcal{I}}$ on $\mathfrak{U} \subset \mathscr{X}_3^+(P)$ is given by the following conjugations. For $(\sigma_1, \tau_1) \in \mathfrak{U}$, let*

$$\eta_t^{\alpha} = \begin{pmatrix} \frac{e^{-t/3}\left(\sigma_1e^t+1\right)}{\sigma_1+1} & \frac{\sigma_1e^{-t/3}\left(e^t-1\right)(\tau_1+1)}{(\sigma_1+1)\tau_1} & 0 \\ 0 & e^{-t/3} & 0 \\ 0 & 0 & \frac{(\sigma_1+1)e^{2t/3}}{\sigma_1e^t+1} \end{pmatrix}$$

and

$$\eta_t^{\gamma} = \begin{pmatrix} \frac{(\sigma_1+1)e^{2t/3}}{\sigma_1e^t+1} & 0 & 0 \\ 0 & e^{-t/3} & 0 \\ 0 & \frac{\sigma_1e^{-t/3}\left(e^t-1\right)(\tau_1+1)}{\sigma_1+1} & \frac{e^{-t/3}\left(\sigma_1e^t+1\right)}{\sigma_1+1} \end{pmatrix}.$$

We define the matrix η_t^{β} in terms of its entries below:

$$(\eta_t^{\beta})_{11} = 0,$$

$$(\eta_t^{\beta})_{12} = \frac{e^{-t/3}\left(\tau_1+1\right)\left(\sigma_1^2e^t-1\right)}{\left(\sigma_1+1\right)\tau_1}$$

$$(\eta_t^\beta)_{13} = \frac{e^{-t/3}\left(\sigma_1^2 e^t(\tau_1+1)+\sigma_1 e^t\tau_1-1\right)}{(\sigma_1+1)\tau_1}$$
$$(\eta_t^\beta)_{21} = 0$$
$$(\eta_t^\beta)_{22} = -\frac{e^{-t/3}\left(\sigma_1+\sigma_1^2 e^t(\tau_1+1)-\tau_1\right)}{(\sigma_1+1)\tau_1}$$
$$(\eta_t^\beta)_{23} = -\frac{\sigma_1 e^{-t/3}\left(\sigma_1 e^t(\tau_1+1)+e^t\tau_1+1\right)}{(\sigma_1+1)\tau_1}$$
$$(\eta_t^\beta)_{31} = \frac{(\sigma_1+1)e^{2t/3}\tau_1}{\sigma_1 e^t+1}$$
$$(\eta_t^\beta)_{32} = \frac{(\tau_1+1)\left(\sigma_1^2 e^t(\tau_1+2)+\sigma_1\left(2e^t\tau_1+1\right)+\sigma_1^3 e^{2t}+e^t\tau_1\right)}{(\sigma_1+1)e^{t/3}\tau_1(\sigma_1 e^t+1)}$$
$$(\eta_t^\beta)_{33} = \frac{\sigma_1^3 e^{2t}(\tau_1+1)+\sigma_1^2 e^t\left(\left(e^t+3\right)\tau_1+2\right)+\sigma_1\left(\left(4e^t+1\right)\tau_1+1\right)+\left(e^t+1\right)\tau_1}{(\sigma_1+1)e^{t/3}\tau_1(\sigma_1 e^t+1)}.$$

Then the flow

$$\rho_t = \begin{cases} \alpha \mapsto \eta_t^\alpha \rho(\alpha)(\eta_t^\alpha)^{-1} \\ \beta \mapsto \eta_t^\beta \rho(\beta)(\eta_t^\beta)^{-1} \\ \gamma \mapsto \eta_t^\gamma \rho(\gamma)(\eta_t^\gamma)^{-1} \end{cases}$$

covers the flow $\Phi_{\mathcal{I}}^t$.

Appendix A. Proof of Theorem C, Part a

In this appendix, we give a proof of Theorem C, Part a, which we restate here.

Theorem A.1. *Let* $\delta = \alpha\gamma^{-1}$ *be a figure eight curve on a pair of pants* P *and let* $\mathcal{Q}$ *be a symplectic leaf in* $\widehat{\mathfrak{C}}(P)$. *The restriction of the function* $\mathsf{tr}_\delta + \mathsf{tr}_{\delta^{-1}}\big|_{\mathcal{Q}} \colon \mathcal{Q} \to \mathbb{R}$ *attains a unique minimum. Moreover, every orbit of the Hamiltonian flow of* $\mathsf{tr}_\delta + \mathsf{tr}_{\delta^{-1}}\big|_{\mathcal{Q}}$ *is periodic, and there is a unique fixed point.*

Here we prove that the symmetrized trace is a proper function on symplectic leaves, and that it is strictly convex along any mixed flow. The proof of the theorem is then identical to the proof of Theorem 5.1 in Section 5.3, and we therefore leave it out.

We begin by computing the trace function associated to δ^{-1} in coordinates.

Lemma A.2. *Let* $\delta = \alpha\gamma^{-1}$ *and* $L = (\ell_{\alpha,1}, \ell_{\alpha,2}, \ell_{\beta,1}, \ell_{\beta,2}, \ell_{\gamma,1}, \ell_{\gamma,2}) \in \mathbb{R}^6_{>0}$ *be a length vector defining a symplectic leaf* $\mathcal{Q}_L$. *Then*

$$\mathsf{tr}_{\delta^{-1}}\big|_{\mathcal{Q}_L} = \frac{1}{\sigma_1^2\tau_1\ell_{\alpha,1}\left(\ell_{\alpha,2}\ell_{\beta,1}\ell_{\beta,2}\ell_{\gamma,1}\ell_{\gamma,2}\right)^{2/3}}\cdot$$
$$\Bigg((\tau_1+1)(\sigma_1+\tau_1+1)\ell_{\alpha,1}^2\ell_{\gamma,1}\sqrt[3]{\ell_{\alpha,2}^2\ell_{\beta,1}\ell_{\beta,2}^4} + \sigma_1\ell_{\alpha,1}\Bigg(\tau_1(\tau_1+1)\ell_{\gamma,1}\sqrt[3]{\ell_{\alpha,2}^2\ell_{\beta,1}\ell_{\beta,2}^4} +$$
$$\sigma_1\tau_1^2\ell_{\gamma,2}\sqrt[3]{\ell_{\alpha,2}^2\ell_{\beta,1}\ell_{\beta,2}} + \sigma_1(\sigma_1+1)\ell_{\gamma,1}\ell_{\gamma,2}\sqrt[3]{\ell_{\alpha,2}^2\ell_{\beta,1}^4\ell_{\beta,2}}\Bigg) +$$

$$\sigma_1\Bigg(\sigma_1\tau_1\sqrt[3]{\ell_{\alpha,2}}\left(\ell_{\alpha,1}\ell_{\gamma,1}\ell_{\gamma,2}\right)^{2/3}\left(\sigma_1\ell_{\beta,1}+\tau_1\ell_{\beta,2}\right)+\tau_1\left(\tau_1+1\right)\ell_{\beta,2}\sqrt[3]{\ell_{\alpha,1}^5\ell_{\alpha,2}\ell_{\gamma,1}^2\ell_{\gamma,2}^2}+$$
$$\left(\sigma_1+\tau_1+1\right)\ell_{\beta,1}\ell_{\beta,2}\sqrt[3]{\ell_{\alpha,1}^5\ell_{\alpha,2}\ell_{\gamma,1}^2\ell_{\gamma,2}^2}+\sigma_1\tau_1\Bigg(\ell_{\gamma,2}\sqrt[3]{\ell_{\alpha,2}^2\ell_{\beta,1}\ell_{\beta,2}}+$$
$$\sqrt[3]{\ell_{\alpha,1}^4\ell_{\beta,1}^2\ell_{\beta,2}^2\ell_{\gamma,1}\ell_{\gamma,2}}+\sqrt[3]{\ell_{\alpha,1}^4\ell_{\beta,1}^2\ell_{\beta,2}^2\ell_{\gamma,1}^4\ell_{\gamma,2}}+\sqrt[3]{\ell_{\alpha,1}^4\ell_{\beta,1}^2\ell_{\beta,2}^2\ell_{\gamma,1}\ell_{\gamma,2}^4}\Bigg)+$$
$$\ell_{\alpha,2}\Bigg(\sigma_1^2\tau_1\sqrt[3]{\ell_{\alpha,1}\ell_{\beta,1}^2\ell_{\beta,2}^2\ell_{\gamma,1}\ell_{\gamma,2}^4}+\left(\tau_1+1\right)\Bigg(\tau_1\sqrt[3]{\ell_{\alpha,1}^4\ell_{\beta,1}^2\ell_{\beta,2}^2\ell_{\gamma,1}\ell_{\gamma,2}}+\sqrt[3]{\ell_{\alpha,1}^4\ell_{\beta,1}^2\ell_{\beta,2}^2\ell_{\gamma,1}^4\ell_{\gamma,2}}\Bigg)+$$
$$\sigma_1\Bigg(\tau_1^2\sqrt[3]{\ell_{\alpha,1}\ell_{\beta,1}^2\ell_{\beta,2}^2\ell_{\gamma,1}\ell_{\gamma,2}}+\sqrt[3]{\ell_{\alpha,1}^4\ell_{\beta,1}^2\ell_{\beta,2}^2\ell_{\gamma,1}^4\ell_{\gamma,2}}+\tau_1\Bigg(\sqrt[3]{\ell_{\alpha,1}\ell_{\beta,1}^2\ell_{\beta,2}^2\ell_{\gamma,1}\ell_{\gamma,2}}+$$
$$\sqrt[3]{\ell_{\alpha,1}^4\ell_{\beta,1}^2\ell_{\beta,2}^2\ell_{\gamma,1}\ell_{\gamma,2}}+\sqrt[3]{\ell_{\alpha,1}\ell_{\beta,1}^2\ell_{\beta,2}^2\ell_{\gamma,1}^4\ell_{\gamma,2}}+\sqrt[3]{\ell_{\alpha,1}^4\ell_{\beta,1}^2\ell_{\beta,2}^2\ell_{\gamma,1}^4\ell_{\gamma,2}}+$$
$$\sqrt[3]{\ell_{\alpha,1}\ell_{\beta,1}^2\ell_{\beta,2}^2\ell_{\gamma,1}\ell_{\gamma,2}^4}+\sqrt[3]{\ell_{\alpha,1}^4\ell_{\beta,1}^2\ell_{\beta,2}^2\ell_{\gamma,1}\ell_{\gamma,2}^4}\Bigg)\Bigg)\Bigg)\Bigg)\Bigg).$$

Proof. The proof of this fact is a computation, found in Section 4 of the Mathematica code. The function `InvtraceFigure8` will give the above output with the length vectors as input. □

We now move on to prove properness of the symmetrized trace function.

Proposition A.3. *Let $\delta = \alpha\gamma^{-1}$ and $L = (\ell_{\alpha,1}, \ell_{\alpha,2}, \ell_{\beta,1}, \ell_{\beta,2}, \ell_{\gamma,1}, \ell_{\gamma,2}) \in \mathbb{R}^6_{>0}$ be a length vector defining a symplectic leaf $\mathcal{Q}_L$. Then the function $\mathsf{tr}_\delta + \mathsf{tr}_{\delta^{-1}}\big|_{\mathcal{Q}_L} : \mathcal{Q}_L \to \mathbb{R}$ is proper. In particular, it realizes a minimum in $\mathcal{Q}_L$.*

Proof. By Lemma A.2, both tr_δ and $\mathsf{tr}_{\delta^{-1}}$ are positive functions. In Proposition 5.3, we proved that tr_δ is proper. Hence we only need to show that $\mathsf{tr}_{\delta^{-1}}$ is proper.

Let $(\sigma_{1,n}, \tau_{1,n})_{n\in\mathbb{N}}$ be a sequence such that as n goes to ∞, $(\sigma_{1,n}, \tau_{1,n})$ goes to a tuple in $\{(\infty,\infty), (0,\infty), (\infty,0), (x,0), (0,y) : x, y \geq 0\}$. We need to show that in any of these cases, $\mathsf{tr}_\delta(\sigma_{1,n}, \tau_{1,n}) \to \infty$ as $n \to \infty$. Notice that all the variables are positive and that all the signs on the monomials are positive as well. Hence, it is enough to find terms in the expression in Lemma A.2 that diverges along any of the above sequences.

(a) Assume $(\sigma_{1,n}, \tau_{1,n}) \to (\infty, \infty)$, then the term
$$\frac{\sigma_{1,n}^2\tau_{1,n}\sqrt[3]{\ell_{\alpha,2}}\left(\ell_{\alpha,1}\ell_{\gamma,1}\ell_{\gamma,2}\right)^{2/3}\left(\sigma_{1,n}\ell_{\beta,1}+\tau_{1,n}\ell_{\beta,2}\right)}{\sigma_{1,n}^2\tau_{1,n}\ell_{\alpha,1}\left(\ell_{\alpha,2}\ell_{\beta,1}\ell_{\beta,2}\ell_{\gamma,1}\ell_{\gamma,2}\right)^{2/3}} \xrightarrow{n\to\infty} \infty.$$

(b) Assume $(\sigma_{1,n}, \tau_{1,n}) \to (0, \infty)$, then the term
$$\frac{\left(\tau_{1,n}+1\right)\left(\sigma_{1,n}+\tau_{1,n}+1\right)\ell_{\alpha,1}^2\ell_{\gamma,1}\sqrt[3]{\ell_{\alpha,2}^2\ell_{\beta,1}\ell_{\beta,2}^4}}{\sigma_{1,n}^2\tau_{1,n}\ell_{\alpha,1}\left(\ell_{\alpha,2}\ell_{\beta,1}\ell_{\beta,2}\ell_{\gamma,1}\ell_{\gamma,2}\right)^{2/3}} \xrightarrow{n\to\infty} \infty.$$

(c) Assume $(\sigma_{1,n}, \tau_{1,n}) \to (\infty, 0)$, then the term
$$\frac{\sigma_{1,n}^2\tau_{1,n}\sqrt[3]{\ell_{\alpha,2}}\left(\ell_{\alpha,1}\ell_{\gamma,1}\ell_{\gamma,2}\right)^{2/3}\left(\sigma_{1,n}\ell_{\beta,1}+\tau_{1,n}\ell_{\beta,2}\right)}{\sigma_{1,n}^2\tau_{1,n}\ell_{\alpha,1}\left(\ell_{\alpha,2}\ell_{\beta,1}\ell_{\beta,2}\ell_{\gamma,1}\ell_{\gamma,2}\right)^{2/3}} \xrightarrow{n\to\infty} \infty.$$

(d) Assume $(\sigma_{1,n},\tau_{1,n})\to(x,0)$ or $(0,y)$ for $x,y\geq 0$, then the term

$$\frac{\ell_{\alpha,1}^2\ell_{\gamma,1}\sqrt[3]{\ell_{\alpha,2}^2\ell_{\beta,1}\ell_{\beta,2}^4}}{\sigma_{1,n}^2\tau_{1,n}\ell_{\alpha,1}\left(\ell_{\alpha,2}\ell_{\beta,1}\ell_{\beta,2}\ell_{\gamma,1}\ell_{\gamma,2}\right)^{2/3}}\xrightarrow{n\to\infty}\infty.$$

This finishes to proof. □

We finish by proving convexity.

Proposition A.4. *Let $\delta=\alpha\gamma^{-1}$ and $L=(\ell_{\alpha,1},\ell_{\alpha,2},\ell_{\beta,1},\ell_{\beta,2},\ell_{\gamma,1},\ell_{\gamma,2})\in\mathbb{R}^6_{>0}$ be a length vector defining a symplectic leaf $\mathcal{Q}_L$. The function $\mathsf{tr}_\delta+\mathsf{tr}_{\delta^{-1}}\big|_{\mathcal{Q}_L}\colon\mathcal{Q}_L\to\mathbb{R}$ is strictly convex along any mixed flow.*

Proof. Since we proved in Theorem 5.4 that tr_δ is strictly convex, we only have to show that the function $\mathsf{tr}_{\delta^{-1}}$ is strictly convex along any mixed flow. Consider first the mixed flow $\Psi_a^t=\widehat{\Phi}_{\mathcal{E}}^{at}\circ\widehat{\Phi}_{\mathcal{I}}^t$. By Section 6 of the Mathematica code, using the function `InvtraceFigure8` and `testfMix1` as input, we obtain that

$$\frac{\partial^2}{\partial t^2}(\mathsf{tr}_{\delta^{-1}}(\Psi_a^t(\sigma_1,\tau_1)))=\frac{e^{-t(2a+1)}}{\sigma_1^2\tau_1\ell_{\alpha,1}\left(\ell_{\alpha,2}\ell_{\beta,1}\ell_{\beta,2}\ell_{\gamma,1}\ell_{\gamma,2}\right)^{2/3}}\cdot$$

$$\Bigg(\ell_{\alpha,1}^2\ell_{\gamma,1}\sqrt[3]{\ell_{\alpha,2}^2\ell_{\beta,1}\ell_{\beta,2}^4}\left(a^2\sigma_1\tau_1e^{at+t}+8a^2e^t\tau_1+(a+1)^2\sigma_1e^{at}+(1-2a)^2e^{2t}\tau_1^2+(2a+1)^2\right)+$$

$$\sigma_1e^{at}\ell_{\alpha,1}\Bigg(a^2e^t\tau_1\ell_{\gamma,1}\sqrt[3]{\ell_{\alpha,2}^2\ell_{\beta,1}\ell_{\beta,2}^4}+(a-1)^2e^{2t}\tau_1^2\ell_{\gamma,1}\sqrt[3]{\ell_{\alpha,2}^2\ell_{\beta,1}\ell_{\beta,2}^4}+$$

$$\sigma_1\tau_1^2e^{(a+2)t}\ell_{\gamma,2}\sqrt[3]{\ell_{\alpha,2}^2\ell_{\beta,1}\ell_{\beta,2}}+(a-1)^2\sigma_1^2e^{2at}\ell_{\gamma,1}\ell_{\gamma,2}\sqrt[3]{\ell_{\alpha,2}^2\ell_{\beta,1}^4\ell_{\beta,2}}+\sigma_1e^{at}\ell_{\gamma,1}\ell_{\gamma,2}\sqrt[3]{\ell_{\alpha,2}^2\ell_{\beta,1}^4\ell_{\beta,2}}\Bigg)+$$

$$\sigma_1\Bigg((a+1)^2\sigma_1^2\tau_1^2e^{(3a+2)t}\ell_{\gamma,2}\sqrt[3]{\ell_{\alpha,2}^2\ell_{\beta,1}\ell_{\beta,2}}+$$

$$\sigma_1\tau_1^2e^{2(a+1)t}\left(\ell_{\alpha,2}\sqrt[3]{\ell_{\alpha,1}\ell_{\beta,1}^2\ell_{\beta,2}^2\ell_{\gamma,1}\ell_{\gamma,2}}+\ell_{\beta,2}\sqrt[3]{\ell_{\alpha,1}^2\ell_{\alpha,2}\ell_{\gamma,1}^2\ell_{\gamma,2}^2}\right)+$$

$$(a+1)^2e^{at}\left(\ell_{\alpha,2}\sqrt[3]{\ell_{\alpha,1}^4\ell_{\beta,1}^2\ell_{\beta,2}^2\ell_{\gamma,1}^4\ell_{\gamma,2}}+\ell_{\beta,1}\ell_{\beta,2}\sqrt[3]{\ell_{\alpha,1}^5\ell_{\alpha,2}\ell_{\gamma,1}^2\ell_{\gamma,2}^2}\right)+$$

$$\sigma_1e^{2at}\left(\ell_{\alpha,2}\sqrt[3]{\ell_{\alpha,1}^4\ell_{\beta,1}^2\ell_{\beta,2}^2\ell_{\gamma,1}^4\ell_{\gamma,2}}+\ell_{\beta,1}\ell_{\beta,2}\sqrt[3]{\ell_{\alpha,1}^5\ell_{\alpha,2}\ell_{\gamma,1}^2\ell_{\gamma,2}^2}\right)+$$

$$a^2\sigma_1^2\tau_1e^{3at+t}\sqrt[3]{\ell_{\alpha,2}}\left(\ell_{\beta,1}\left(\ell_{\alpha,1}\ell_{\gamma,1}\ell_{\gamma,2}\right)^{2/3}+\sqrt[3]{\ell_{\alpha,1}\ell_{\alpha,2}^2\ell_{\beta,1}^2\ell_{\beta,2}^2\ell_{\gamma,1}\ell_{\gamma,2}^4}\right)+$$

$$a^2\tau_1e^{at+t}\left(\left(\ell_{\beta,1}+1\right)\ell_{\beta,2}\sqrt[3]{\ell_{\alpha,1}^5\ell_{\alpha,2}\ell_{\gamma,1}^2\ell_{\gamma,2}^2}+\ell_{\alpha,2}\left(\sqrt[3]{\ell_{\alpha,1}^4\ell_{\beta,1}^2\ell_{\beta,2}^2\ell_{\gamma,1}\ell_{\gamma,2}}+\sqrt[3]{\ell_{\alpha,1}^4\ell_{\beta,1}^2\ell_{\beta,2}^2\ell_{\gamma,1}^4\ell_{\gamma,2}}\right)\right)\Bigg)\Bigg)\Bigg)\Bigg)$$

This quantity is positive for any $a\in\mathbb{R}$ and any coordinates.

Now consider the mixed flow $\Psi_a^t=\widehat{\Phi}_{\mathcal{E}}^t\circ\widehat{\Phi}_{\mathcal{I}}^{at}$. From Section 6 of the Mathematica code this time using `testfMix2` as input, we obtain that

$$\frac{\partial^2}{\partial t^2}(\mathsf{tr}_{\delta^{-1}}(\Psi_a^t(\sigma_1,\tau_1)))=\frac{e^{-t(2+a)}}{\sigma_1^2\tau_1\ell_{\alpha,1}\left(\ell_{\alpha,2}\ell_{\beta,1}\ell_{\beta,2}\ell_{\gamma,1}\ell_{\gamma,2}\right)^{2/3}}\cdot$$

$$\Bigg(\Bigg(\ell_{\alpha,1}^2\ell_{\gamma,1}\sqrt[3]{\ell_{\alpha,2}^2\ell_{\beta,1}\ell_{\beta,2}^4}\left(\sigma_1\tau_1e^{at+t}+(a+1)^2\sigma_1e^t+(a-2)^2\tau_1^2e^{2at}+8\tau_1e^{at}+(a+2)^2\right)+$$
$$e^t\sigma_1\ell_{\alpha,1}\Bigg((a-1)^2\tau_1^2e^{2at}\ell_{\gamma,1}\sqrt[3]{\ell_{\alpha,2}^2\ell_{\beta,1}\ell_{\beta,2}^4}+\tau_1e^{at}\ell_{\gamma,1}\sqrt[3]{\ell_{\alpha,2}^2\ell_{\beta,1}\ell_{\beta,2}^4}+$$
$$a^2\sigma_1\tau_1^2e^{2at+t}\ell_{\gamma,2}\sqrt[3]{\ell_{\alpha,2}^2\ell_{\beta,1}\ell_{\beta,2}}+a^2\sigma_1e^t\ell_{\gamma,1}\ell_{\gamma,2}\sqrt[3]{\ell_{\alpha,2}^2\ell_{\beta,1}^4\ell_{\beta,2}}+$$
$$(a-1)^2\sigma_1^2e^{2t}\ell_{\gamma,1}\ell_{\gamma,2}\sqrt[3]{\ell_{\alpha,2}^2\ell_{\beta,1}^4\ell_{\beta,2}}\Bigg)+\sigma_1\Bigg((a+1)^2\sigma_1^2\tau_1^2e^{(2a+3)t}\ell_{\gamma,2}\sqrt[3]{\ell_{\alpha,2}^2\ell_{\beta,1}\ell_{\beta,2}}+$$
$$a^2\sigma_1\tau_1^2e^{2(a+1)t}\left(\ell_{\alpha,2}\sqrt[3]{\ell_{\alpha,1}\ell_{\beta,1}^2\ell_{\beta,2}^2\ell_{\gamma,1}\ell_{\gamma,2}}+\ell_{\beta,2}\sqrt[3]{\ell_{\alpha,1}^2\ell_{\alpha,2}\ell_{\gamma,1}^2\ell_{\gamma,2}^2}\right)+$$
$$(a-1)^2\tau_1^2e^{2at+t}\left(\ell_{\alpha,2}\sqrt[3]{\ell_{\alpha,1}^4\ell_{\beta,1}^2\ell_{\beta,2}^2\ell_{\gamma,1}\ell_{\gamma,2}}+\ell_{\beta,2}\sqrt[3]{\ell_{\alpha,1}^5\ell_{\alpha,2}\ell_{\gamma,1}^2\ell_{\gamma,2}^2}\right)+$$
$$(a+1)^2e^t\left(\ell_{\alpha,2}\sqrt[3]{\ell_{\alpha,1}^4\ell_{\beta,1}^2\ell_{\beta,2}^2\ell_{\gamma,1}^4\ell_{\gamma,2}}+\ell_{\beta,1}\ell_{\beta,2}\sqrt[3]{\ell_{\alpha,1}^5\ell_{\alpha,2}\ell_{\gamma,1}^2\ell_{\gamma,2}^2}\right)+$$
$$a^2\sigma_1e^{2t}\left(\ell_{\alpha,2}\sqrt[3]{\ell_{\alpha,1}^4\ell_{\beta,1}^2\ell_{\beta,2}^2\ell_{\gamma,1}^4\ell_{\gamma,2}}+\ell_{\beta,1}\ell_{\beta,2}\sqrt[3]{\ell_{\alpha,1}^5\ell_{\alpha,2}\ell_{\gamma,1}^2\ell_{\gamma,2}^2}\right)+$$
$$\sigma_1^2\tau_1e^{(a+3)t}\sqrt[3]{\ell_{\alpha,2}}\left(\ell_{\beta,1}\left(\ell_{\alpha,1}\ell_{\gamma,1}\ell_{\gamma,2}\right)^{2/3}+\sqrt[3]{\ell_{\alpha,1}\ell_{\alpha,2}^2\ell_{\beta,1}^2\ell_{\beta,2}^2\ell_{\gamma,1}\ell_{\gamma,2}^4}\right)+$$
$$e^{t(1+a)}\tau_1\Bigg(\left(\ell_{\beta,1}+1\right)\ell_{\beta,2}\sqrt[3]{\ell_{\alpha,1}^5\ell_{\alpha,2}\ell_{\gamma,1}^2\ell_{\gamma,2}^2}+$$
$$\ell_{\alpha,2}\left(\sqrt[3]{\ell_{\alpha,1}^4\ell_{\beta,1}^2\ell_{\beta,2}^2\ell_{\gamma,1}\ell_{\gamma,2}}+\sqrt[3]{\ell_{\alpha,1}^4\ell_{\beta,1}^2\ell_{\beta,2}^2\ell_{\gamma,1}^4\ell_{\gamma,2}}\right)\Bigg)\Bigg)\Bigg)\Bigg).$$

This quantity is also positive for any $a\in\mathbb{R}$ and any coordinates. Hence, the function $t\mapsto \mathsf{tr}_\delta(\Psi_a^t(\sigma_1,\tau_1))+\mathsf{tr}_{\delta^{-1}}(\Psi_a^t(\sigma_1,\tau_1))$ is strictly convex for any (σ_1,τ_1). □

Appendix B. Proof of Lemma 2.8

Proof. Since the cross ratio is a projective invariant, we can assume that the flags are in the following positions:

$$p_1=\begin{bmatrix}1\\0\\0\end{bmatrix},\quad \ell_1=\begin{bmatrix}0:1:1\end{bmatrix}$$
$$p_2=\begin{bmatrix}0\\1\\0\end{bmatrix},\quad \ell_2=\begin{bmatrix}1:0:1\end{bmatrix}$$
$$p_3=\begin{bmatrix}0\\0\\1\end{bmatrix},\quad \ell_3=\begin{bmatrix}1:x:0\end{bmatrix}$$
$$p_4=\begin{bmatrix}1\\y\\z\end{bmatrix},\quad \ell_4=\begin{bmatrix}-wz-y:1:w\end{bmatrix}$$

where $x, y, z, w \in \mathbb{R} \smallsetminus \{0\}$. The lines appearing in the first cross ratio in the lemma are given by

$$\overline{p_1p_2} = \big[0:0:1\big], \quad \overline{p_1p_3} = \big[0:1:0\big], \quad \overline{p_1p_4} = \big[0:z:-y\big].$$

To take the cross ratio of the four lines, we choose the line $h = \overline{p_1p_4}$ to identify it with $\mathbb{R} \cup \{\infty\}$. We have that

$$h = \big[-z:0:1\big] = \left\{ \begin{bmatrix} 1 \\ b \\ z \end{bmatrix} \ : \ b \in \mathbb{R} \right\}$$

and we choose the isomorphism

$$\begin{aligned} h &\to \mathbb{R} \\ \begin{bmatrix} 1 \\ b \\ z \end{bmatrix} &\mapsto b. \end{aligned} \tag{25}$$

The intersections of the relevant lines with h are

$$\ell_1 \cap h = \begin{bmatrix} 1 \\ -z \\ z \end{bmatrix}, \ \overline{p_1p_2} \cap h = \begin{bmatrix} 0 \\ 1 \\ 0 \end{bmatrix}, \ \overline{p_1p_3} \cap h = \begin{bmatrix} 1 \\ 0 \\ z \end{bmatrix}, \ \overline{p_1p_4} \cap h = \begin{bmatrix} 1 \\ y \\ z \end{bmatrix}.$$

Under the above identification of h with $\mathbb{R} \cup \{\infty\}$, we have that

$$\ell_1 \cap h \mapsto -z, \quad \overline{p_1p_2} \cap h \mapsto \infty, \quad \overline{p_1p_3} \cap h \mapsto 0, \quad \overline{p_1p_4} \cap h \mapsto y.$$

Their cross ratio is therefore

$$\mathsf{cr}(\ell_1, \overline{p_1p_2}, \overline{p_1p_3}, \overline{p_1p_4}) = \frac{-y}{y+z}.$$

On the other hand

$$\mathsf{cr}_1(F_1, F_2, F_3, F_4) = -\frac{\left(\big[0:1:1\big] \begin{bmatrix} 0 \\ 1 \\ 0 \end{bmatrix}\right)\left(\big[0:1:0\big] \begin{bmatrix} 1 \\ y \\ z \end{bmatrix}\right)}{\left(\big[0:1:1\big] \begin{bmatrix} 1 \\ y \\ z \end{bmatrix}\right)\left(\big[0:1:0\big] \begin{bmatrix} 0 \\ 1 \\ 0 \end{bmatrix}\right)} = \frac{-y}{y+z}$$

as desired.

For the second cross ratio, we do a similar computation. The lines appearing in the second cross ratio are

$$\overline{p_3p_1} = \big[1:0:0\big], \quad \overline{p_1p_3} = \big[0:1:0\big], \quad \overline{p_1p_4} = \big[y:-1:0\big].$$

Using the same projective line h as above and using the identification in (25), we have that

$$\ell_3 \cap h = \begin{bmatrix} 1 \\ -1/x \\ z \end{bmatrix} \mapsto \frac{-1}{x}, \qquad \overline{p_3p_4} \cap h = \begin{bmatrix} 1 \\ y \\ z \end{bmatrix} \mapsto y$$

$$\overline{p_3p_1} \cap h = \begin{bmatrix} 1 \\ 0 \\ z \end{bmatrix} \mapsto 0, \qquad \overline{p_3p_2} \cap h = \begin{bmatrix} 0 \\ 1 \\ 0 \end{bmatrix} \mapsto \infty.$$

Thus

$$\mathsf{cr}(\ell_3, \overline{p_3p_4}, \overline{p_3p_1}, \overline{p_3p_2}) = \frac{-1-xy}{xy}.$$

On the other hand,

$$\mathsf{cr}_2(F_1, F_2, F_3, F_4) = -\frac{\left([1:x:0]\begin{bmatrix} 1 \\ y \\ z \end{bmatrix}\right)\left([0:1:0]\begin{bmatrix} 0 \\ 1 \\ 0 \end{bmatrix}\right)}{\left([1:x:0]\begin{bmatrix} 0 \\ 1 \\ 0 \end{bmatrix}\right)\left([0:1:0]\begin{bmatrix} 1 \\ y \\ z \end{bmatrix}\right)} = \frac{-1-xy}{xy}$$

as desired. □

References

[BD14] Francis Bonahon and Guillaume Dreyer, *Parameterizing Hitchin components*, Duke Math. J. **163** (2014), no. 15, 2935–2975.

[BD17] ———, *Hitchin characters and geodesic laminations*, Acta Math. **218** (2017), no. 2, 201–295.

[BL23] Martin J. Bridgeman and François Labourie, *Ghost polygons, Poisson bracket and convexity*, Preprint, arXiv:2307.04380 [math.GT] (2023), 2023.

[CCFW24] Fernando Camacho-Cadena, James Farre, and Anna Wienhard, *Invariant multi-functions and Hamiltonian flows for surface group representations*, Preprint, arXiv:2410.05154 [math.GT] (2024), 2024.

[CdS01] Ana Cannas da Silva, *Lectures on symplectic geometry*, Lect. Notes Math., vol. 1764, Berlin: Springer, 2001.

[CFM21] Marius Crainic, Rui Loja Fernandes, and Ioan Mărcuţ, *Lectures on Poisson geometry*, Grad. Stud. Math., vol. 217, Providence, RI: American Mathematical Society (AMS), 2021.

[CTT20] Alex Casella, Dominic Tate, and Stephan Tillmann, *Moduli spaces of real projective structures on surfaces*, MSJ Mem., vol. 38, Tokyo: Mathematical Society of Japan, 2020.

[DKS24] Daniel C. Douglas, Richard Kenyon, and Haolin Shi, *Dimers, webs, and local systems*, Trans. Am. Math. Soc. **377** (2024), no. 2, 921–950 (English).

[FG06] Vladimir Fock and Alexander Goncharov, *Moduli spaces of local systems and higher Teichmüller theory*, Publ. Math., Inst. Hautes Étud. Sci. **103** (2006), 1–211.

[FG07] ———, *Moduli spaces of convex projective structures on surfaces*, Adv. Math. **208** (2007), no. 1, 249–273.

[FR99] Vladimir Fock and A. A. Rosly, *Poisson structure on moduli of flat connections on Riemann surfaces and the r-matrix*, Moscow Seminar in mathematical physics, Providence, RI: American Mathematical Society, 1999, pp. 67–86.

[GHJW97] K. Guruprasad, J. Huebschmann, L. Jeffrey, and A. Weinstein, *Group systems, groupoids, and moduli spaces of parabolic bundles*, Duke Math. J. **89** (1997), no. 2, 377–412.

[Gol84] William M. Goldman, *The symplectic nature of fundamental groups of surfaces*, Advances in Mathematics **54** (1984), no. 2, 200–225.

[Gol86] ———, *Invariant functions on Lie groups and Hamiltonian flows of surface group representations*, Invent. Math. **85** (1986), no. 2, 263–302. MR 846929

[Gol90] ———, *Convex real projective structures on compact surfaces*, J. Differ. Geom. **31** (1990), no. 3, 791–845.

[Ker83] Steven P. Kerckhoff, *The Nielsen realization problem*, Ann. Math. (2) **117** (1983), 235–265.

[KO24] Richard Kenyon and Nicholas Ovenhouse, *Eigenvalues of matrix products*, Preprint, arXiv:2407.10786 [math.CO] (2024), 2024.

[Kos04] Vladimir Petrov Kostov, *The Deligne–Simpson problem—a survey*, Journal of Algebra **281** (2004), no. 1, 83–108.

[LZ21] John Loftin and Tengren Zhang, *Coordinates on the augmented moduli space of convex* $\mathbb{RP}^2$ *structures*, J. Lond. Math. Soc., II. Ser. **104** (2021), no. 4, 1930–1972.

[Mar10] Ludovic Marquis, *Espace des modules marqués des surfaces projectives convexes de volume fini*, Geometry & Topology **14** (2010), no. 4, 2103 – 2149.

[MS17] Dusa McDuff and Dietmar Salamon, *Introduction to symplectic topology*, third ed., Oxford Graduate Texts in Mathematics, Oxford University Press, Oxford, 2017. MR 3674984

[Pal13] Frederic Palesi, *Introduction to positive representations and Fock–Goncharov coordinates*, preprint, 2013.

[Sik01] Adam S. Sikora, SL_n*-character varieties as spaces of graphs*, Trans. Amer. Math. Soc. **353** (2001), no. 7, 2773–2804. MR 1828473

[Sun21] Zhe Sun, *Rank N swapping algebra for* PGL_n *Fock-Goncharov* $\mathcal{X}$ *moduli space*, Math. Ann. **380** (2021), no. 3-4, 1311–1353.

[SWZ20] Zhe Sun, Anna Wienhard, and Tengren Zhang, *Flows on the* $\mathrm{PGL}(V)$*-Hitchin component*, Geom. Funct. Anal. **30** (2020), no. 2, 588–692.

[SZ17] Zhe Sun and Tengren Zhang, *The Goldman symplectic form on the PGL(V)-Hitchin component*, Preprint, arXiv:1709.03589 [math.DG] (2017), 2017.

[Thu86] William P. Thurston, *Earthquakes in two-dimensional hyperbolic geometry*, Low dimensional topology and Kleinian groups, Symp. Warwick and Durham 1984, Lond. Math. Soc. Lect. Note Ser. 112, 91-112 (1986)., 1986.

[Wei83] Alan Weinstein, *The local structure of Poisson manifolds*, J. Differ. Geom. **18** (1983), 523–557.

[Wol82] Scott Wolpert, *The Fenchel-Nielsen deformation*, Ann. Math. (2) **115** (1982), 501–528.

[Wol83] ———, *On the symplectic geometry of deformations of a hyperbolic surface*, Ann. Math. (2) **117** (1983), 207–234.

[WZ18] Anna Wienhard and Tengren Zhang, *Deforming convex real projective structures*, Geometriae Dedicata **192** (2018), 327–360.

Max Planck Institute for Mathematics in the Sciences, Inselstr. 22, 04103 Leipzig, Germany

Email address: fernando.camacho@mis.mpg.de